FOSSIL ENERGY

185
05/11/80 MJ.

D. 1595

DOE/MC/03103-2

MASTER

INVESTIGATIONS OF ENHANCED OIL RECOVERY THROUGH USE OF CARBON DIOXIDE

Progress Report for the Period
July 7, 1978—December 31, 1979

Date Published—June 1980

Work Performed for the Department of Energy
Under Contract No. DE-AC21-78MC03103

Louisiana State University
Baton Rouge, Louisiana

U. S. DEPARTMENT OF ENERGY

DOE/MC/03103-2
Distribution Category UC-92a

INVESTIGATIONS OF ENHANCED OIL RECOVERY THROUGH USE OF CARBON DIOXIDE

Progress Report for the Period
July 7, 1978—December 31, 1979

W. R. Whitehead, O. K. Kimbler,
R. M. Hoshman, and J. R. Hervey
Department of Petroleum Engineering
Louisiana State University
Baton Rouge, Louisiana 70803

C. D. Locke, *Technical Project Officer*
Morgantown Energy Technology Center
P.O. Box 880
Morgantown, West Virginia 26505

Work Performed for the Department of Energy
Under Contract No. DE-AC21-78MC03103
(formerly ET-78-S-01-3101)

Date Published—June 1980

U.S. DEPARTMENT OF ENERGY

TABLE OF CONTENTS

ABSTRACT

Procurement, construction, and installation of unconsolidated sand packs and all peripheral equipment required for conducting displacement studies at pressures up to 5000 psi is complete and the equipment is in routine use. One of the most significant accomplishments to date has been the design, construction and testing of sampling equipment which permits samples to be taken at pressures up to 3000 psi during displacements and phase behavior studies. This equipment was developed through cooperation with Precision Sampling Corp., Baton Rouge, Louisiana.

A total of 21 displacements have been made using synthetic crudes, one of which was formulated to serve as an analog of a typical West Texas crude. The data obtained to date suggest that miscibility can be generated between pure carbon dioxide and this oil at a pressure of 1100 psig. At a displacement temperature of 109°F, miscibility is generated through multiple contacts and the preponderance of data suggest, but do not yet prove, that the generation mechanism is one of condensation rather than vaporization. In displacements in which the injection gas was a mixture of carbon dioxide and methane, the minimum miscibility pressure appears to increase approximately linearly with increasing methane content.

Increased methane concentrations over those originally present were observed in all displacements where the pressure was less than that required for first contact miscibility.

Thus it was tentatively concluded that the presence of a methane bank is not in itself an indication that miscibility was not attained, but only an indication that the mechanism was one of generation of miscibility through mass transfer (multiple contacts).

LIST OF TABLES

LIST OF FIGURES

I. INTRODUCTION

Research at Louisiana State University on the use of CO_2 as an enhanced recovery process is keyed to the development of a basic understanding of the mechanism(s) by which miscibility is generated between the injected fluid and a reservoir oil. Various mechanisms have been proposed by earlier investigators which involved (1) the vaporization of intermediate molecular weight hydrocarbons into the CO_2 by a multiple contact mechanism and (2) the vaporization of higher molecular weight hydrocarbons (up to perhaps C_{20}). These mass transfer mechanisms are augmented and perhaps even supplanted under certain conditions by the strikingly high solubility of CO_2 in oil. It appears likely that the dominance of a particular mechanism may be dictated by a number of variables such as temperature, pressure, injected gas composition, oil composition, and the presence and distribution of an aqueous phase.

The manner in which miscibility is developed by mass transfer cannot be readily discerned without some means for determining the in-situ compositional history which takes place during and after the development of miscibility during an actual displacement of oil by CO_2. The only possible means for obtaining such data would appear to be the development of high pressure sampling techniques which could remove insignificant quantities (microliter size samples) from the flowing stream during consolidated core

and slim tube (sand pack) displacements. Such samples would be amenable to analysis through modifications of standard gas chromatography procedures. The development of such equipment and procedures has been a paramount concern of this research effort since its inception.

Laboratory displacements have traditionally focused on the recovery efficiency associated with that portion of a porous medium actually swept by a displacing fluid. For operational reasons this has usually dictated the use of either unconsolidated sand packs (slim tubes) or outcrop sandstone cores. It is the opinion of the principal investigators on this project that such recovery efficiency data is of little utility alone and must be supplemented by visual observations of the flowing (or produced) stream, compositional data, and selected supportive PVT experiments. The project aim is to obtain such data over a wide variety of conditions.

Displacements in sand packs can be used as a rapid means of studying such things as how fluid compositions and temperature affect minimum miscibility pressures and how these same variables influence mass transfer between phases under flowing conditions. Sand packs are also useful as screening devices because they allow rapid turnaround time between displacements. A disadvantage is that the effects of variations in water saturation cannot be readily studied.

The use of consolidated cores will permit the study of the effects of water saturation on CO_2 flooding and allows

the study of the process as a tertiary recovery tool. The presence of high water saturations may influence the time to reach mass transfer equilibrium. Also, because of the pore size distribution, capillary forces much like those encountered in reservoir rocks will be attained in the consolidated cores. This may emphasize recovery differences between miscible and near miscible displacement conditions. The primary disadvantage in using consolidated cores is the long period of time required for a displacement since small pressure gradients must be maintained. Furthermore, the turnaround time for a displacement is very long, with the net result being that the time-frame for a single displacement will be in the order of weeks instead of hours or days.

When a primary objective of a study is to delineate mechanisms, there are distinct advantages to be realized from the use of synthetic or simulated crude oils since they can be well characterized. In many instances an oil can be formulated which will show striking similarities to certain types of naturally occuring crudes. Thus, properly chosen and formulated synthetic crudes can act as time saving screening devices for developing and testing concepts which can later be validated in systems utilizing the prototype crude. Such an approach is being used in this project with one of the synthetic crudes employed being similar in many respects to certain West Texas crudes. Since reservoir conditions in the Gulf Coast and the midcontinent areas are frequently quite different from those encountered in West

Texas, particularly in respect to temperature, it is anticipated that all work on oils of this type will be done on an actual crude. One such oil, from the Brookhaven Field in Mississippi, will be used to represent such reservoirs.

Usually, CO_2 flooding implies the use of relatively pure CO_2 as an injection fluid. It may not be necessary or even desirable to use pure CO_2 since the presence of certain other components might not be detrimental and in some cases could even prove to be beneficial. This could be of major importance since many sources of CO_2 contain impurities. Furthermore, field application of the CO_2 process would in many cases result in the early breakthrough of CO_2 with the attendant necessity for recycling. In this case the produced CO_2 will contain substantial quantities of hydrocarbon components from the oil. It may be both technically and economically advantageous to reinject the produced gas without surface treatment other than normal oil-gas separation. The effects of the presence of certain components that could be contained in the CO_2 injection fluid are a major concern in the present research program.

The primary task associated with this project has been to design, procure and construct the experimental facilities necessary to support a continuing effort in the area of enhanced oil recovery with immediate application to the CO_2 process. This work has progressed nicely in view of substantial delays associated with a move to new physical facilities and with procurement problems. The most formidable

problem, that of taking and analyzing small samples under displacement conditions, is believed to be essentially solved thus making the remaining tasks experimentally possible.

II. EXPERIMENTAL EQUIPMENT AND PROCEDURES

Displacement Equipment and Procedures

All displacements discussed in this report were made in unconsolidated sand packs using synthetic crudes. The sand packs were constructed using 1" OD by 5/8" ID stainless steel tubing approximately twenty feet in length. Ferrule type fittings containing 350 mesh stainless steel screens were attached to the ends and adapted to receive 1/8" Ruska high pressure fittings. The assembly was pressure tested to 8000 psi prior to packing. The twenty-foot sections were suspended vertically in a forty-foot shaft adjacent to the laboratory. A vertical arrangement was used to maximize gravity segregation between the injection fluid and the reservoir oil during displacement. The tubes were packed dry with a 70 mesh and finer Ottawa sand. A complete sieve analysis of the sand is shown in Table A.1 of Appendix A. Dense packing was achieved by vibrating the tubes during placement of the sand. The porosity was measured on each pack by evacuating the pack and then saturating it with Soltrol 170. The sand packs had an average porosity of 25.7% and an average permeability of 11.6 darcies. When a forty-foot flow path was desired two twenty-foot lengths were connected in series using 1/8" OD stainless steel tubing and Ruska fittings.

The sand packs were heated by circulating a mixture of ethylene glycol and water through 1/4" OD copper tubing that was tightly wound around the entire length of the 1" OD

stainless steel tubing. Heat loss was minimized by thoroughly insulating the sand pack assembly and all connecting tubing. A schematic of the temperature control equipment is shown in Figure 2.1

All displacements were conducted while maintaining a constant pressure drop across the sand packs. This was accomplished by means of 6000 psi Tescom back pressure regulators.

The effluent from the packs was visually observed by means of a high pressure capillary visual cell located immediately upstream from a sampling point. An LED-Phototransistor sensor was built into the visual cell body to electronically detect phase charges and/or changes in light transmission which might result from major compositional changes. Output from the sensor was recorded on a strip chart recorder. Location of the sampling point immediately downstream of the visual cell permitted the sampling of equilibrium phases during an immiscible displacement and sequential sampling through the transition zone during a miscible displacement. Details of the sampling point and sampling technique are discussed in a later section. The effluent was flashed to atmospheric pressure in a glass separatory funnel from which oil was withdrawn into graduated cylinders. The gas production was measured by means of a wet test meter which was vented into an exhaust air duct. All displacements were terminated at a producing GOR of 30,000 SCF/STB.

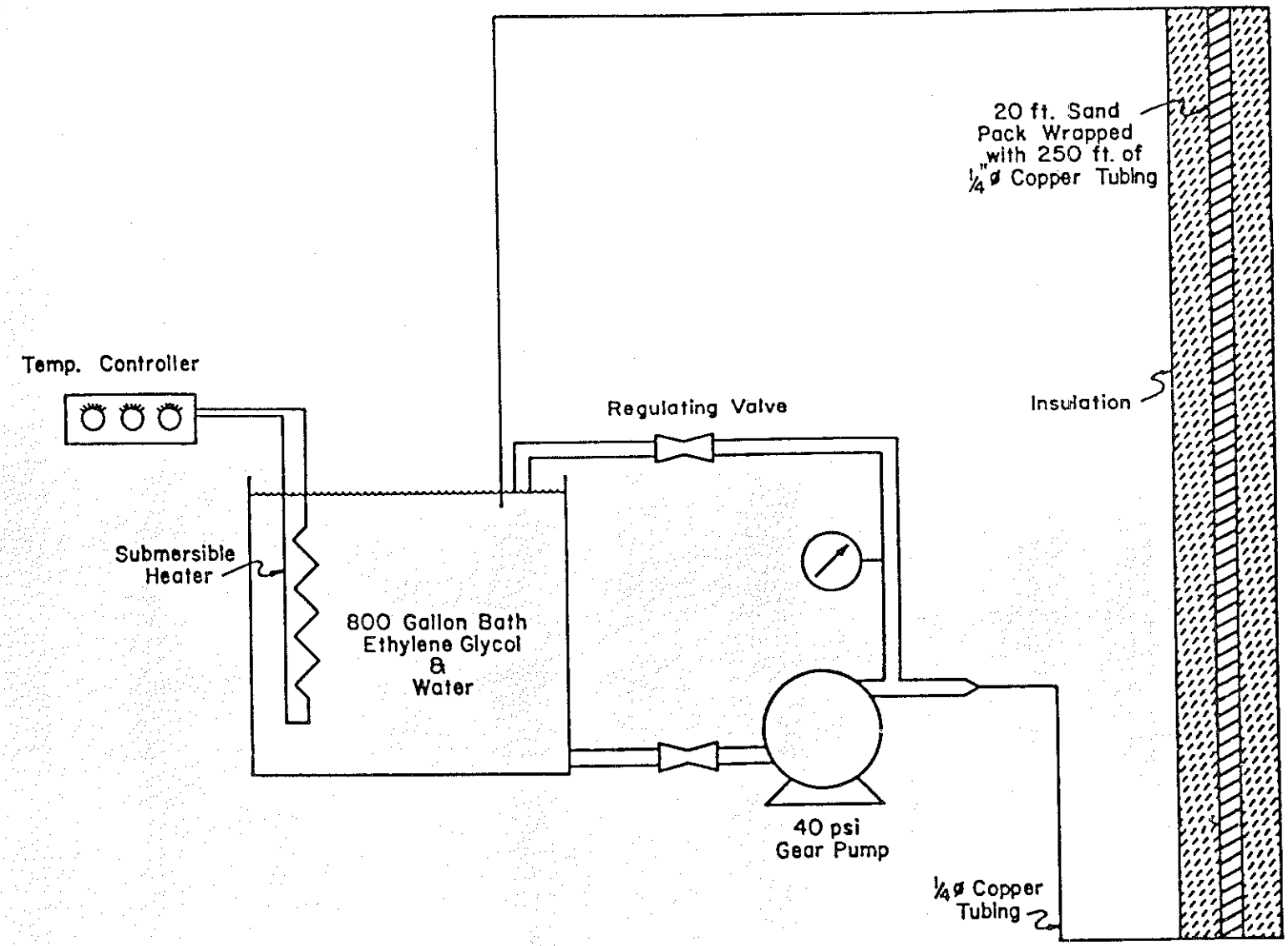

FIGURE 2.1 TEMPERATURE CONTROL OF SAND PACKS

Different equipment arrangements upstream of the sand pack were necessary for charging the pack with live oil and for displacement by CO_2 and CO_2-methane mixtures. The arrangement used for saturation is shown in Figure 2.2. The oil phase was charged to the packs from the 37,000 cc, 3000 psi titanium sphere in which it was mixed. The mixing procedure is described elsewhere. The live oil, above its saturation pressure was injected into the Soltrol-saturated pack by means of a Whitey diaphragm-type laboratory feed pump which pumped methane saturated water into the bottom of the titanium vessel. Saturation was considered complete when both the effluent gas-oil ratio and the effluent composition matched those of the injected oil.

Figure 2.3 shows the arrangement used during displacements. The injection fluid was delivered to the pack from a 316 stainless steel transfer vessel fitted with a floating piston. The fluid was preheated in a controlled temperature water both prior to injection into the sand pack. Water was used to drive the floating piston.

Although not shown in the schematic drawings, auxilliary safety equipment is an integral part of the displacement set-up. Valves are located at all points necessary to isolate any portion of the equipment which might develop leaks. Sensors set to monitor flammability limits are strategically placed to detect even minor leaks and facilities are available for rapidly flooding exhaust vents with CO_2 if flammable limits should be approached.

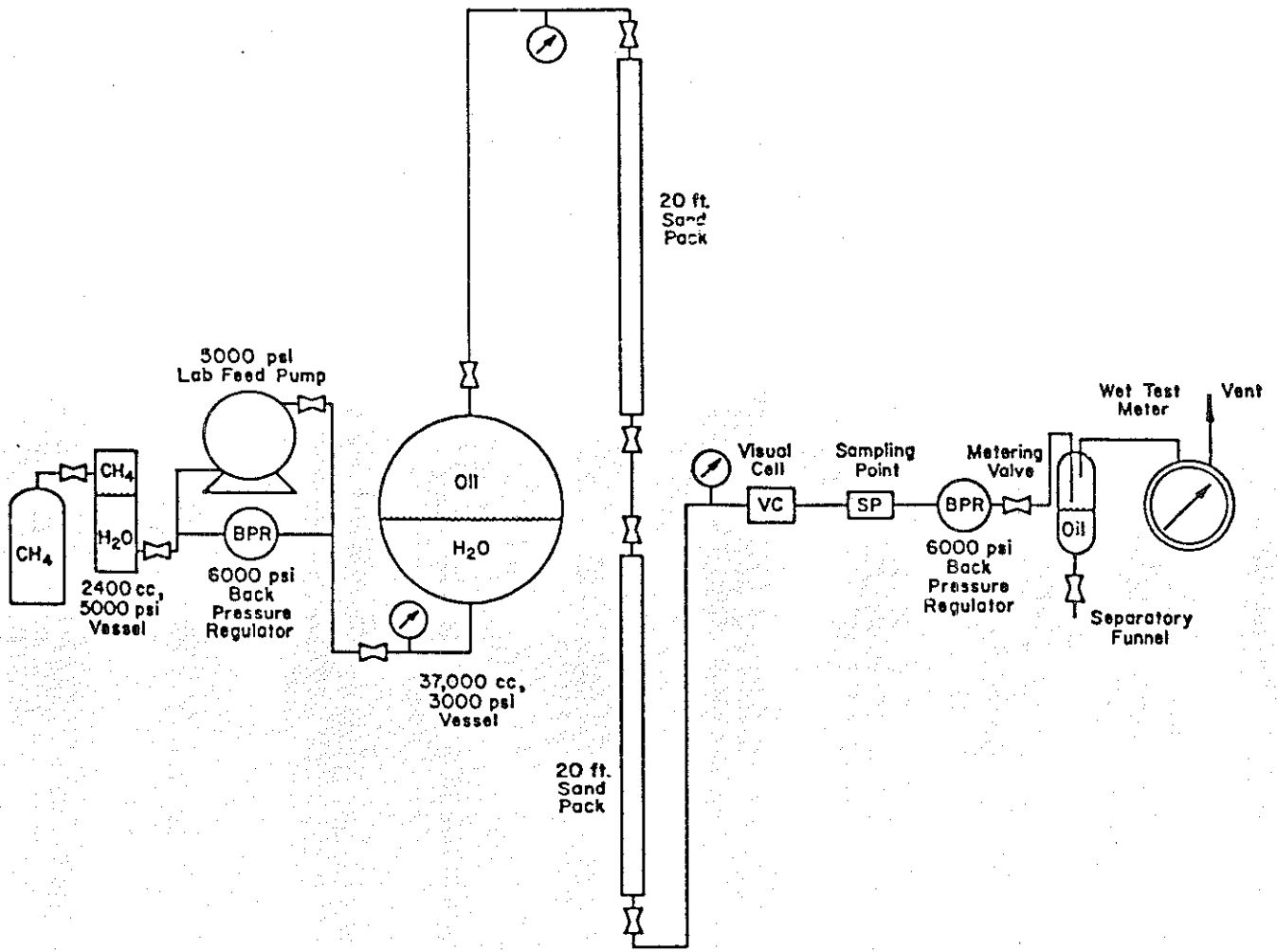

FIGURE 2.2 FORTY FOOT SAND PACK
(Arrangement for Saturation with Live Oil)

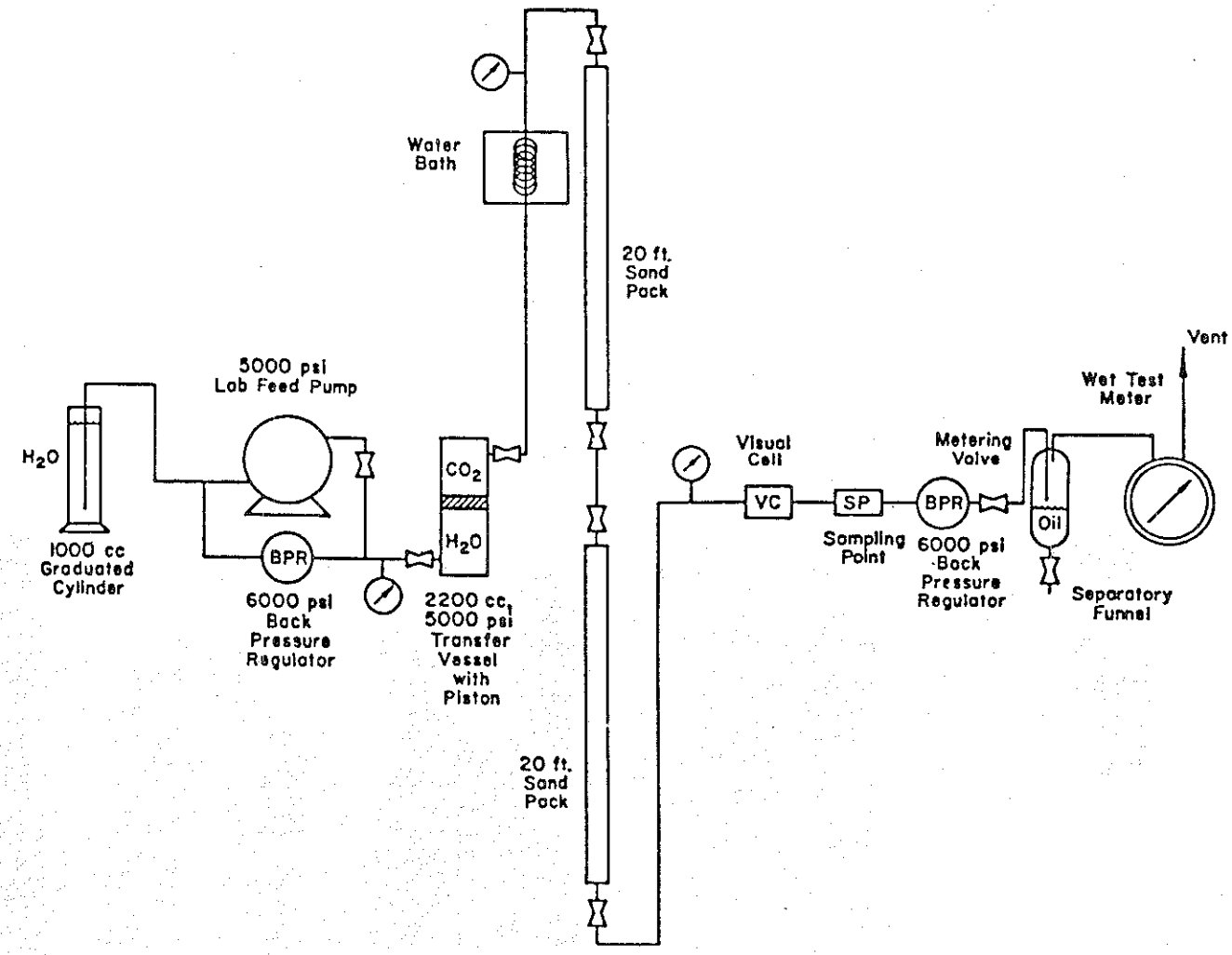

FIGURE 2.3 FORTY FOOT SAND PACK
(Arrangement for Displacement)

Fluid Mixing Facilities and Procedures

The facility for mixing synthetic crudes and for reconstituting crude oils is shown in Figure 2.4. In either case those constituents which are liquid at room temperature and atmospheric pressure are first charged into the sphere. Water is pumped into the bottom of the vessel until it is completely liquid filled. Ethane and heavier components are then metered in the liquid phase into the vessel by means of a Ruska Mercury pump. A 6000 psi back pressure regulator in parallel with a Whitey feed pump maintains the desired pressure level in the vessel as these components are added. Methane is charged to the vessel in the vapor phase. The purity of all components used is given in Table A.2 of Appendix A. After addition of all components, the contents are thoroughly mixed by rocking the vessel on its support. A sample of the mix is taken for chromatographic analysis and for the determination of bubble point pressure, gas-oil ratio, formation volume factor, and molecular weight of the C_7 plus fraction. If adjustments in composition are required they are made at this time. The facility permits sufficient quantities of oil to be mixed at one time to supply the requirements for all PVT and displacement studies contemplated for that oil. This consistency in oil properties from one experiment to another is considered to be of major importance since the effect on miscibility pressure of minor changes in oil composition has not yet been established.

The facility for mixing injection fluid is shown in

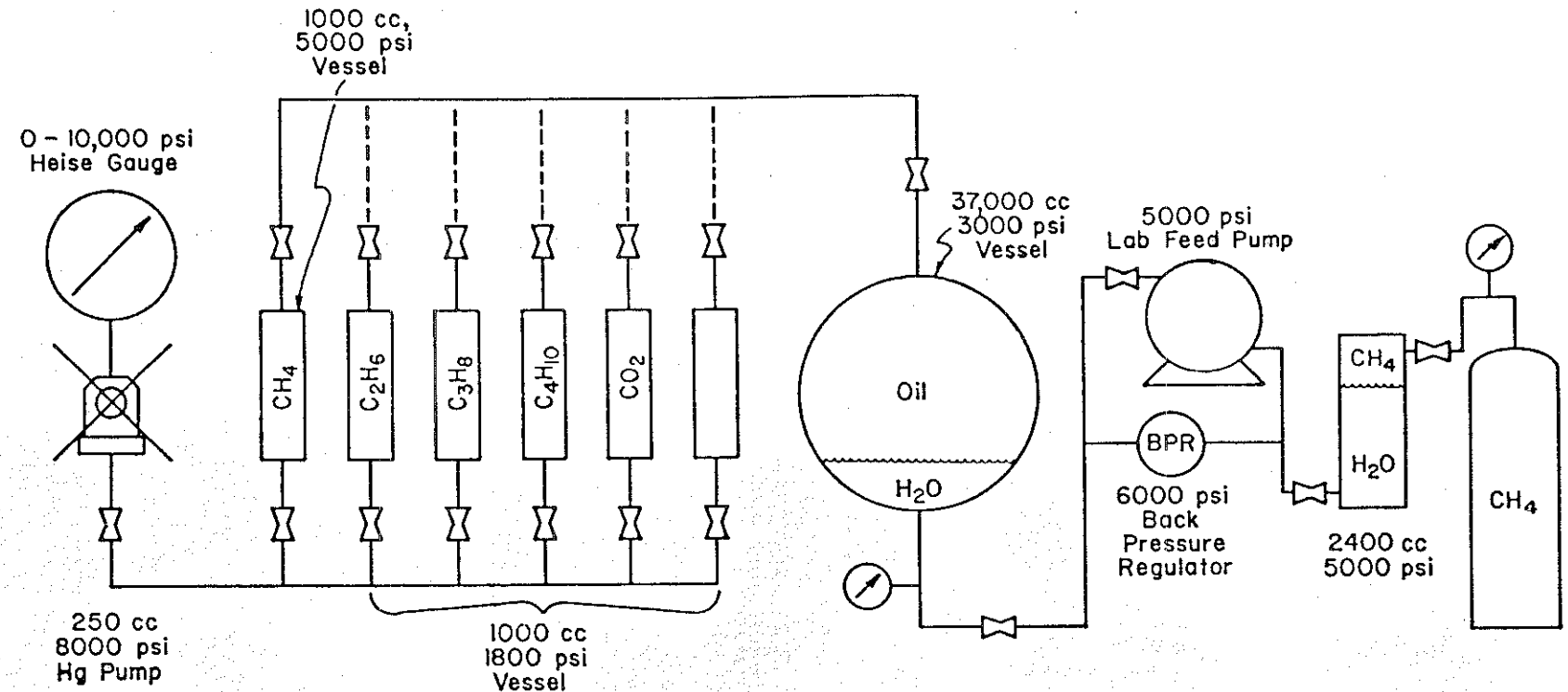

FIGURE 2.4 MIXING FACILITY FOR RESERVOIR OIL

Figure 2.5. It is identical to that described above except that a stainless steel transfer vessel is substituted for the titanium sphere.

PVT Equipment

Figure 2.6 is a schematic of the PVT equipment used in this study. The arrangement consists of a 10,000 psi Ruska windowed condensate cell, two blind cells, and two Ruska mercury pumps. The cells are enclosed in an air bath for temperature control. The condensate cell has been modified to allow the installation of high pressure sampling facilities which are discussed later. This modification also allows sampling of any phase that appears during the PVT studies. The air bath has a window through which the cell contents can be viewed via a mirror inside the bath. A Gaertner cathetometer (Model No. M-912) is used to measure phase volumes. As a safety precaution the air bath is heated by forcing air over a finned-tube heat exchanger through which a heated mixture of ethelyene glycol and water is circulated. Air from the box is continually exhausted through a ventilation duct that contains a flammability limit detector.

Sampling and Analysis

Central to this project is the requirement that high pressure samples of any phase be obtainable during displacements and PVT studies. This is accomplished by means of custom designed, high pressure, microliter syringes and

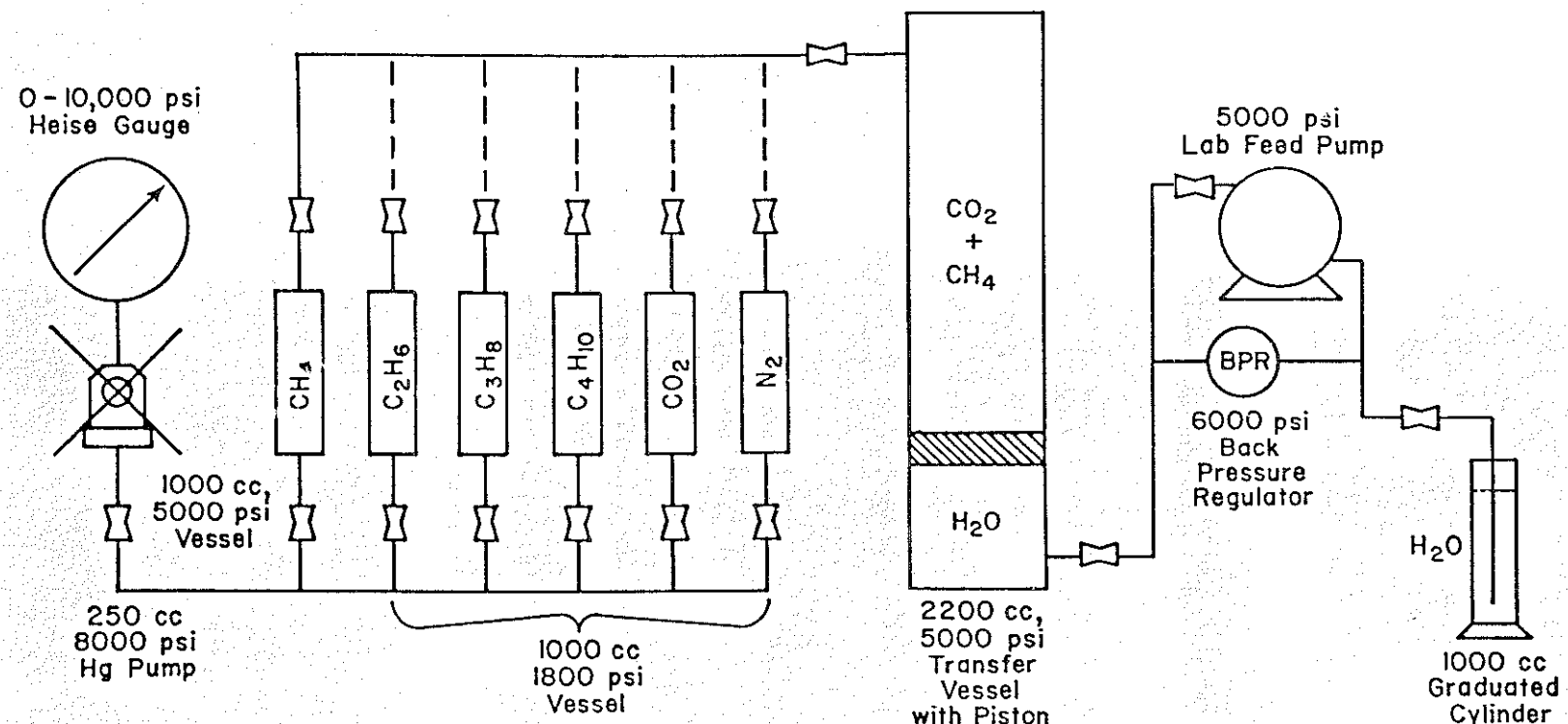

FIGURE 2.5 MIXING FACILITY FOR INJECTION FLUID

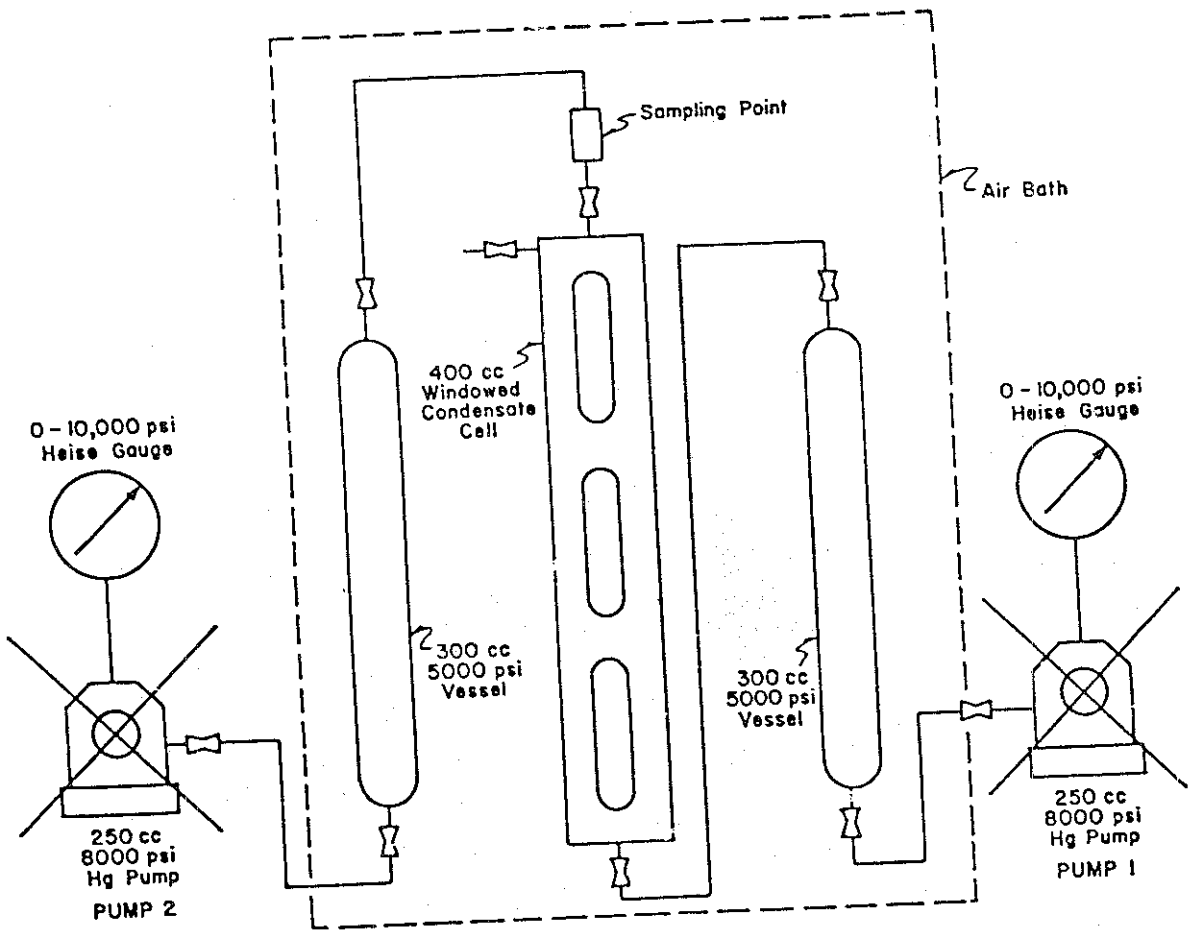

FIGURE 2.6 PVT CELL

sampling yokes developed in cooperation with Precision Sampling Corp., Baton Rouge, Louisiana.

In essence the sampling yoke is a stainless steel block designed to mount permanently in a flow line. The flowing stream is conducted through a 1/16" diameter hole drilled longitudinally through the block. A slide valve operating perpendicularly to the hole permits a sampling needle to be inserted directly into the flowing stream. The slide is sealed with preloaded teflon seals and locks into the closed position as a precaution against accidental opening. No purging is required since no dead space is introduced during the sampling operation.

A special high-pressure 15 microliter sampling syringe attaches to the sampling needle. The syringe contains internal valving which allows a sample to be withdrawn without the introduction of dead space. The only dead space which exists within the system is a minute annular volume which exists between the inside diameter of the needle and a stylet which occupies most of the internal volume of the needle. The resulting 0.001 inch annular width has a volume which is insignificant in comparison to the sample volume (5 μl) normally taken. The trapped sample can be either injected immediately into a gas chromatograph or held under pressure for several hours. Since each analysis requires an appreciable period of time, it is not uncommon during a displacement to have several samples awaiting analysis. The sampling system has been used routinely at pressures up to 2500 psi

and on occasion up to 3000 psi. It appears likely that presently contemplated improvements will raise the working pressure even higher. At the present time the sampling system is considered experimental and is not offered commercially by Precision Sampling. It is believed, however, that it may be made available after all modifications have been thoroughly tested.

Analyses of samples were made using a Hewlett-Packard Model 5840 gas chromatograph coupled to a Hewlett-Packard Model 9825C post-run calculator. Numerous column types and valving arrangements were tested in an attempt to obtain the best possible analysis. The most successful arrangement for analyzing samples taken during displacements of synthetic crudes proved to be an 8-foot long, 1/8 in. diameter, Chromosorb 102 column with a back-flush valve. All analyses were made using a thermal conductivity detector. The chromatograph was calibrated using the NGPA Natural Gas Reference Standard and a custom blend of C_5 through C_{10} and Soltrol 170. At the start of each analysis the oven temperature was set at 50°C, the injection port temperature at 290°C, the detector temperature at 300°C, the back-flush valve temperature at 300°C, and the carrier gas (helium) flow rate at 30 ml/min. After injection of the sample the oven temperature remained at 50°C for two minutes, after which the temperature was increased at 30°C per minute until a maximum temperature of 240°C was reached. All components through C_{10} had been eluted from the column at the end of 20 minutes. The back-

flush valve then automatically reversed the flow of the carrier gas through the column and the base line was automatically rezeroed. The C_{11} plus fraction was thus backflushed out of the column and through the thermal conductivity detector for analysis. The chromatograph was preprogramed to take the area counts obtained from the analysis and the response factors determined from the calibration runs and compute and print out a complete analysis of each sample.

III. EXPERIMENTAL RESULTS

As mentioned previously, all displacements have been conducted using well characterized synthetic crudes. The bulk of the work has been accomplished using an oil designed to have a composition and PVT properties which would be typical of many West Texas crude oils. A paper by Rathmell et al.* (1971) reports a study of three oils having appreciably different characteristics. The oil designated by Rathmell as Crude A was chosen as the prototype upon which the composition of this synthetic oil was based. A comparison of Rathmell's Crude A and this synthetic crude is shown in Table 3.1. Compositions of both synthetic crudes and all injection fluids used in this study are shown in Table 3.2.

Displacement Data

A total of twenty-one displacements were conducted in the unconsolidated sand packs. All displacements were made at a temperature of 109°F which corresponds to the reservoir temperature of Crude A reported by Rathmell. Table 3.3 lists pertinent data concerning each run. Run 1 was the only displacement in which synthetic Crude B was used. The composition of this crude, differed from reservoir fluid A only in that it contained naphtha and did not contain heptane and octane. This oil was abandoned after the first run

*Rathmell, J.J., F.I. Stalkup, and R.C. Hassinger, "A Laboratory Investigation of Miscible Displacement by Carbon Dioxide", SPE Preprint No. 3483, October 1971.

Table 3.1

Comparison of Rathmell's Crude A

And Synthetic Crude Used In This Study

	Rathmell's Crude A	Reservoir Fluid A
C_1	17.07	17.24
C_2	6.41	6.52
C_3	7.82	6.83
C_4	6.72	6.37
C_5	2.69	2.70
C_6	5.19	5.13
C_{6+}	54.10	55.21
C_{7+} Density, gm/cc	0.8780	0.753
C_{7+} Molecular Weight	222	161
Bubble Point Pressure	845 psig	705 psig
Reservoir Temperature	109°F	109°F
Solution GOR, SCF/bbl	317	450

Table 3.2

Composition of Reservoir Oil and Displacing Fluid

Expressed in Mole Percent

Component	Reservoir Fluid A	Reservoir Fluid B	Injected Gas A	Injected Gas B	Injected Gas C
CO_2			100.0	87.49	75.19
C_1	17.24	12.55		12.51	24.81
C_2	6.52	5.55			
C_3	6.83	4.97			
C_4	6.37	10.19			
C_5	2.70	2.79			
C_6	5.13	5.49			
C_7	7.20				
C_8	7.50				
C_9	6.25	7.43			
C_{10}	5.78	4.51			
Soltrol	28.50	31.45			
Naphtha		15.11			
Molecular Weight C_7+	161.1				
density gm/cc	0.656		0.605*		0.306*
C_7+	0.753				
viscosity, cp.	0.340		0.048*	0.0293*	0.0265*
Bubble Point	705 psig	740 psig			
B_o	1.238 bbl/STB @ 109°F	1.267 bbl/STB @ 109°F			

*estimated at displacement pressure

Table 3.3

Summary of CO_2 Displacements

Run	Core Length	Crude Composition	Injection Fluid	Pressure	CO_2 Breakthrough Recovery	Ultimate Recovery	Condition
1	20	Reservoir Fluid B	CO_2	1100	85.9	92.3	Miscible
2	20	Soltrol	Nitrogen	850	21.5	56.1	Immiscible
3	20	Reservoir Fluid A	CO_2	1100	80.9	89.8	Immiscible
4	20	Reservoir Fluid A	CO_2	1850	74.8	93.0	Miscible
5	20	Reservoir Fluid A	CO_2	1200	90.9	96.1	Miscible
6	40	Soltrol	Nitrogen	800	20.0	54.6	Immiscible
7	40	Reservoir Fluid A	CO_2	1200	89.6	94.9	Miscible
8	40	Reservoir Fluid A	CO_2	1500	86.5	95.4	Miscible
9	40	Reservoir Fluid A	CO_2	1000	77.5	80.6	Immiscible
10	40	Reservior Fluid A	CO_2	1300	87.9	97.8	Miscible
11	40	Reservoir Fluid A	87.5% CO_2 12.5% C_1	1800	91.2	94.3	Miscible
12	40	Reservoir Fluid A	87.5% CO_2 12.5% C_1	1500	84.6	91.9	Immiscible
13	40	Reservoir Fluid A	87.5% CO_2 12.5% C_1	1400	83.2	88.1	Immiscible
14	40	Reservoir Fluid A	87.5% CO_2 12.5% C_1	950	67.9	72.1	Immiscible
15	40	Reservoir Fluid A	87.5% CO_2 12.5% C_1	1600	86.0	93.5	Miscible
16	40	Reservoir Fluid A	75.0% CO_2 25.0% C_1	2000	82.4	93.5	Miscible
17	40	Reservoir Fluid A	75.0% CO_2 25.0% C_1	1700	80.0	85.7	Immiscible
18	40	Reservoir Fluid A	75.0% CO_2 25.0% C_1	1800	80.3	86.8	Immiscible
19	40	Reservior Fluid A	75.0% CO_2 25.0% C_1	1900	82.6	89.6	Miscible
20	40	Reservoir Fluid A	C_1	4000	79.4	84.6	Miscible
21	40	Reservoir Fluid A	C_1	3700	76.5	80.7	Miscible

because the resulting chromatogram did not have as many clearly defined discrete peaks as reservoir fluid A. Runs one through five were conducted in a 20 foot pack while the remainder of the runs were conducted in a forty-foot system.

Two immiscible displacements, (Runs 2 and 6), using Soltrol as a reservoir fluid and nitrogen as an injection fluid, were conducted to determine the minimum recovery to be expected during an immiscible flood in which very little swelling was taking place in the reservoir fluid. One displacement was in a twenty-foot pack and the other in a forty-foot pack. The runs showed good agreement in both breakthrough and ultimate recovery.

Runs seven through twenty-one were conducted in the forty-foot system using reservoir fluid A. In runs seven through ten pure carbon dioxide was used as the injection fluid. A mixture of 12.5 mole percent methane and 87.5 mole percent carbon dioxide was used as the injection fluid during runs eleven through fifteen. The concentration of methane in the injection fluid was increased to 25 mole percent in runs sixteen through nineteen. The last two displacements were conducted using pure methane as the displacing fluid. Since the displacement pressures in these last two exceeded the maximum working pressure of the sampling syringe, no samples were taken.

A total of ninety samples taken during fifteen displacements were analyzed. The results of these analyses are given in Table B.1 of Appendix B. Also presented in the

table is the recovery up to the time each sample was taken and the phase state of each sample. Table B.2 (Appendix B) presents modified analyses of the same samples obtained by subtracting from the observed values those quantities of the components associated with the injection fluid. The data shown in Tables 3.4, 3.5, and 3.6 were derived from the modified analyses shown in Table B.2. The mole fraction of each component listed was divided by the mole fraction of that component originally present in the reservoir oil. Thus, values greater than one indicate an increase in concentration of a component or group of components, whereas a value less than one indicates a decrease.

Breakthrough (appearance of CO_2 in the effluent) and ultimate recovery data from those displacements which used carbon dioxide as the injection fluid are plotted in Figure 3.1. The volume of oil produced up to the time of interest is multiplied by the formation value factor and then decreased by the volume of dead space associated with the connecting tubing and control panel. The quantity thus obtained is divided by the total pore volume of the sand pack to yield the fractional recovery up to that time. A plot of recovery as a function of pressure is a very important tool in determining the minimum miscibility pressure.

Both breakthrough and ultimate recoveries increase as the displacement pressure approaches the minimum miscibility pressure. Once this pressure has been exceeded there are no appreciable increases in recovery. This trend was observed

Table 3.4

Normalized Concentrations of Components in the Transition Zone of the 40 Foot Displacements Using CO_2 as a Displacement Fluid

Run	Pressure	Percent Recovery	C_1	C_2	C_3	C_4	C_5	C_6	C_7	C_8	C_9	C_{10}	Soltrol	C_2- C_4	C_5+
7	1200	91.9	1.67	1.37	1.05	0.89	0.82	0.79	0.78	0.78	0.78	0.86	0.81	1.10	0.80
7	1200	93.7	2.98	3.49	1.55	0.65	0.40	0.32	0.30	0.29	0.00	0.00	0.27	1.87	0.24
7	1200	94.9	0.45	2.52	1.91	1.65	1.39	2.13	1.03	0.82	0.77	0.12	0.64	2.02	0.83
8	1500	86.5	0.96	0.96	0.97	0.99	0.98	0.98	0.99	1.02	1.02	0.96	1.05	0.97	1.02
8	1500	88.5	1.02	0.99	0.95	0.95	0.96	0.95	0.96	0.99	1.00	0.91	1.06	0.96	1.01
8	1500	89.6	1.01	0.98	0.93	0.93	0.94	0.94	0.96	0.98	0.98	0.90	1.09	0.95	1.01
8	1500	91.8	1.02	0.99	0.93	0.91	0.90	0.90	0.92	0.95	0.95	0.95	1.12	0.94	1.01
8	1500	93.2	0.91	0.93	0.91	0.86	0.90	0.93	0.94	0.97	0.98	0.91	1.20	0.91	1.06
9	1000	80.6	0.93	1.49	1.05	0.94	0.93	0.93	0.95	0.95	0.98	1.01	0.97	1.17	0.98
9	1000	80.6	0.30	3.84	1.83	1.19	0.97	0.87	0.83	0.78	0.76	0.76	0.73	2.30	0.78
10	1300	88.7	1.00	0.99	0.99	0.99	1.02	1.03	1.04	1.03	1.00	1.00	0.98	0.99	1.00
10	1300	90.6	0.99	0.98	0.98	0.98	1.00	0.99	1.01	1.00	0.99	1.01	1.02	0.98	1.01
10	1300	92.9	1.01	1.02	0.99	0.97	0.98	0.98	0.98	0.99	0.97	1.01	1.02	0.99	1.00
10	1300	94.7	0.83	0.89	0.89	0.93	1.07	1.14	1.04	1.10	1.10	1.05	1.07	0.90	1.08

Table 3.5

Normalized Concentrations of Components in the Transition Zone of the 40 Foot Displacements Using 12.5% C_1H_4 - 87.5% CO_2 as a Displacement Fluid

Run	Pressure	Percent Recovery	C_1	C_2	C_3	C_4	C_5	C_6	C_7	C_8	C_9	C_{10}	Soltrol	C_2- C_4	C_5+
12	1500	84.6	1.76	1.04	0.94	0.90	0.88	0.87	0.86	0.83	0.82	0.85	0.76	0.96	0.80
12	1500	84.6	4.45	0.71	0.23	0.14	0.09	0.06	0.13	0.16	0.17	0.21	0.41	0.36	0.27
12	1500	88.5	1.40	1.06	0.99	0.98	0.97	0.96	0.96	0.91	0.91	0.93	0.83	1.01	0.89
12	1500	91.2	0.85	1.32	1.20	.98	0.83	0.73	0.81	0.81	0.85	0.92	1.19	1.16	0.99
13	1400	83.2	1.37	0.91	0.81	0.82	0.86	0.89	0.91	0.92	0.93	0.93	0.94	0.85	0.92
13	1400	83.2	3.69	0.93	0.32	0.17	0.15	0.16	0.17	0.18	0.18	0.16	0.17	0.48	0.17
13	1400	86.6	1.13	1.06	0.89	0.86	0.86	0.96	0.96	0.97	0.96	0.95	1.00	0.94	0.98
13	1400	88.1	0.28	1.97	2.04	1.38	1.06	1.00	0.94	0.92	0.90	0.86	0.90	1.82	0.92
14	950	67.9	1.56	1.14	0.98	0.89	0.85	0.85	0.85	0.84	0.84	0.83	0.83	1.00	0.84
14	950	67.9	4.74	0.80	0.19	0.07	0.07	0.07	0.14	0.14	0.16	0.12	0.17	0.34	0.15
14	950	70.7	3.70	2.65	0.59	0.16	0.09	0.07	0.16	0.15	0.16	0.12	0.19	1.17	0.16
14	950	70.7	0.28	1.90	1.25	1.08	1.07	1.08	1.08	1.07	1.07	1.07	1.06	1.40	1.07
15	1600	86.0	1.11	1.03	0.98	0.97	0.97	0.97	0.97	0.97	0.97	0.97	0.96	0.99	0.97
15	1600	87.2	0.96	0.93	0.94	0.98	1.02	1.04	1.04	1.05	1.04	1.04	1.02	0.95	1.03
15	1600	90.0	1.07	0.94	0.92	0.93	0.97	1.00	1.02	1.03	1.02	1.01	0.99	0.93	1.00
15	1600	92.1	1.65	1.02	0.91	0.88	0.85	0.86	0.86	0.84	0.82	0.78	0.77	0.94	0.80
15	1600	92.6	1.97	0.98	0.91	0.89	0.85	0.82	0.80	0.77	0.71	0.65	0.63	0.93	0.70

Table 3.6

Normalized Concentrations of Components in the Transition Zone of the 40 Foot Displacements Using 25% C_1H_4 – 75% CO_2 as a Displacement Fluid

Run	Pressure	Percent Recovery	C_1	C_2	C_3	C_4	C_5	C_6	C_7	C_8	C_9	C_{10}	Soltrol	C_2– C_4	C_5+
16	2000	82.4	1.02	1.01	1.01	1.01	1.00	1.00	1.00	0.99	0.99	0.98	0.99	1.01	0.99
16	2000	85.5	1.03	0.94	0.95	0.96	0.97	0.98	1.00	1.01	1.01	1.01	1.02	0.95	1.01
16	2000	89.4	1.44	0.99	0.91	0.87	0.86	0.85	0.86	0.86	0.87	0.85	0.87	0.93	0.86
16	2000	91.3	3.72	1.06	0.66	0.38	0.22	0.04	0.12	0.10	0.08	0.05	0.07	0.71	0.08
16	2000	91.3	1.14	1.08	1.05	1.04	1.06	1.05	1.04	0.98	0.94	0.88	0.85	1.05	0.92
17	1700	80.0	2.28	1.06	0.82	0.71	0.68	0.68	0.69	0.69	0.69	0.68	0.69	0.86	0.77
17	1700	83.5	2.07	1.15	0.89	0.77	0.73	0.73	0.73	0.73	0.73	0.72	0.71	0.93	0.72
17	1700	83.5	4.93	0.84	0.27	0.13	0.11	0.03	0.12	0.12	0.11	0.10	0.09	0.40	0.10
17	1700	85.3	1.44	1.39	1.09	0.92	0.89	0.88	0.87	0.85	0.84	0.81	0.81	1.13	0.83
17	1700	85.3	4.75	1.25	0.46	0.19	0.13	0.03	0.11	0.10	0.09	0.08	0.05	0.62	0.07
18	1800	80.3	2.36	0.97	0.78	0.69	0.66	0.74	0.65	0.65	0.65	0.63	0.65	0.82	0.65
18	1800	80.3	4.90	0.65	0.22	0.10	0.08	0.07	0.08	0.06	0.07	0.06	0.05	0.32	0.06
18	1800	82.1	2.08	0.98	0.83	0.79	0.79	0.79	0.79	0.78	0.78	0.76	0.66	0.87	0.72
18	1800	84.4	1.84	1.20	0.98	0.87	0.84	0.82	0.81	0.80	0.80	0.77	0.67	1.02	0.74
18	1800	85.9	1.43	1.32	1.14	1.02	0.97	0.94	0.92	0.89	0.88	0.83	0.72	1.16	0.81
18	1800	85.9	4.45	1.26	0.55	0.24	0.13	0.11	0.10	0.08	0.08	0.05	0.04	0.69	0.06
19	1900	82.6	1.50	1.00	0.92	0.89	0.88	0.88	0.88	0.87	0.87	0.86	0.86	0.94	0.87
19	1900	85.3	1.72	0.99	0.88	0.83	0.82	0.82	0.82	0.82	0.81	0.80	0.80	0.90	0.81
19	1900	87.8	1.76	1.14	0.94	0.83	0.78	0.77	0.79	0.78	0.79	0.77	0.76	0.97	0.77
19	1900	87.8	4.60	1.00	0.42	0.19	0.12	0.09	0.07	0.05	0.04	0.02	0.03	0.54	0.05

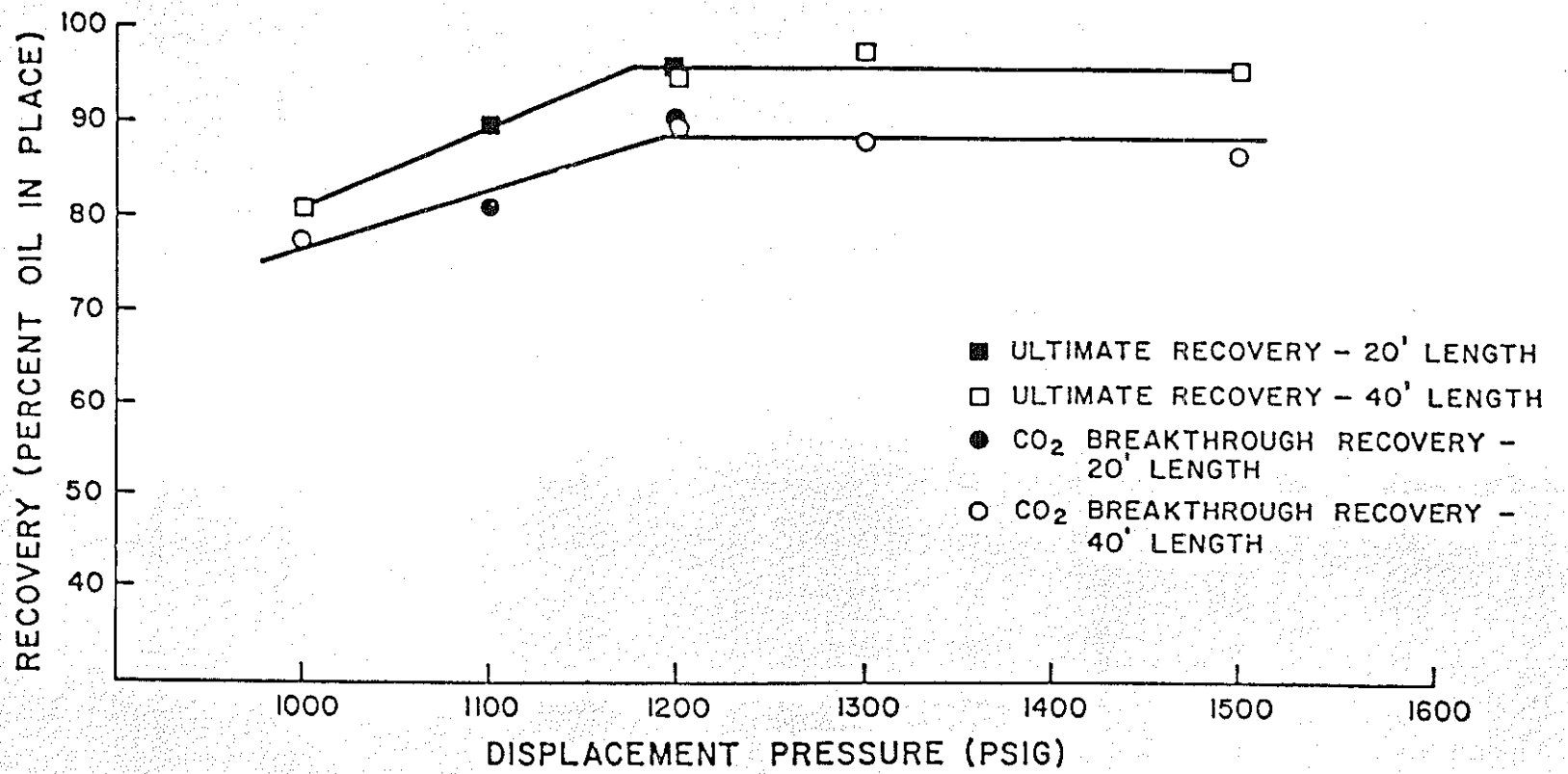

FIGURE 3.1 – RECOVERY OF RESERVOIR FLUID USING 100% CO_2 AS A DISPLACEMENT FLUID

in the recovery plots made for all the displacements and was used in conjunction with phase observations in the visual cell and chromatographic analyses in determining the minimum miscibility pressure for each injection fluid.

Figure 3.2 shows the recoveries obtained when using a mixture of 12.5% methane and 87.5% carbon dioxide as an injection fluid. Recovery plots using 25% methane and 75% carbon dioxide are shown in Figure 3.3. Only carbon dioxide breakthroughs are shown in the figures, even though in some runs this was preceded by a methane breakthrough.

Methane banks were noted in at least one displacement for each compostion of injected gas. These banks appeared either as a two phase flow region where the vapor phase was primarily methane and the liquid phase was a saturated oil, or as a single phase oil with an increased methane concentration. The methane banks associated with two phase flow occurred at lower pressures than did single phase methane banks. In general, the lower the displacement pressure the larger the methane bank. Figures 3.4 through 3.6 are plots of the methane concentrations in the liquid phase plotted as a function of recovery. Data for these plots were obtained from Table B.2 (Appendix B). A discussion of the methane bank and its relationship to miscibility determination appears in the next chapter.

Compositional changes in the effluent during twelve displacements are represented on pseudo-ternary diagrams using carbon dioxide and methane as one pseudocomponent, the

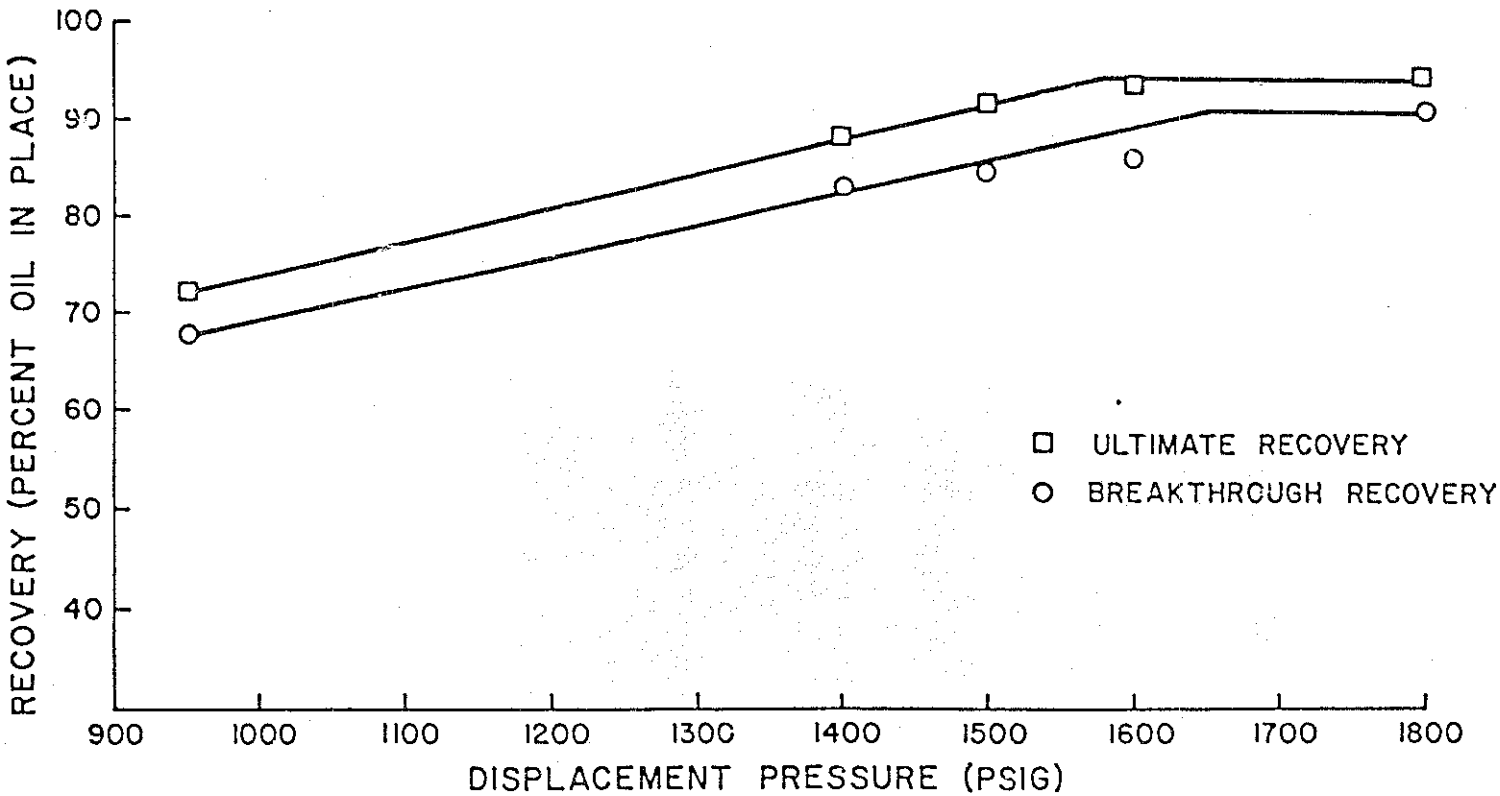

FIGURE 3.2 — RECOVERY OF RESERVOIR FLUID USING 12.5% C_1H_4 - 87.5% CO_2 AS A DISPLACEMENT FLUID

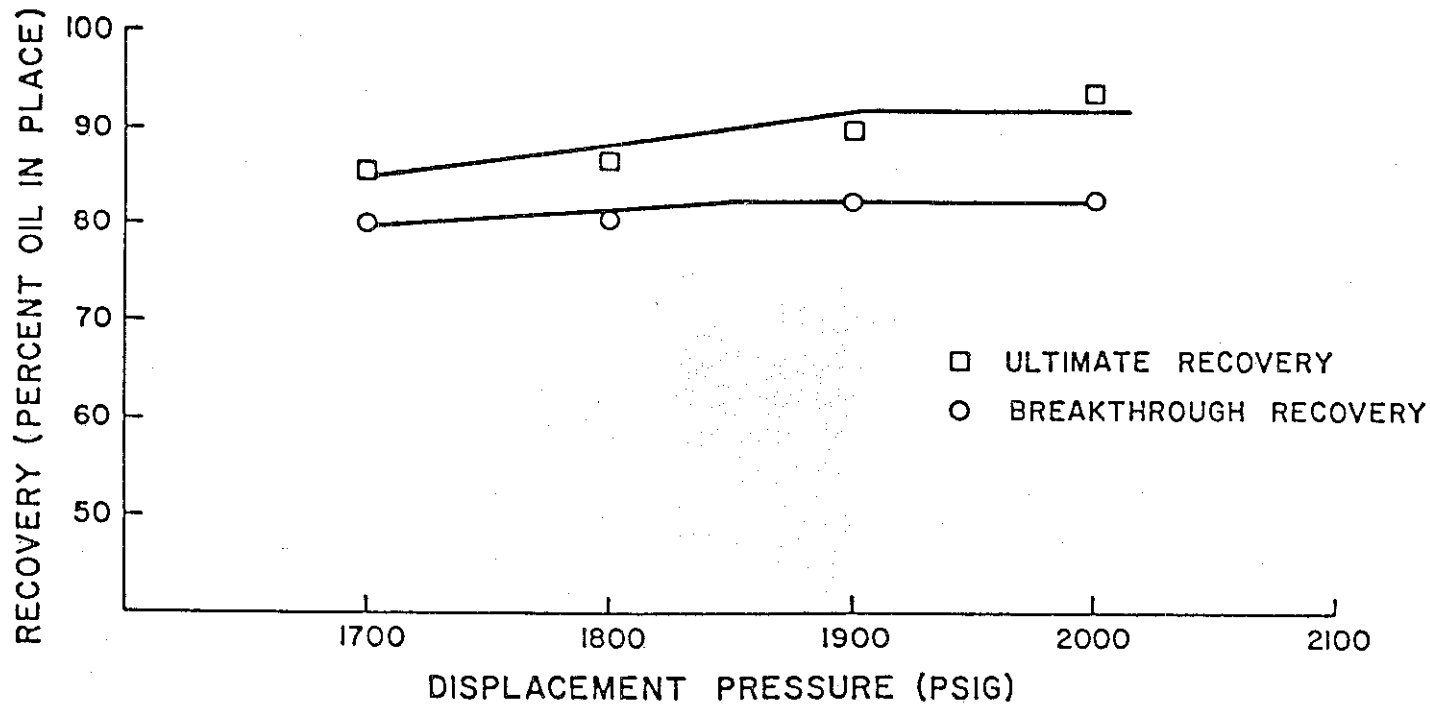

FIGURE 3.3 – RECOVERY OF RESERVOIR FLUID USING 25% C_1H_4 - 75% CO_2 AS A DISPLACEMENT FLUID

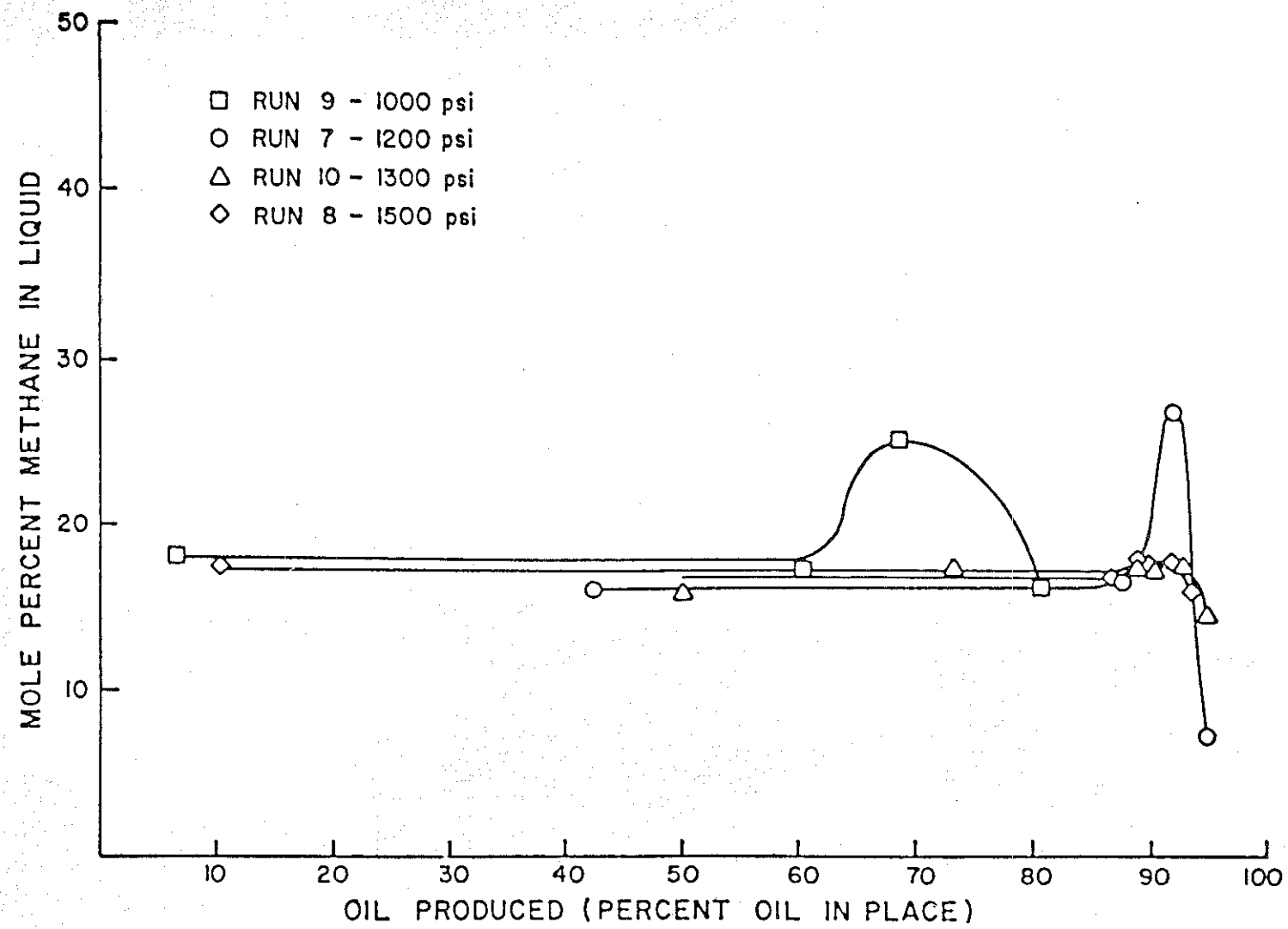

FIGURE 3.4 – METHANE CONCENTRATION IN CRUDE USING 100 % CO_2 AS A DISPLACEMENT FLUID

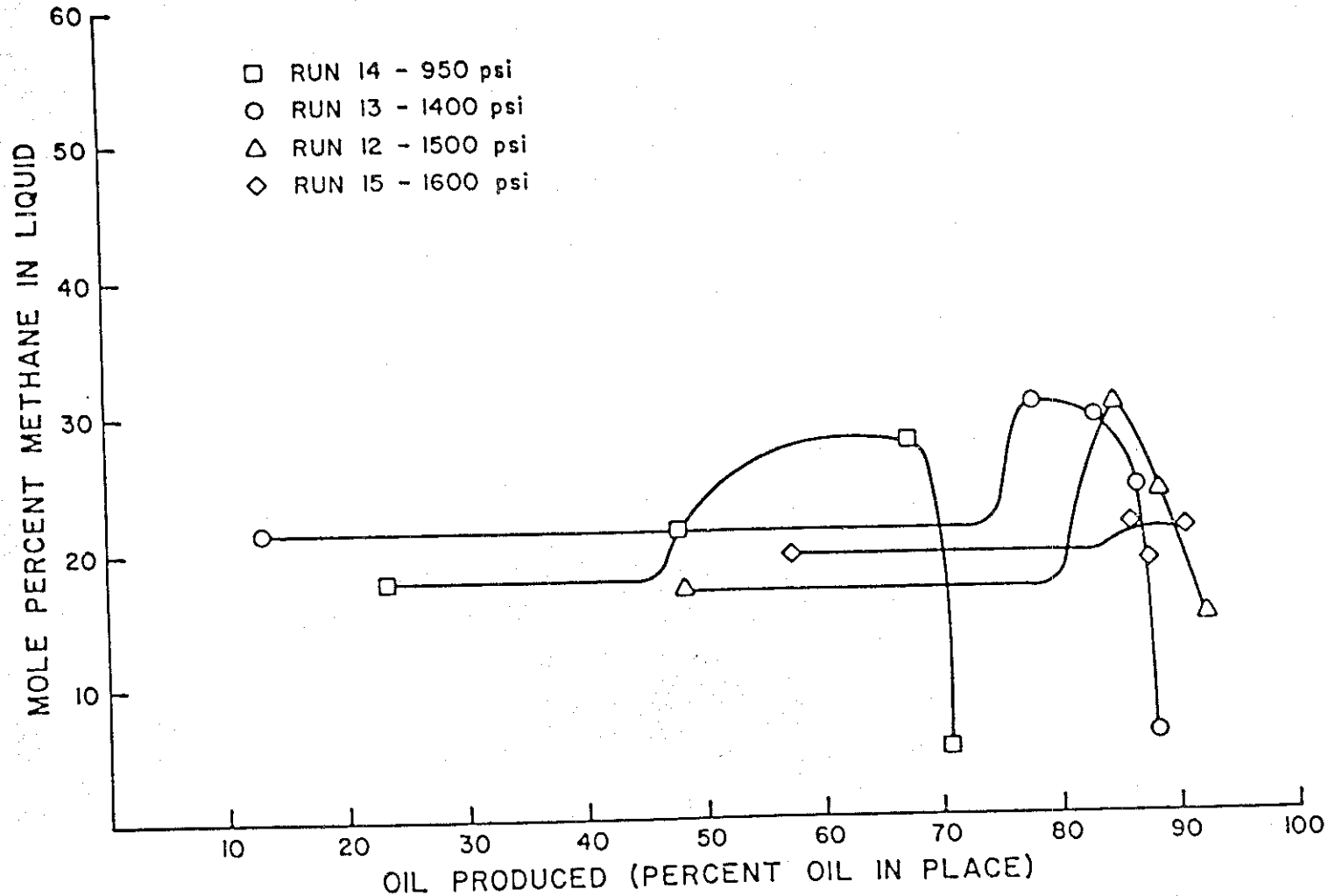

FIGURE 3.5 — METHANE CONCENTRATION IN CRUDE USING 12.5% C_1H_4 - 87.5% CO_2 AS A DISPLACING FLUID

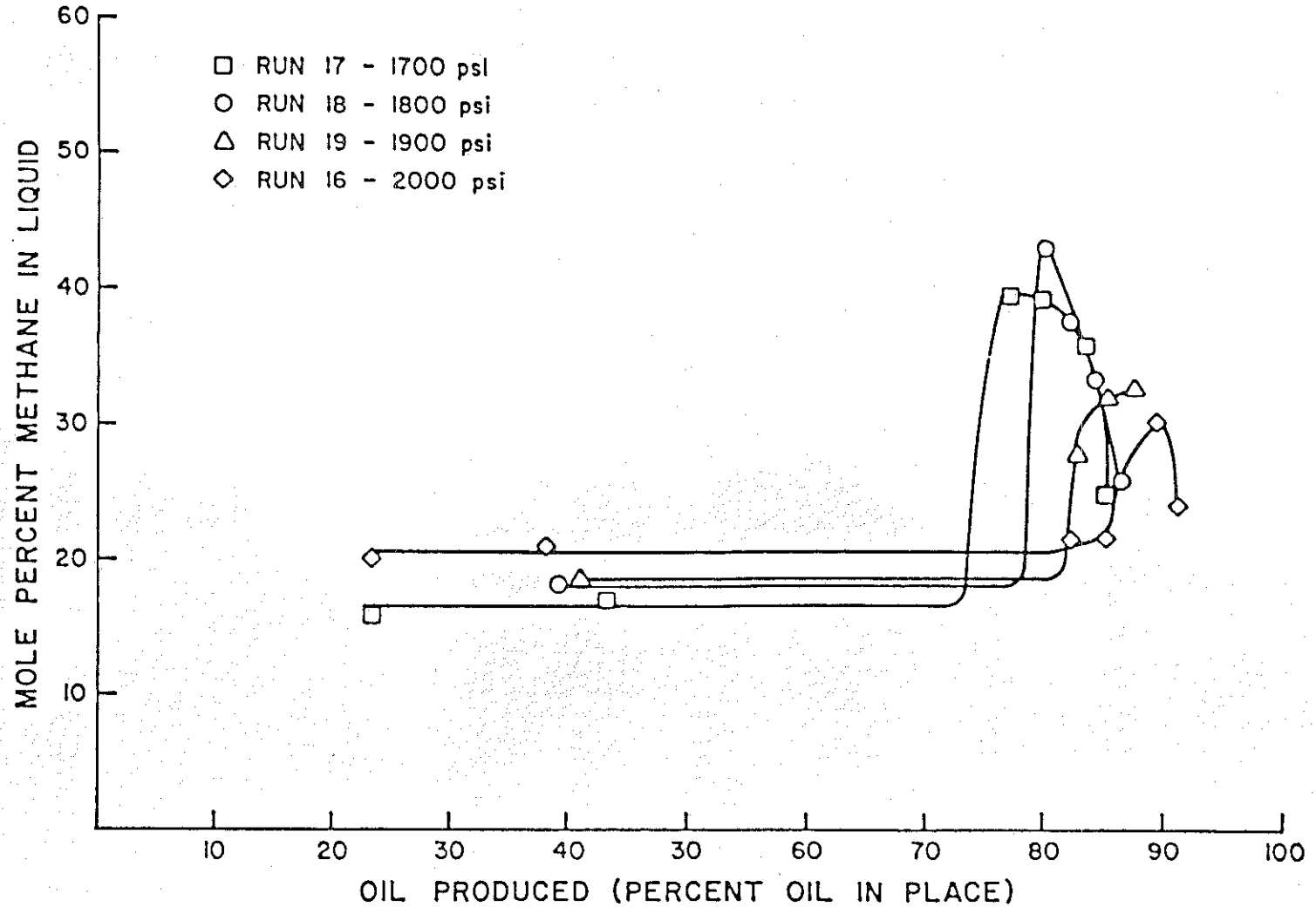

FIGURE 3.6 — METHANE CONCENTRATION IN CRUDE USING 25% C_1H_4 - 75% CO_2 AS A DISPLACEMENT FLUID

intermediates, C_2-C_6, as another and C_7+ as the third. These diagrams are shown as Figures 3.7 through 3.18. Pseudo-ternary diagrams are simplified representations of complex systems and are not quantitatively definitive, but do serve as illustrative tools. All single points on the plots represent a single phase sample and all two phase samples are shown by two points connected by a tie line.

Phase Behavior Data

The phase behavior experiments were conducted to support the displacement studies. Figure 3.19 is a pressure-volume diagram of the injection fluid which contains the highest concentration of methane in a CO_2-C_1 mixture. It shows that this fluid is a single phase at 109°F and all displacement pressure at which it was used. Clearly all mixtures containing less C_1 would likewise be single phase under these same conditions.

Pressure-volume data were obtained for various mixtures of reservoir fluid and injection gases. These data, together with the systems compositions are shown in Appendix C as Tables C.1 through C.12 and Figures C.1 through C.12. Swelling factors were determined at the bubble point pressure for all mixtures. Figures 3.20 and 3.21 show the swelling factors associated with the reservoir fluid - CO_2 and the reservoir fluid - injection fluid (87.13% CO_2, 12.87% C_1) systems respectively. A swelling factor in excess of three was observed in the latter case at high concentrations of injection fluid. These data clearly show why excellent

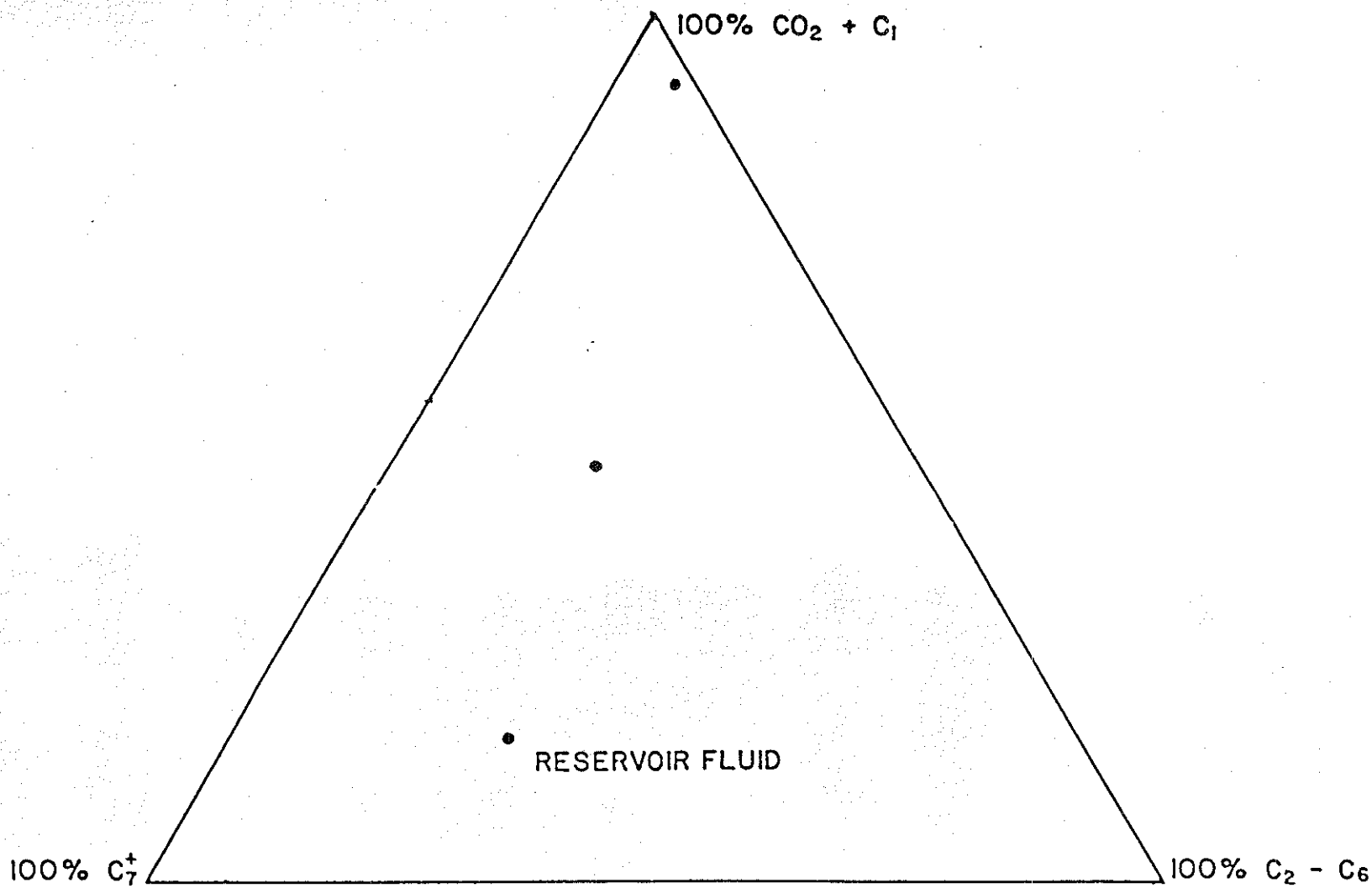

FIGURE 3.7 – COMPOSITION OF EFFLUENT DURING RUN 7 AT 1200 psi

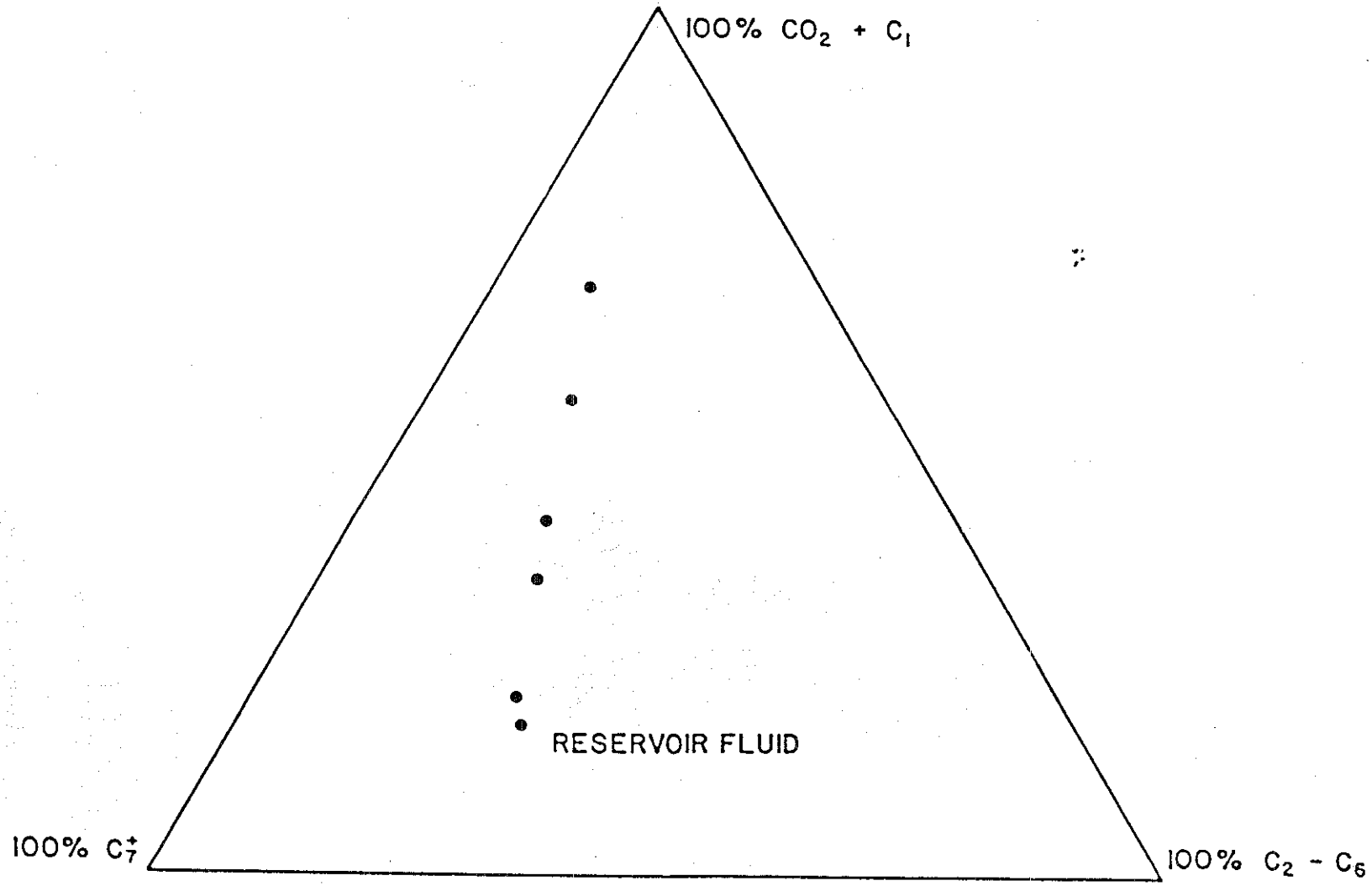

FIGURE 3.8 — COMPOSITION OF EFFLUENT DURING RUN 8 AT 1500 psi

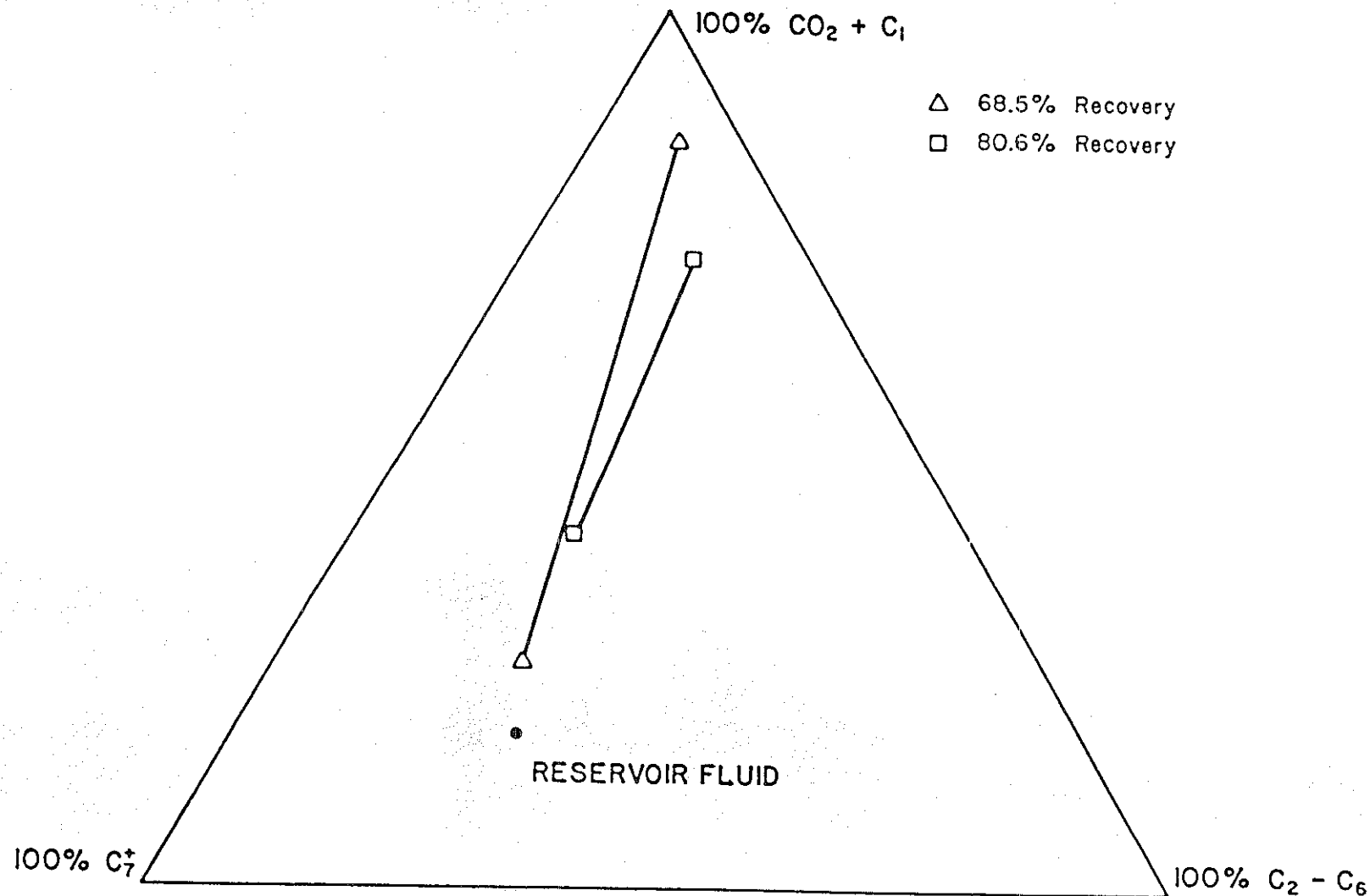

FIGURE 3.9 – COMPOSITION OF EFFLUENT DURING RUN 9 AT 1000 psig USING 100% CO_2 AS A DISPLACEMENT FLUID

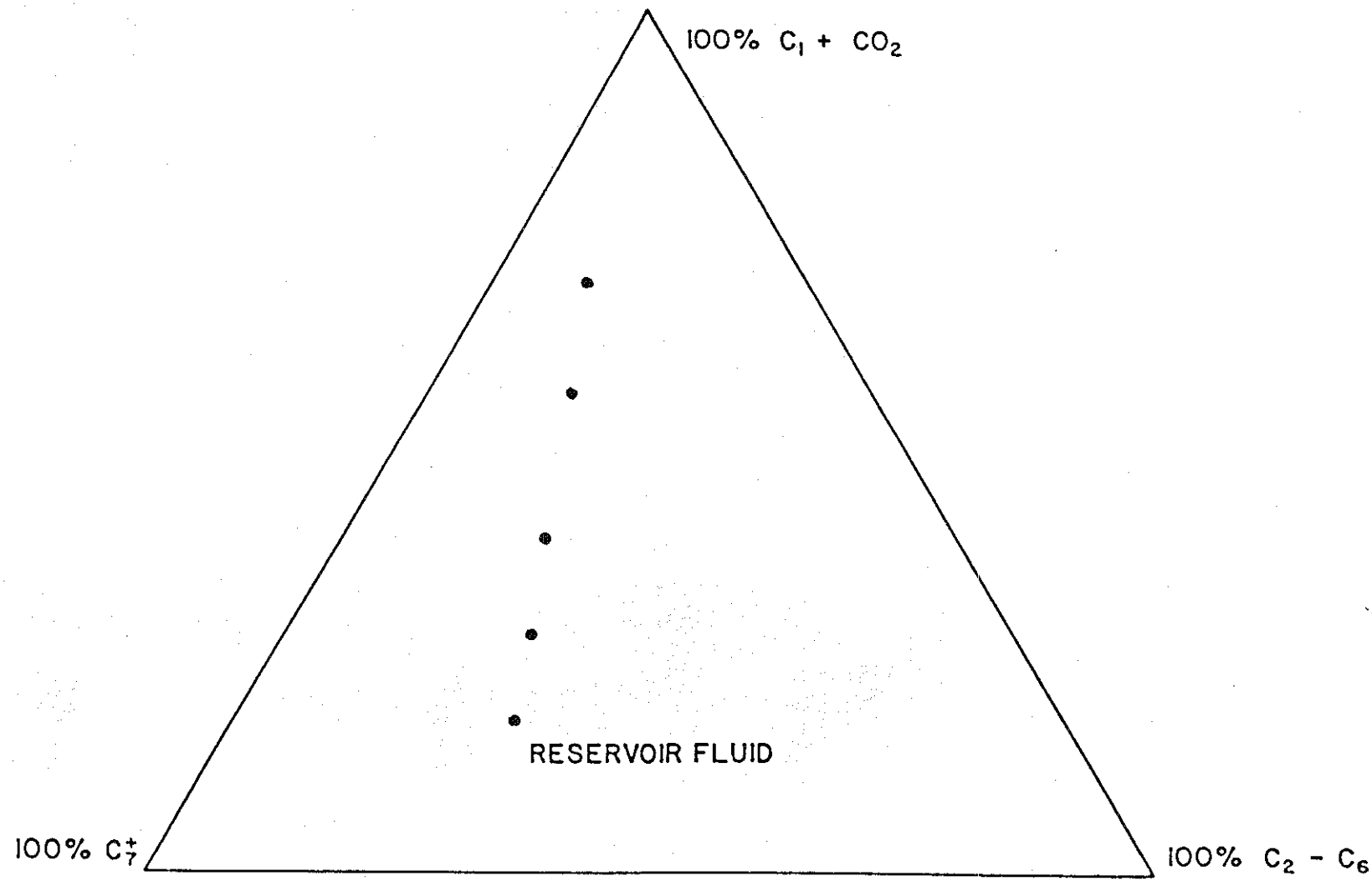

FIGURE 3.10 – COMPOSITION OF EFFLUENT DURING RUN 10 AT 1300 psig USING 100% CO_2 AS A DISPLACEMENT FLUID

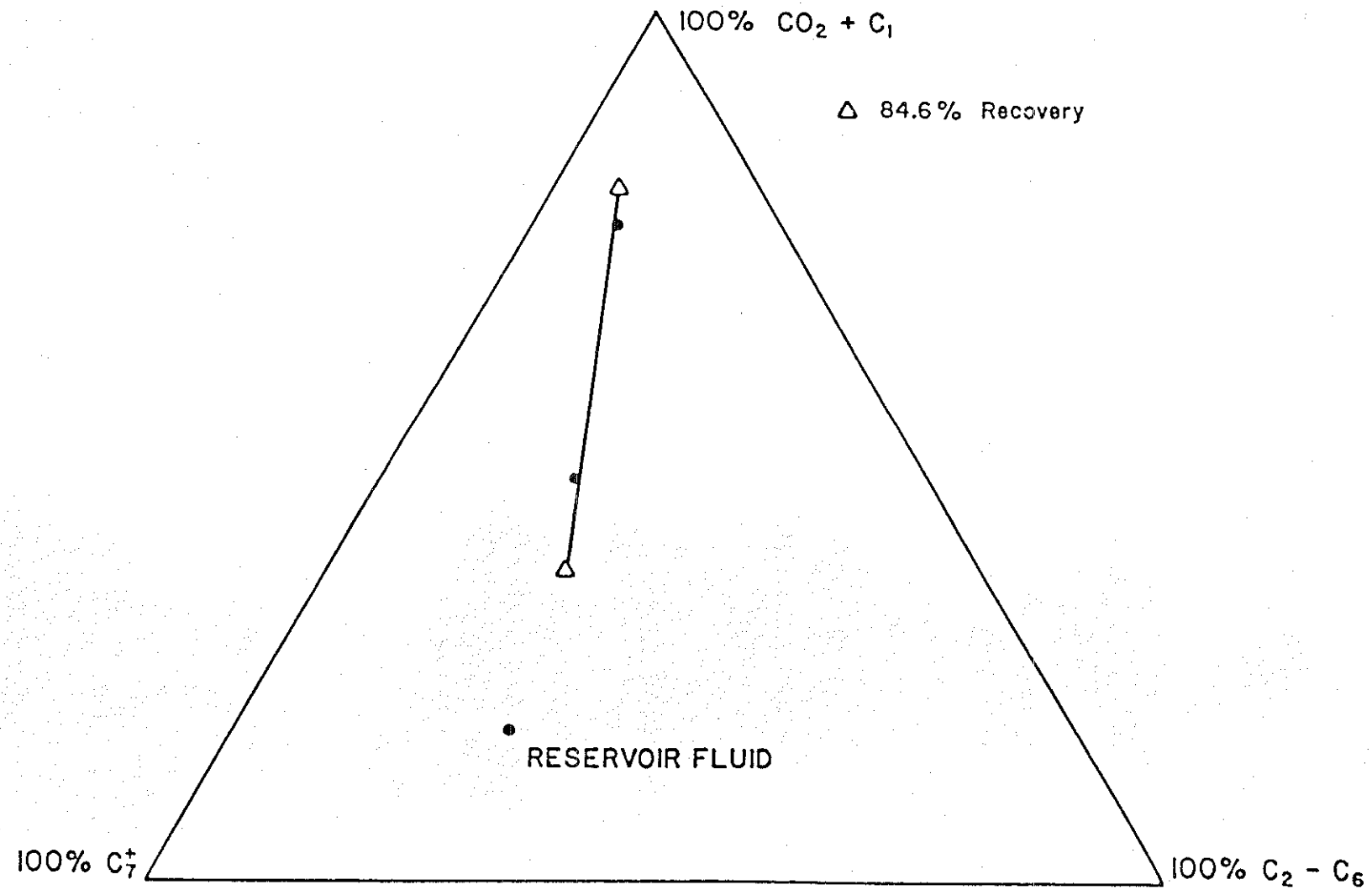

FIGURE 3.11 – COMPOSITION OF EFFLUENT DURING RUN 12 AT 1500 psi USING 12.5% CH_4 – 87.5% CO_2 AS A DISPLACEMENT FLUID

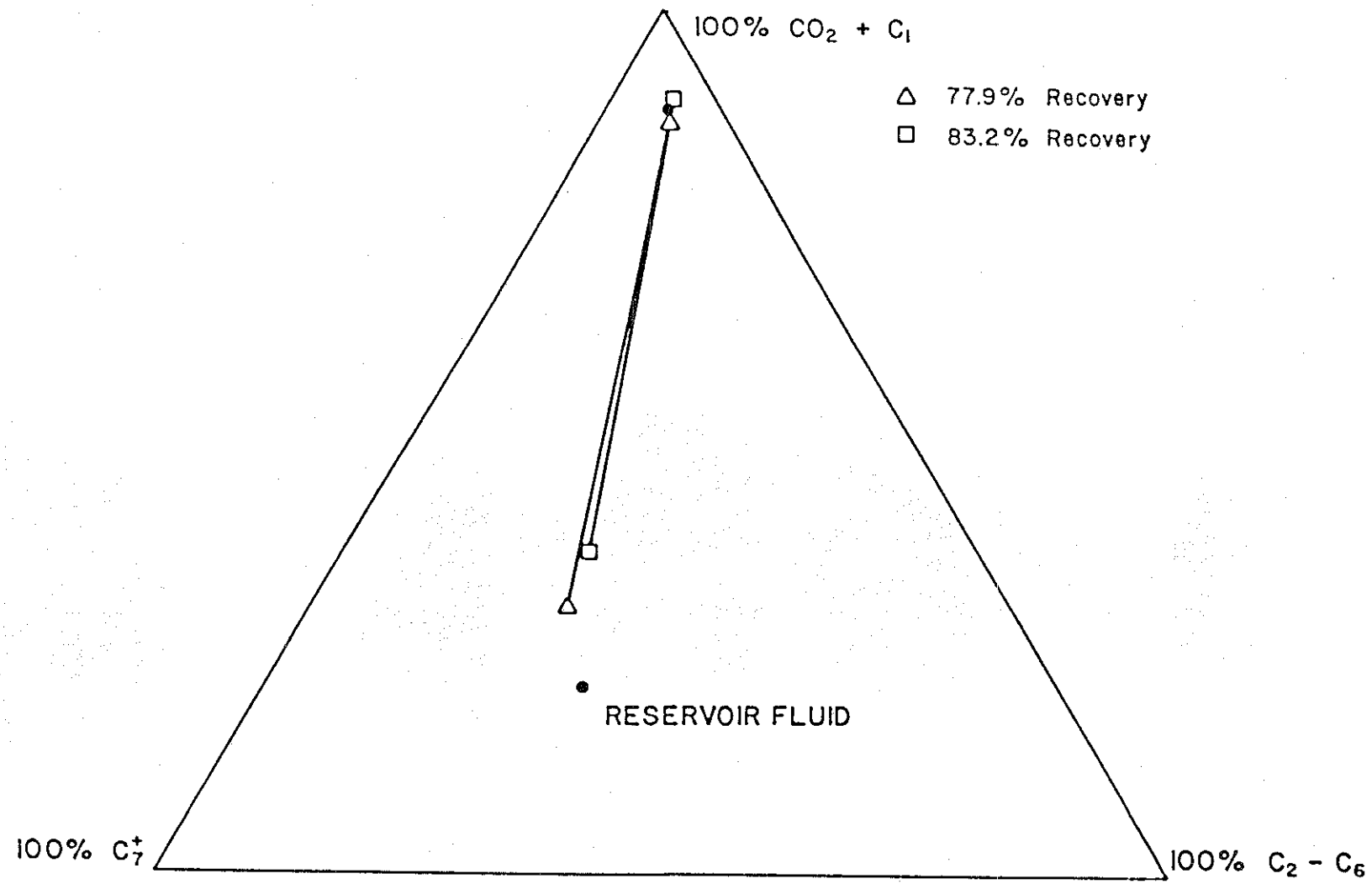

FIGURE 3.12 – COMPOSITION OF EFFLUENT DURING RUN 13 AT 1400 psi USING 12.5% CH_4 – 87.5% CO_2 AS A DISPLACEMENT FLUID

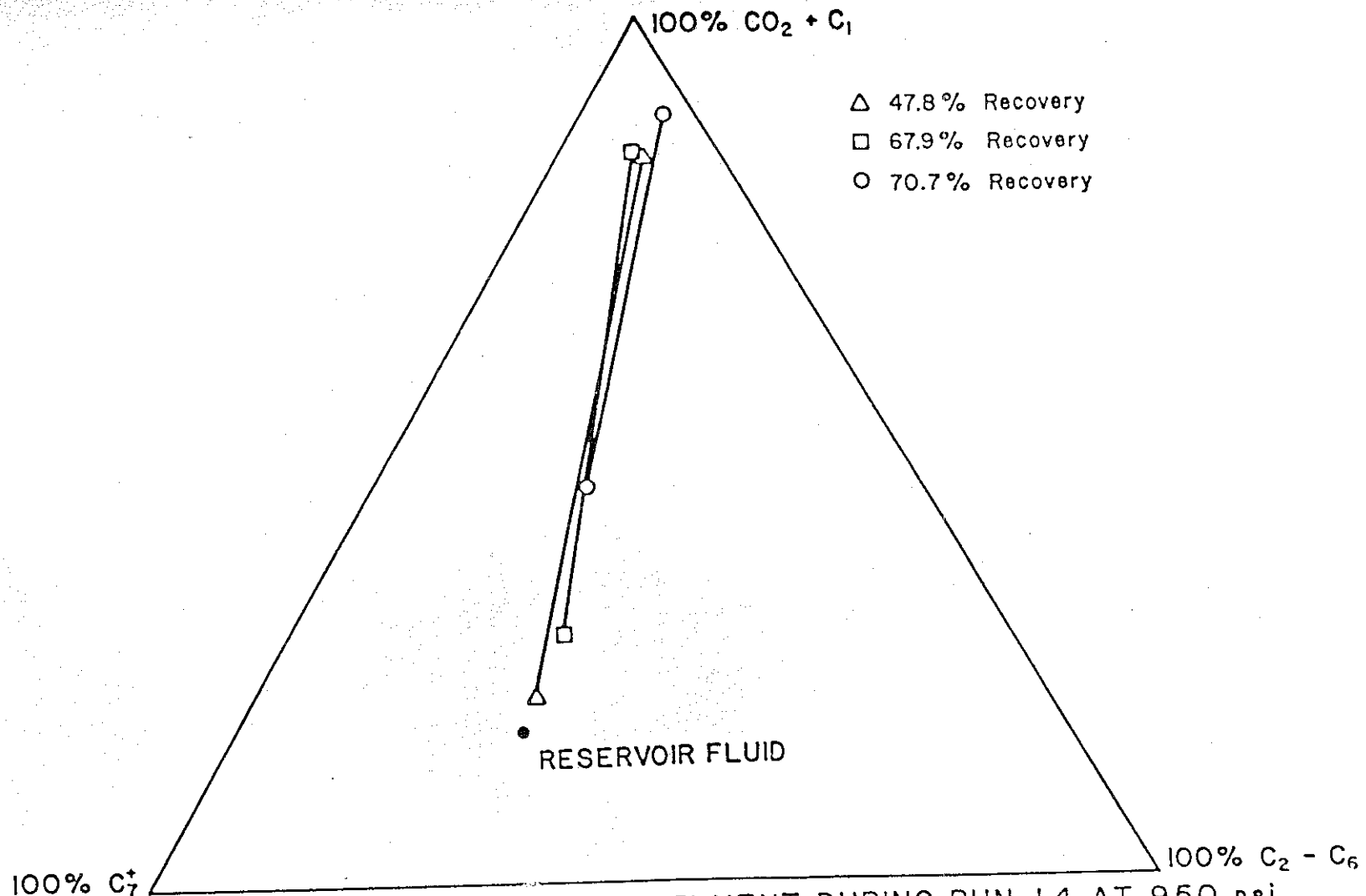

FIGURE 3.13 – COMPOSITION OF EFFLUENT DURING RUN 14 AT 950 psi USING 12.5% CH_4 – CO_2 AS A DISPLACEMENT FLUID

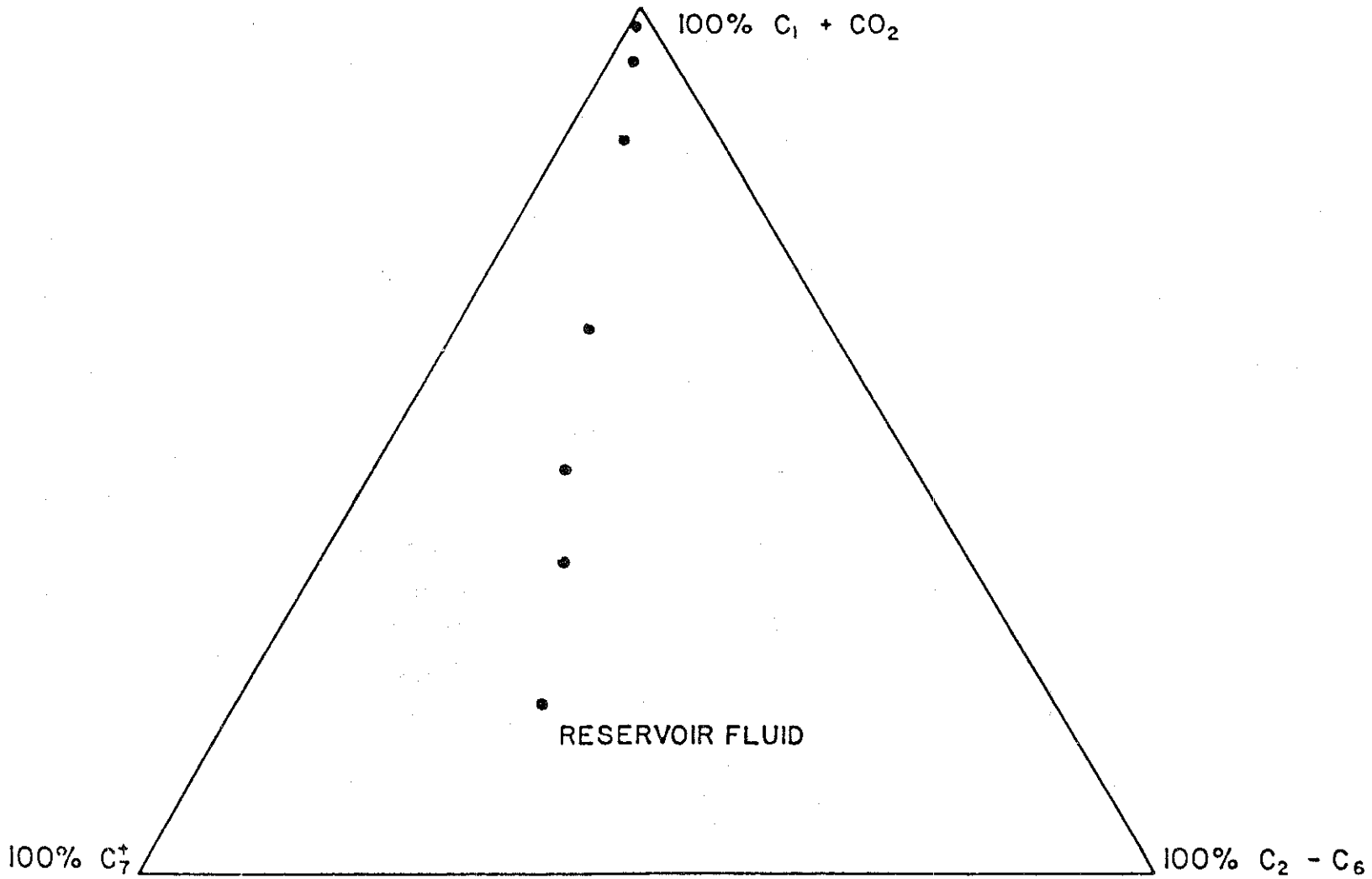

FIGURE 3.14 – COMPOSITION OF EFFLUENT DURING RUN 15 AT 1600 psi USING 12.5% CH_4 – 87.5% CO_2 AS A DISPLACEMENT FLUID

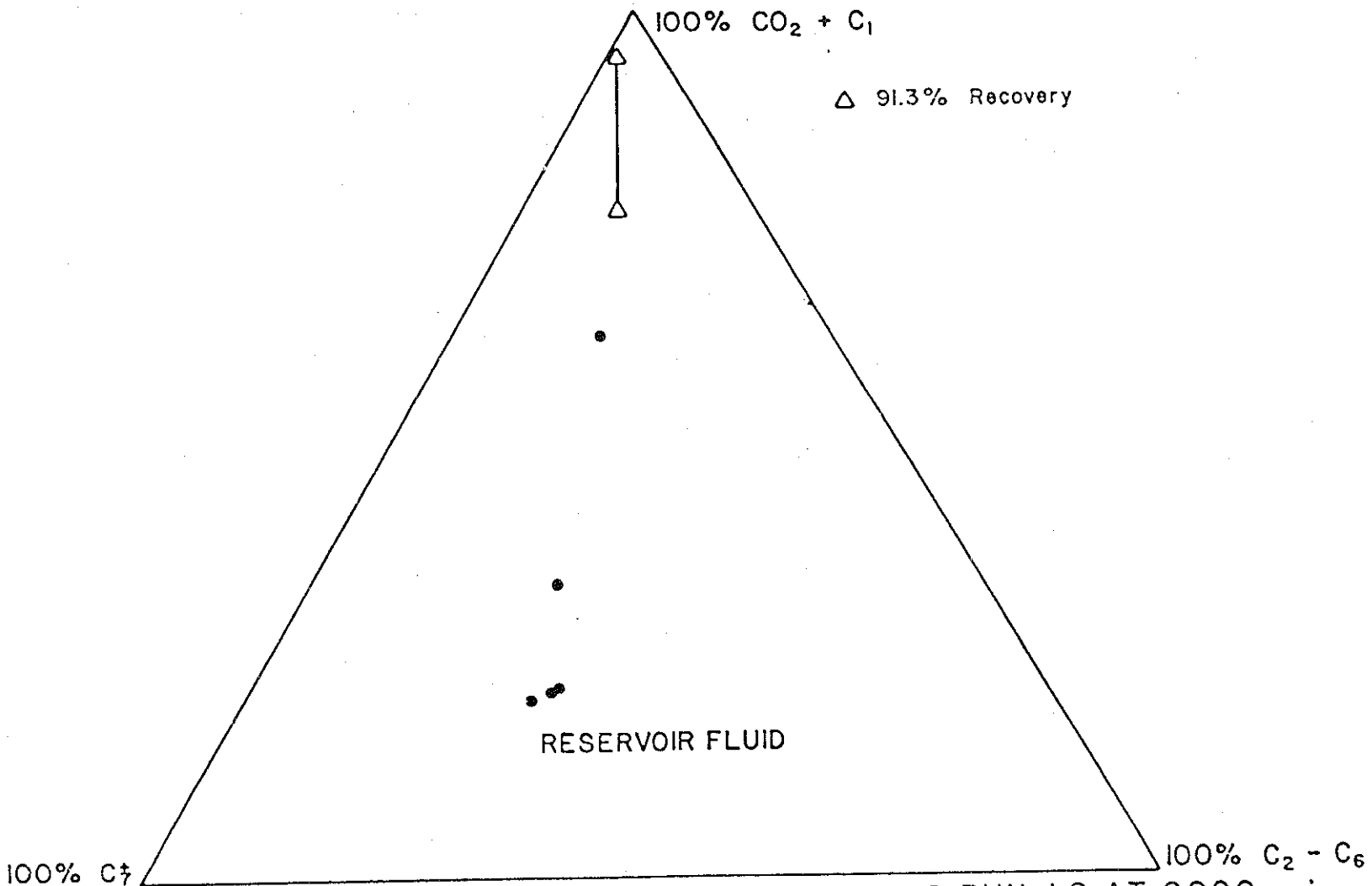

FIGURE 3.15 – COMPOSITION OF EFFLUENT DURING RUN 16 AT 2000 psi USING 25% CH_4 – 75% CO_2 AS A DISPLACEMENT FLUID

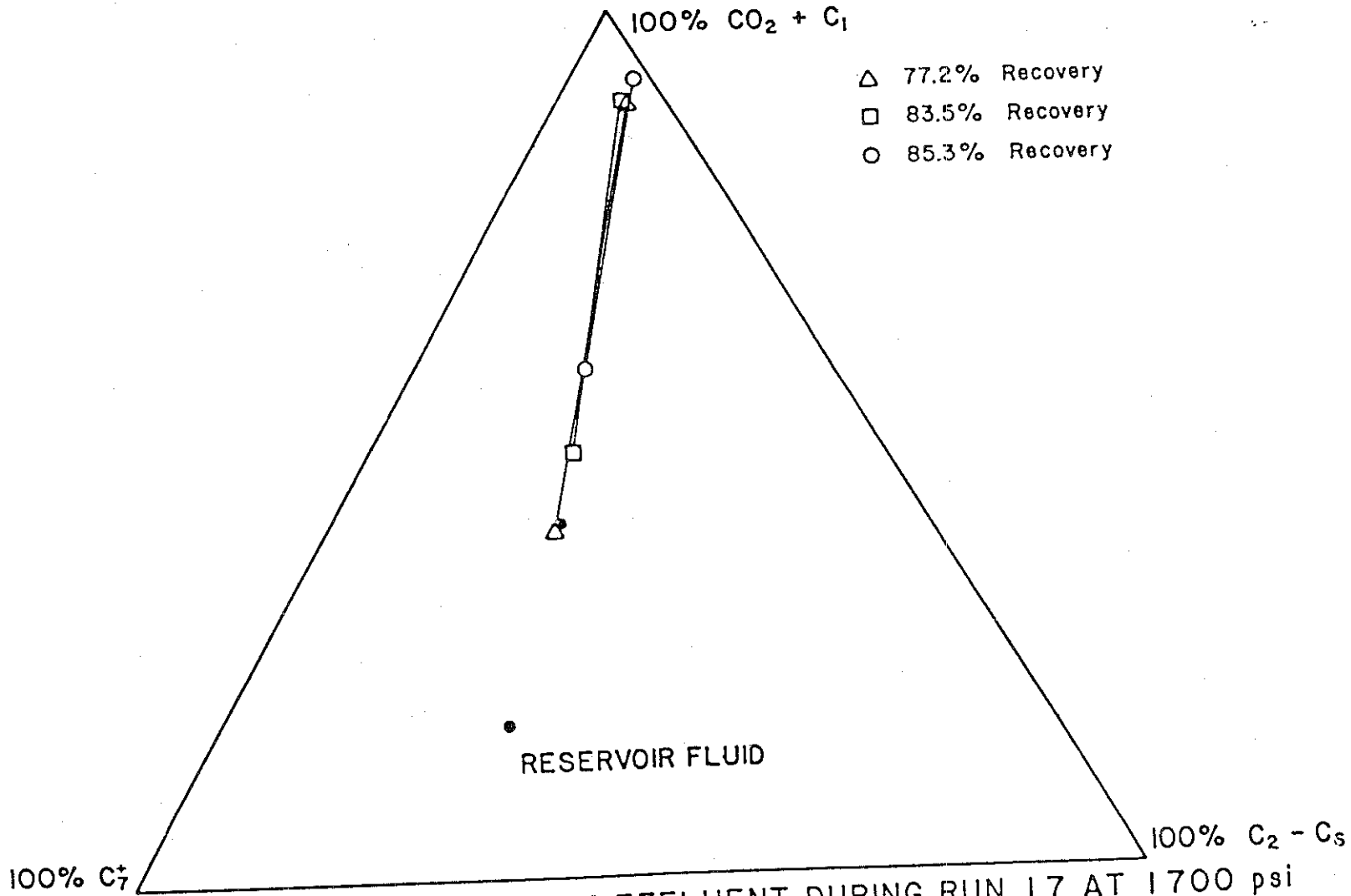

FIGURE 3.16 – COMPOSITION OF EFFLUENT DURING RUN 17 AT 1700 psi USING 25% CH_4 – 75% CO_2 AS A DISPLACEMENT FLUID

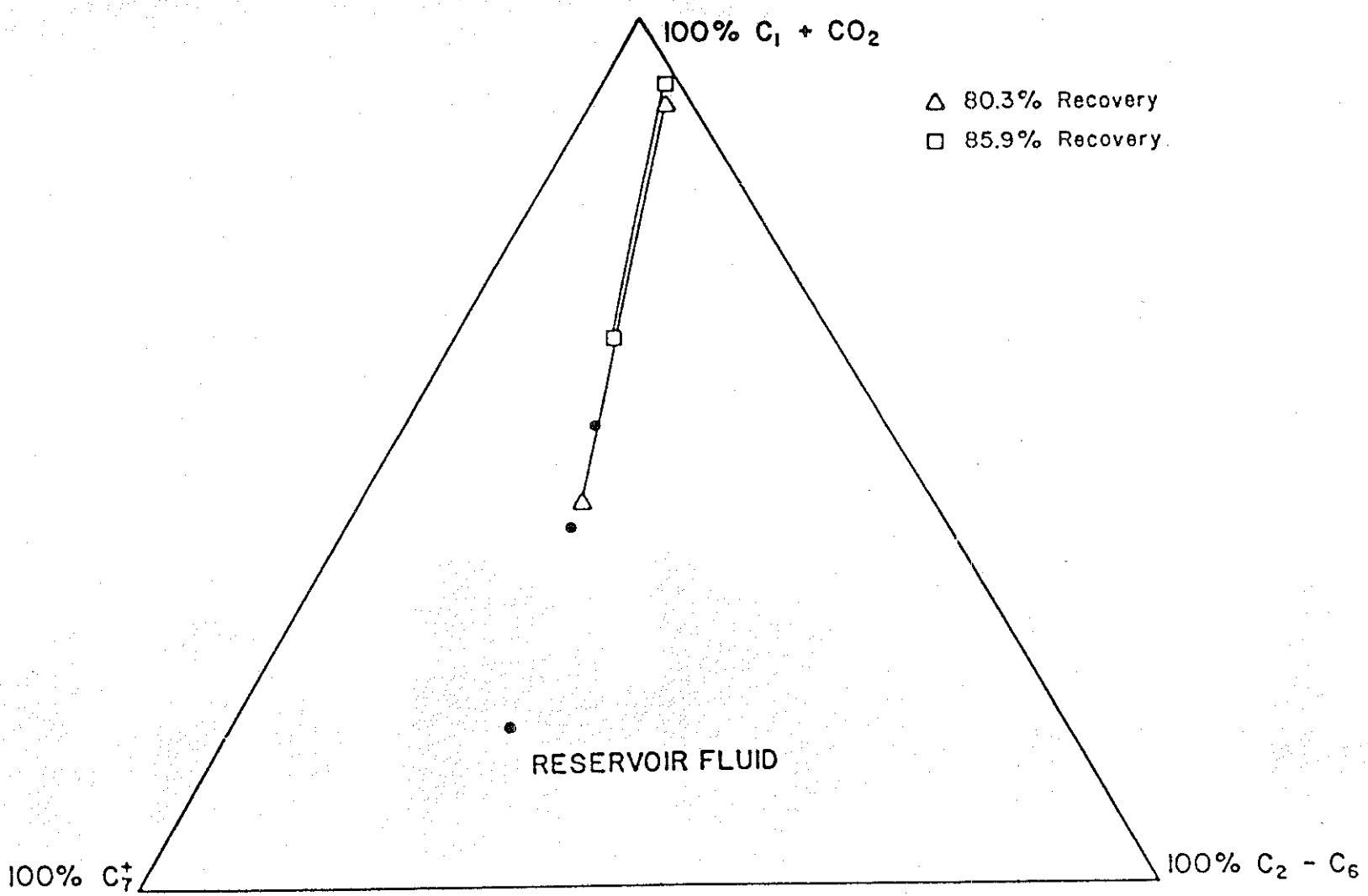

FIGURE 3.17 – COMPOSITION OF EFFLUENT DURING RUN 18 AT 1800 psi USING 25% CH_4 – 75% CO_2 AS A DISPLACEMENT FLUID

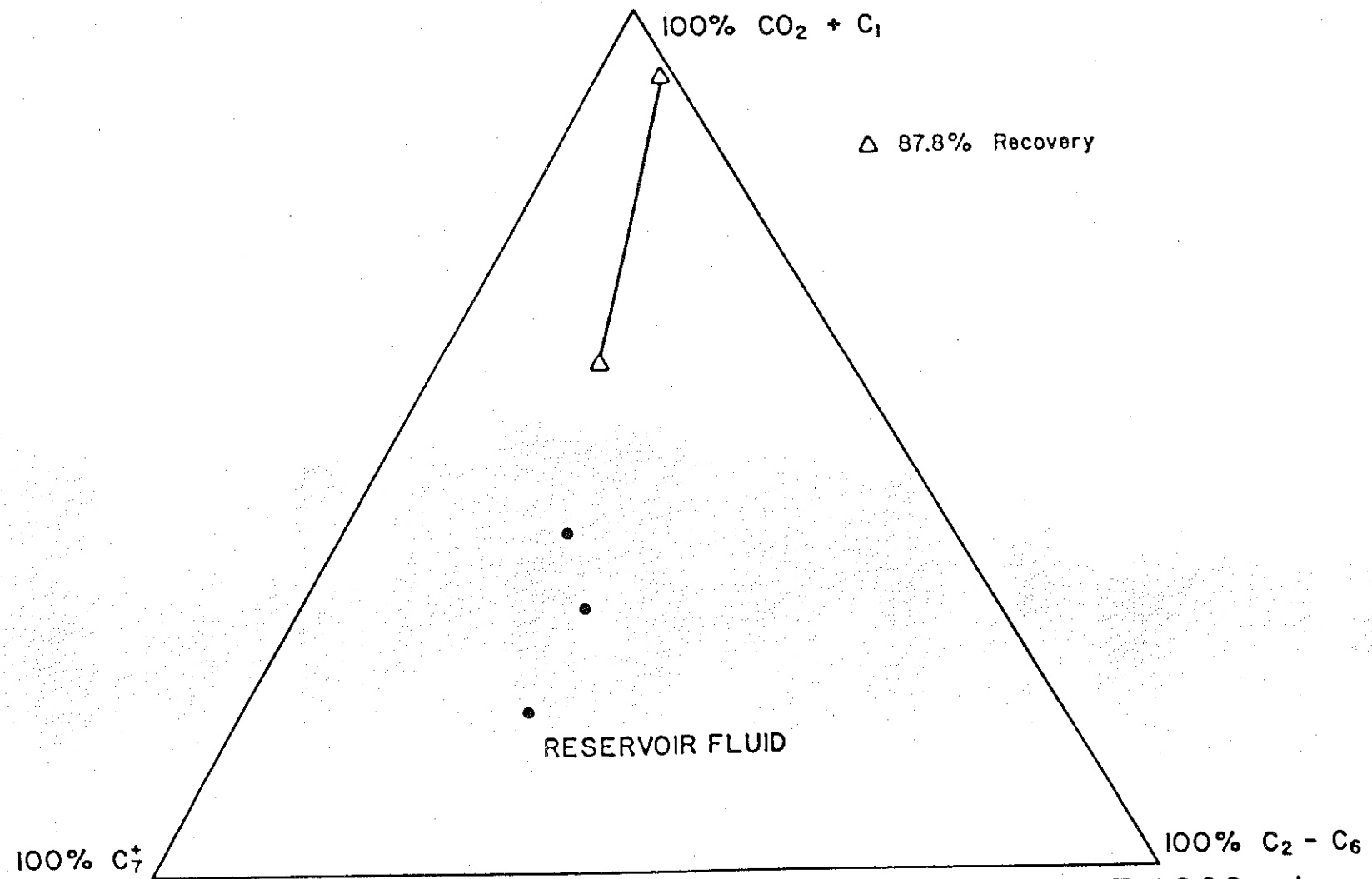

FIGURE 3.18 – COMPOSITION OF EFFLUENT DURING RUN 19 AT 1900 psi
USING 25% CH_4 – 75% CO_2 AS A DISPLACEMENT FLUID

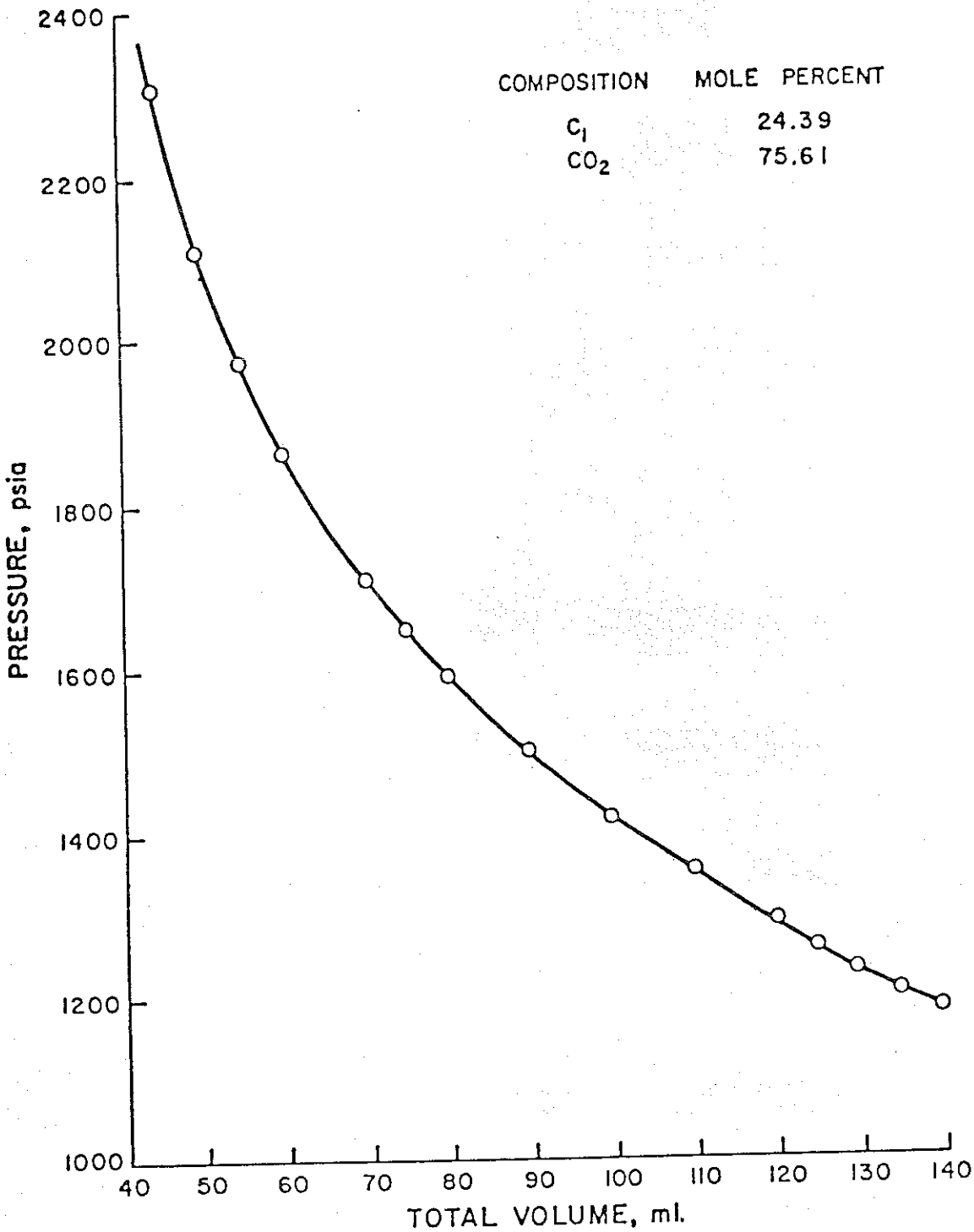

FIGURE 3.19 PRESSURE-VOLUME BEHAVIOR FOR INJECTION FLUID @ 109°F

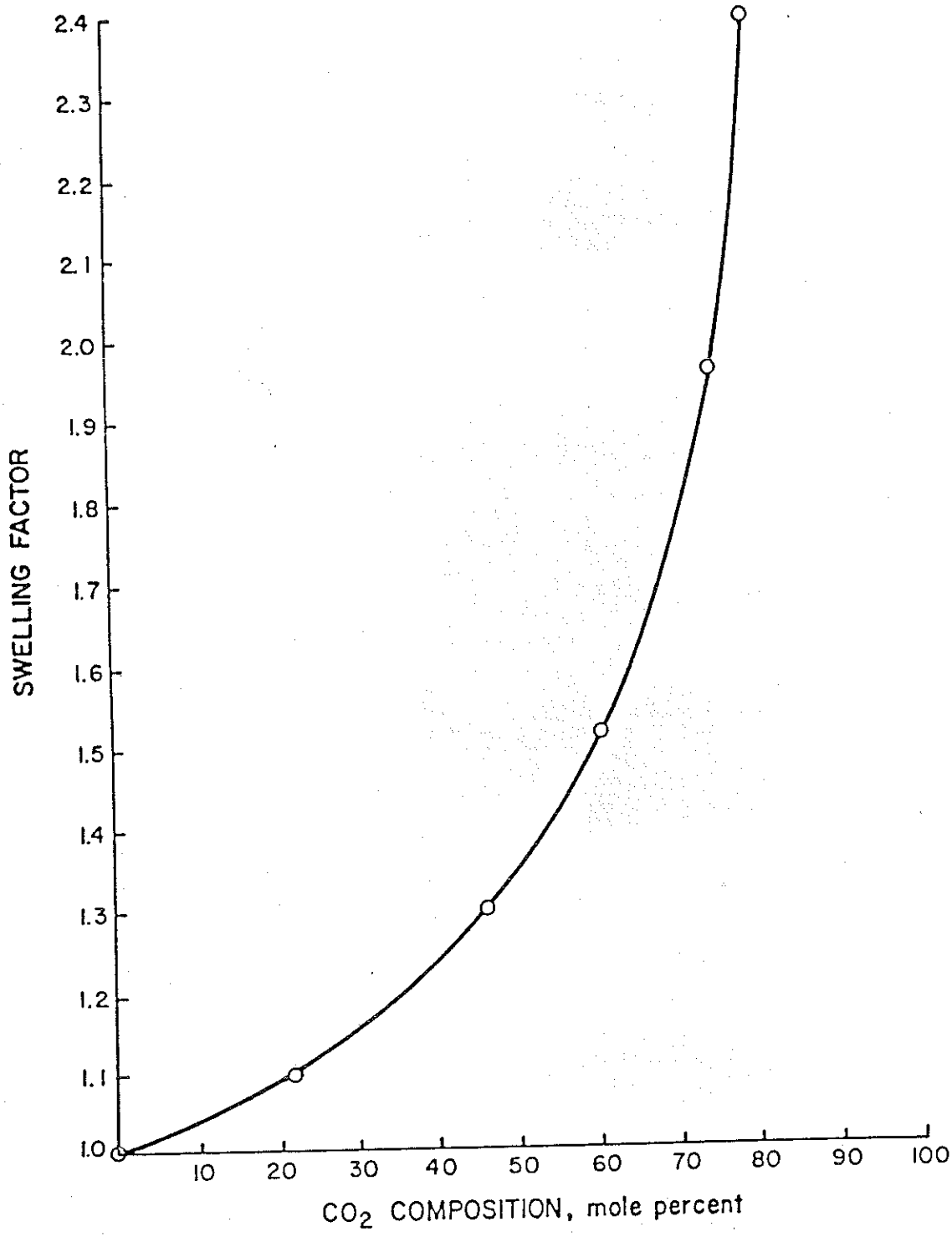

FIGURE 3.20 SWELLING FACTORS FOR MIXTURES OF CO_2 AND RESERVOIR FLUIDS

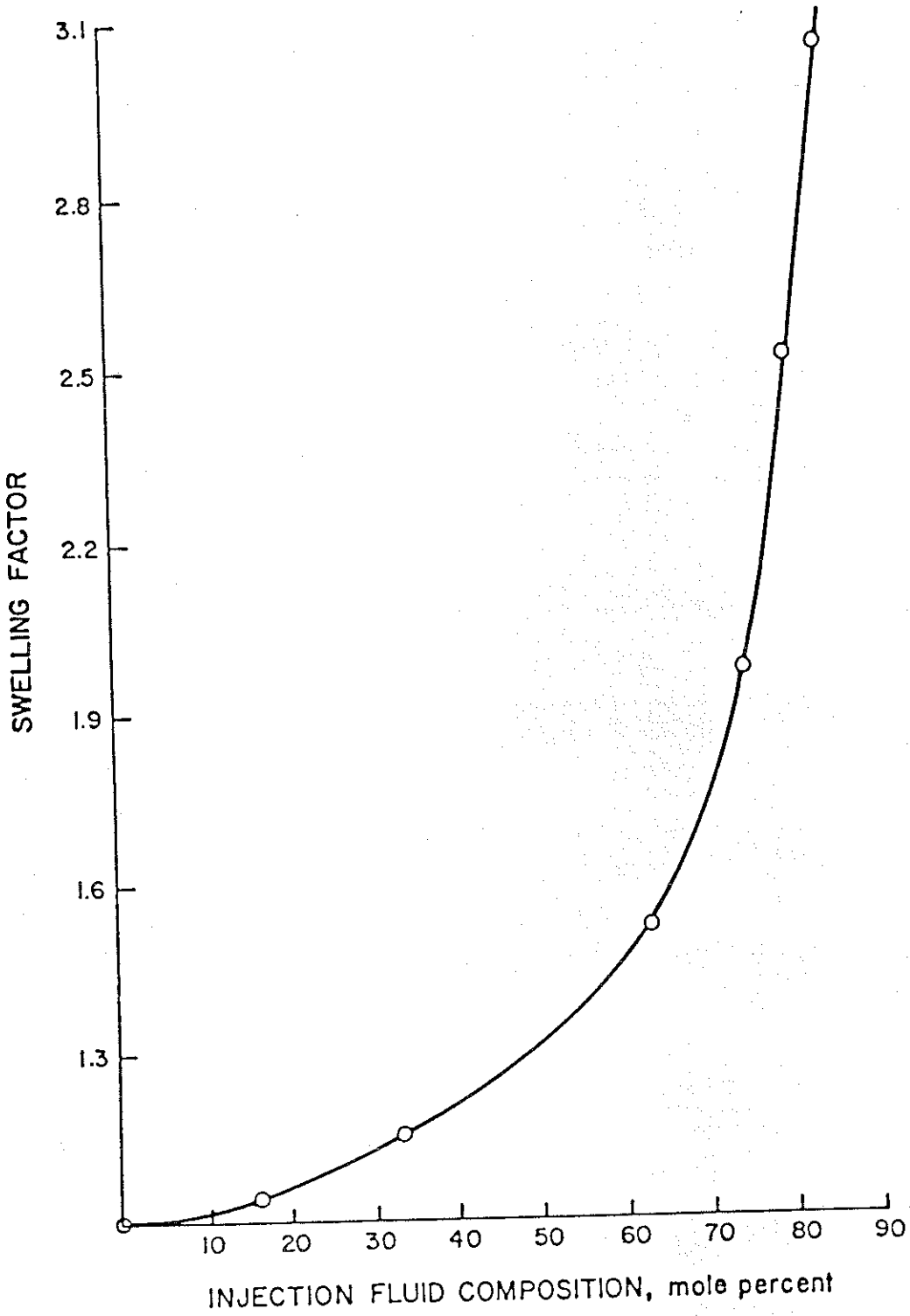

FIGURE 3.21 SWELLING FACTORS FOR MIXTURES OF RESERVOIR FLUID AND INJECTION FLUIDS, 12.76 % C_1H_4 – 87.24 % CO_2

recoveries are obtained in immiscible displacements only slightly below the minimum miscibility pressure and why recovery data alone is a poor criterion for judging whether or not a displacement is miscible.

Pressure-composition diagrams for reservoir fluid-injection fluid systems are presented as Figures 3.22 and 3.23. Figure 3.23 is for an injection fluid composition of 87.13% CO_2 and 12.37% C_1. These figures suggest that first contact miscibility (displacement above the circondenbar) would be expected at displacement pressures in excess of 1225 psig for pure CO_2 and 1725 psig for the CO_2-C_1 mixture.

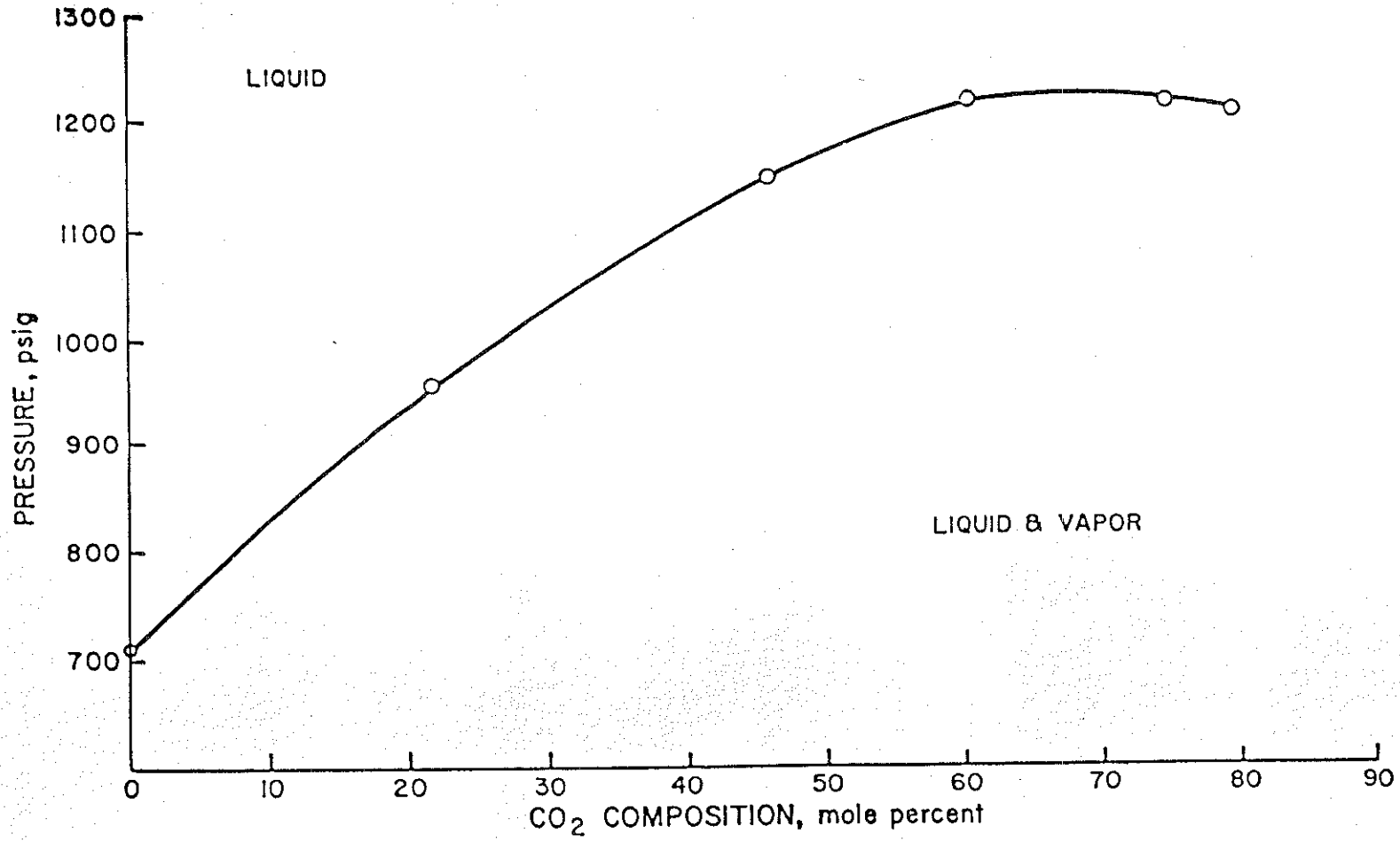

FIGURE 3.22 PRESSURE COMPOSITION DIAGRAM FOR CO_2 AND RESERVOIR FLUID

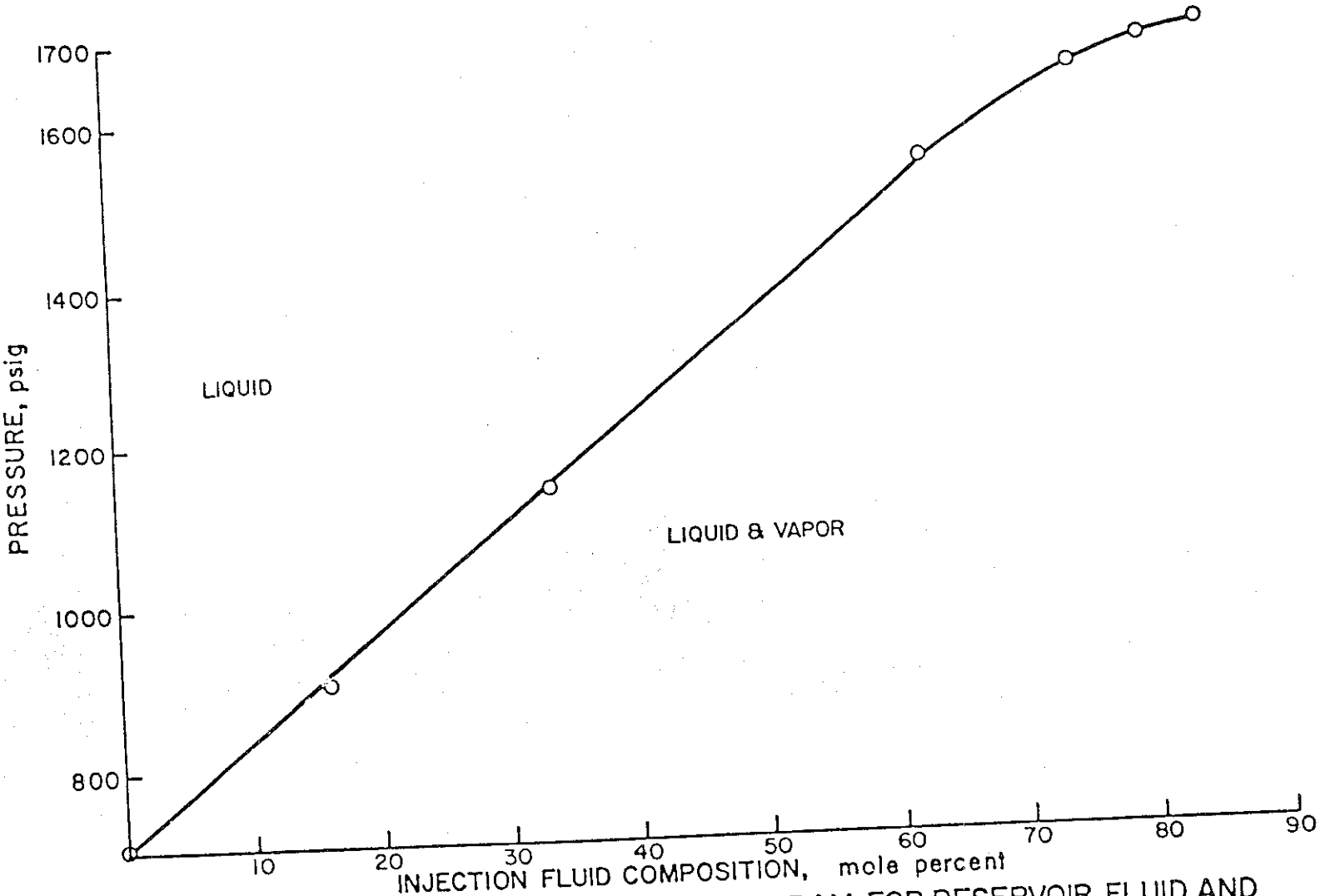

FIGURE 3.23 PRESSURE–COMPOSITION DIAGRAM FOR RESERVOIR FLUID AND INJECTION FLUID, 12.76% C_1H_4– 87.24% CO_2

IV. DISCUSSION OF RESULTS

Minimum Miscibility Pressure

The determination of the pressure at which carbon dioxide can miscibly displace reservoir oil is difficult to determine in that, the viscosity reduction and swelling characteristics of carbon dioxide yield high recoveries even during immiscible floods. This is evidenced by ultimate recoveries of 80.6% during Run 9 and 71.1% during Run 14, both of which were immiscible displacements. Although a direct comparison with carbon dioxide would be invalid, nitrogen only, recovered an average of 55.4% of the Soltrol in place during an immiscible displacement. Immiscible breakthrough recoveries ranges from a minimum of 67.8% with carbon dioxide to 20.8% with nitrogen.

Miscibility pressures were determined using the plots of recovery as a function of displacement pressure Figures 3.1 through 3.3, supplemented by visual and analytical data. Although the recoveries were high, they all exhibited the same general trends; both breakthrough and ultimate recoveries gradually increased then leveled off yielding no additional recovery with pressure increases. The minimum miscibility pressure was chosen as the pressure at the intersection of the extrapolation of the two trends. Visual observations of the phases present in the effluent at breakthrough were very useful in determining miscibility pressure. Two-phase flow at the CO_2 breakthrough was noted in all floods conducted below the MMP (minimum miscibility pressure)

and single phase flow was observed throughout the flood in most of the displacements conducted above the MMP. Interestingly, those runs conducted at pressures slightly higher than the MMP exhibited single phase flow at breakthrough and throughout most of the transition zone, but changed to two phase flow immediately prior to completion of the run.

Figure 4.1 is a plot of minimum miscibility pressure as a function of methane concentration in the injected gas. There is a large gap between 25% and 100% methane where no data were obtained, but it can be seen that an increase in the amount of methane in the injection fluid produced a significant and approximately linear increase in the minimum miscibility pressure. This linearity was somewhat surprising in that it was thought as the concentration of methane in the injected gas increased, not only did the two-phase region as represented on a pseudo-ternary diagram increase, but the slope of the tie lines shifted from a smaller angle to a larger angle with respect to the horizontal axis. Assuming this to be true, the curve connecting the data points in Figure 4.1 would have been concave upward. This was definitely not the case. Furthermore, as can be seen in Figures 3.9 through 3.18, the slopes of the tie lines connecting the vapor phases with liquid phases retain the same slope regardless of the methane concentration in the injected gas.

Increasing the amount of methane in the carbon dioxide also yielded lower breakthrough and ultimate recoveries when

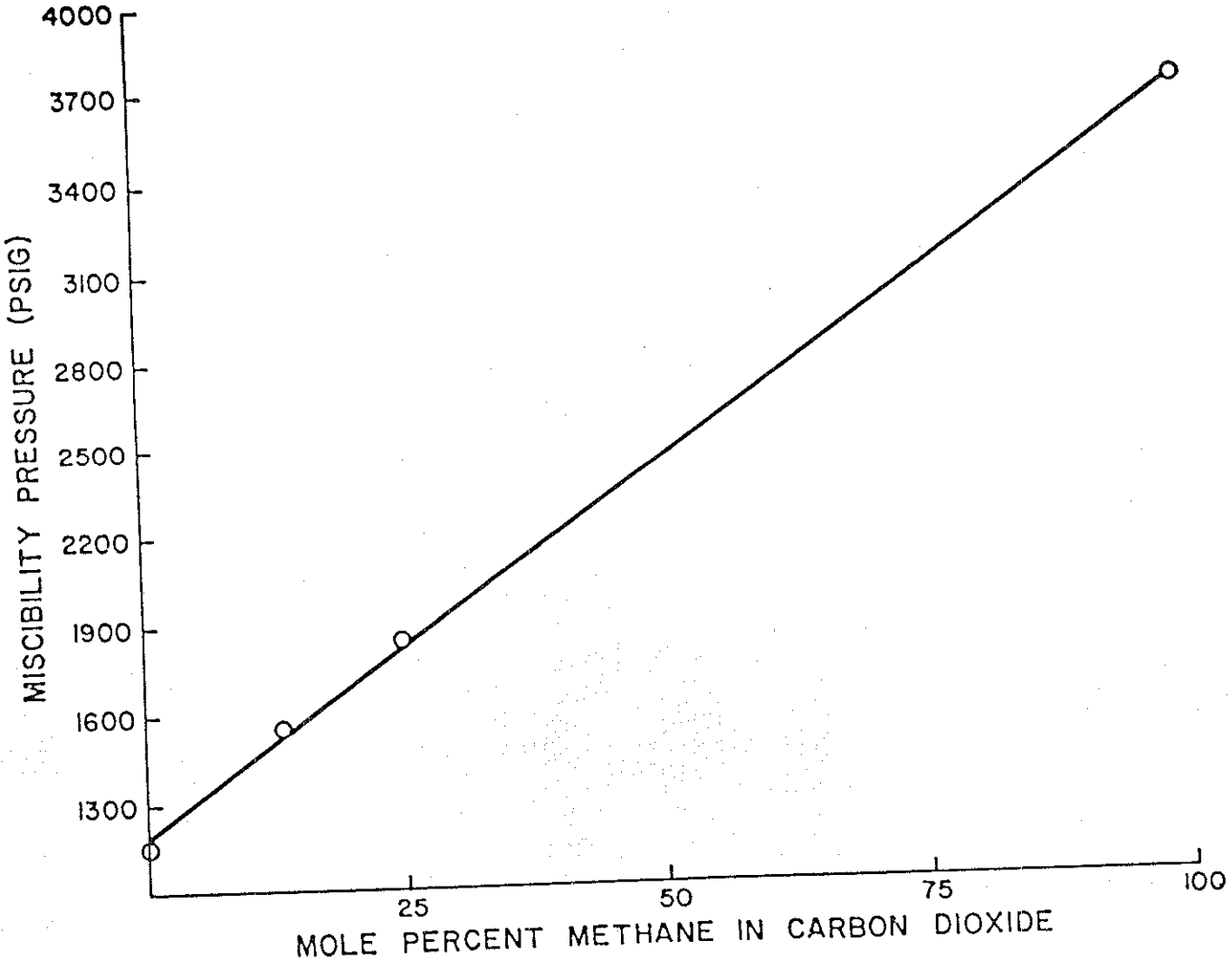

FIGURE 4.1 – MISCIBILITY PRESSURES AS A FUNCTION OF METHANE CONCENTRATION IN DISPLACEMENT FLUID

miscibility was attained. This can be seen in Figure 4.2. These decreasing recoveries are believed to be caused primarily by increased mobility ratios brought about by lower injection fluid viscosities. Very good agreement was attained between recoveries observed in the 20 foot system and recoveries observed in the 40 foot system, as shown in Figure 3.1. During an immiscible displacement, recovery should be constant regardless of system length. However, in displacements where miscibility is developed by multiple contact recoveries should increase with system length. This is because as miscibility is being developed by mass transfer between the carbon dioxide and the in-place fluid, the flood acts as an immiscible displacement with attendant by-passing of oil until miscibility is generated. Once this occurs a longer system will yield better oil recovery. This study shows that miscibility by multiple contacts was readily generated even in the 20 foot system.

Methane Concentration in the Effluent

Increases in methane concentration in the effluent were noted in ten displacements using different injection fluids. This occurred in both miscible and immiscible runs. Typical methane banks are shown in Figures 3.4 through 3.6. Such banks ranged from very large in Run 14 to barely perceptible in Run 15, and occurred during both two-phase flow and as an increased concentration preceding CO_2 breakthrough during displacements which remained single phase throughout.

Of the floods using pure carbon dioxide as the displace-

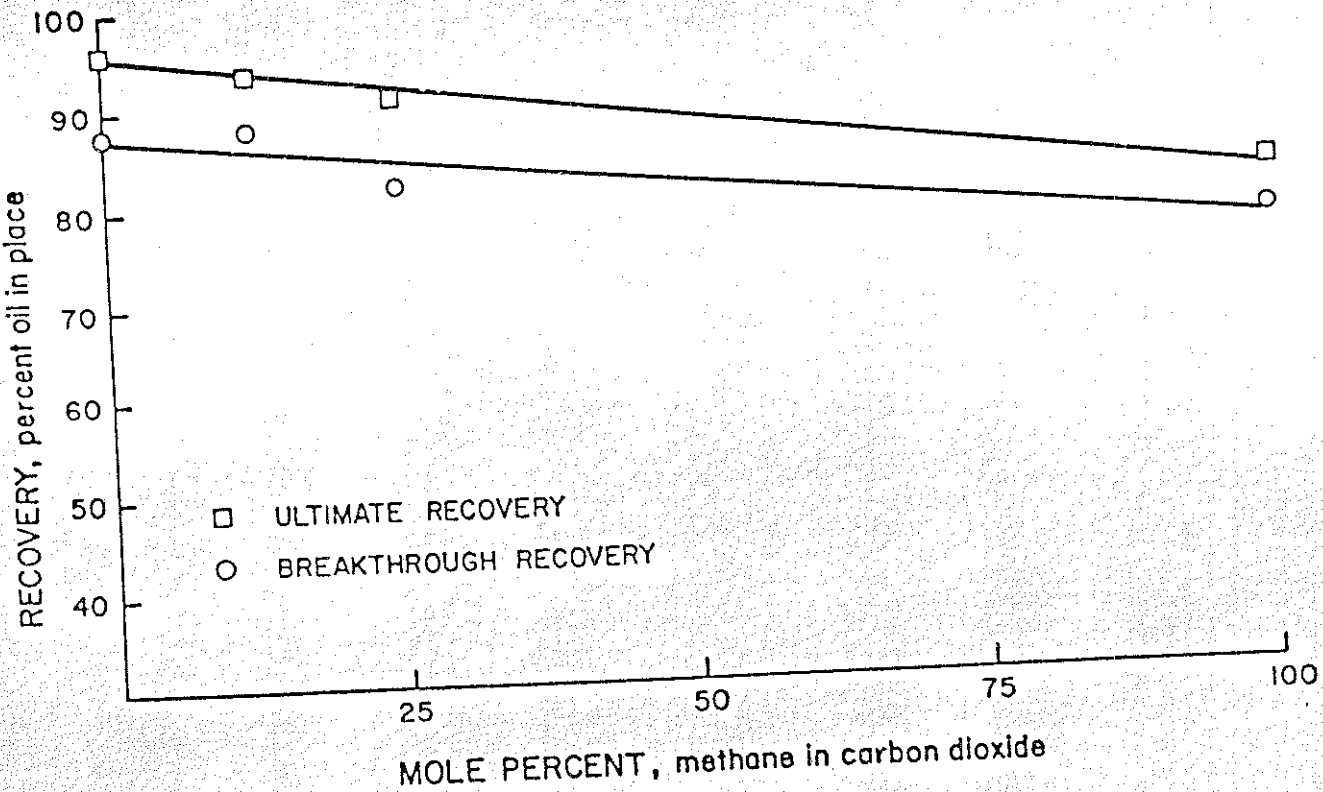

FIGURE 4.2 RECOVERIES AS A FUNCTION OF METHANE CONCENTRATION IN DISPLACEMENT FLUID

ment fluid, Runs 8 and 10, conducted at 1500 and 1300 psi respectively, were judged to exhibit first contact miscibility since these pressures exceeded the cricondenbar. These displacements showed no methane banks while the remaining runs did. In those displacements using the 12.5% methane and 87.5% carbon dioxide mixture as the injected fluid, all runs in which samples were analyzed were conducted at pressures below the cricondenbar and all runs had obvious methane banks. It appears that a methane bank is only generated in those displacements which are either immiscible or in which miscibility was attained by multiple contacts. This indicates that the presence of methane banks should not be used as a criteria to determine miscibility in a flood. For a given system length, as the displacement pressure approaches the cricondenbar the size of the methane bank diminishes.

This phenomenon can be explained in that as miscibility is being generated, carbon dioxide is going into solution in the reservoir oil and subsequently increasing its bubble point pressure. When the bubble point pressure of the new mixture exceeds the displacement pressure, methane will be driven out of the oil. Since the methane is more mobile than the injected carbon dioxide, it moves ahead to contact new oil in which it dissolves. The closer the displacement pressure to the saturation pressure of the original reservoir oil, the less methane can be absorbed by the oil. This results in higher concentration methane banks at lower

displacement pressures and lower concentration banks at higher pressures.

Miscibility Mechanism

It appears likely that no single mechanism is responsible for the generation of miscibility during CO_2 displacements. Previous investigators have proposed both vaporization and condensation as mechanisms and it has been postulated that these may be related to displacement conditions. Since only one oil composition and a single temperature have been investigated to date, no generalizations concerning mechanisms can yet be drawn. The preponderance of data obtained from analyses of samples taken during displacements as well as very limited multiple contact studies in the PVT cell fail to support a vaporization mechanism. Furthermore, although small quantities of the heavier components (C_7+) appear in the CO_2 rich phase the degree of extraction of these materials does not appear to be sufficient to have an effect upon the displacement mechanism. Therefore, our tentative conclusion is that in the present series of runs miscibility has probably been generated through a condensation type mechanism.

V. PROJECT STATUS

Excellent progress has been made on many of the tasks outlined in the original proposal. Unforeseen delays in equipment procurement, obtaining funds for the second year of the project, moving to new facilities, and the development of high-pressure sampling and analysis techniques have caused the project to be several months behind schedule. All equipment for displacing and sampling synthetic crudes in unconsolidated sand packs is operational. Assembly of equipment for conducting displacements in consolidated systems is continuing.

A major obstacle that has been overcome is the development and fabrication of the equipment which allows sampling of reservoir fluid at displacement pressure and temperature. The availability of this equipment should expedite the remaining work on the project. Chromatographic techniques for analyzing samples taken during displacement of synthetic crudes have been perfected. Work is continuing on developing satisfactory techniques for analyzing samples that will be taken during displacements of actual crudes. A crude from the Brookhaven, Mississippi Field has been obtained and is being used in the development of the analysis technique. This crude will also be used for displacement studies.

APPENDIX A

SAND AND FLUID PROPERTIES

Table A.1

Grain Size Distribution of Sand Used

In Unconsolidated Sand Packs

Particle Diameter (microns)	Distribution (Weight Percent)
>210	0.0
210-105	80.5
105-88	16.5
88-74	1.5
< 74	1.5

Table A-2

Purity of Hydrocarbon Components

Component	Purity Mole Percent
Carbon Dioxide*	99.9
Methane*	95.9
Ethane*	95.9
Propane*	95.9
n- Butane*	99.5
n- Pentane**	95.9
n- Hexane**	95.9
n- Heptane**	99.8
n- Octane**	99.9
n- Nonane**	99.9
n- Decane**	99.9
Soltrol***	99.9

*Obtained from Matheson Gas Products of Gonzales, Louisiana
**Obtained from Chemical Sample Company of Columbus, Ohio
***Obtained from Phillips Petroleum Company of Bartlesville, Oklahoma

Table B.1

Table of Fluid Compositions
(Mole %)

Run	Pressure	Percent Recovery	Phase	C_1	C_2	C_3	C_4	C_5	C_6	C_7	C_8	C_9	C_{10}	Soltrol	CO_2
3	1100	3.4	liquid	18.75	6.95	7.02	6.22	2.46	4.81	6.77	6.79	5.75	5.28	29.20	—
3	1100	80.9	liquid	25.08	7.03	6.77	5.94	2.29	4.48	8.18	6.35	5.39	4.87	23.59	0.02
3	1100	86.4	gas	0.66	1.45	2.19	1.11	0.32	0.53	0.73	0.69	0.55	0.48	2.31	88.99
4	1850	47.0	liquid	19.96	7.35	7.30	6.56	2.66	5.15	7.17	7.10	6.02	5.48	25.27	—
4	1850	76.6	liquid	15.00	5.34	5.19	4.58	1.83	3.51	4.97	4.95	4.24	3.94	17.45	29.01
4	1850	91.4	gas	2.34	1.03	1.06	1.00	0.43	0.89	1.35	1.46	1.22	1.22	7.40	80.62
5	1200	37.8	liquid	17.51	6.64	6.96	6.51	2.67	5.27	7.46	7.44	6.15	5.79	27.60	—
5	1200	90.8	liquid	16.05	5.93	5.95	5.27	2.15	4.13	5.84	5.83	4.97	4.55	22.21	17.13
5	1200	96.0	gas	0.87	0.86	1.13	0.80	0.26	0.43	0.58	0.62	0.50	0.52	1.88	91.55
7	1200	42.4	liquid	16.13	6.27	6.86	6.58	2.80	5.36	7.52	7.74	6.41	5.90	28.42	—
7	1200	87.5	liquid	16.65	6.33	6.85	6.38	2.67	5.08	7.15	7.41	6.20	6.50	28.79	—
7	1200	91.9	liquid	19.30	6.17	5.16	4.20	1.65	3.04	4.21	4.31	3.59	3.65	16.47	28.26
7	1200	93.7	liquid	7.71	3.51	1.70	0.69	0.18	0.28	0.36	0.36	0.04	0.09	1.24	83.96
7	1200	94.9	gas	0.95	2.10	1.74	1.44	0.52	1.52	1.03	0.84	0.65	0.09	2.40	86.71
8	1500	10.3	liquid	17.55	6.76	7.13	6.46	2.70	5.10	7.19	7.50	6.24	6.17	27.21	—
8	1500	86.5	liquid	16.06	6.19	6.57	6.07	2.53	4.75	6.79	7.27	6.07	5.63	27.29	4.79
8	1500	88.5	liquid	14.49	5.41	5.45	4.95	2.09	3.01	5.59	6.01	5.03	4.55	23.41	19.12
8	1500	89.6	liquid	12.88	4.79	4.82	4.36	1.84	3.47	4.98	5.33	4.42	4.04	21.53	27.53
8	1500	91.8	liquid	9.93	3.68	3.66	3.23	1.35	2.54	3.66	3.92	3.29	3.24	16.79	44.70
8	1500	93.2	liquid	6.10	2.40	2.47	2.19	0.93	1.77	2.58	2.80	2.35	2.16	12.54	61.71
9	1000	6.6	liquid	18.18	6.96	7.05	6.13	2.48	4.73	6.47	7.01	5.94	5.49	29.56	—
9	1000	60.3	liquid	17.30	6.69	6.99	6.38	2.64	4.95	6.93	7.44	6.20	6.11	28.39	—
9	1000	68.5	liquid	24.47	6.88	6.69	5.88	2.40	4.48	6.38	6.82	5.70	5.28	25.02	—
9	1000	68.5	liquid	25.38	6.14	5.88	5.35	2.30	4.39	6.35	6.83	5.70	5.58	26.10	—
9	1000	69.1	gas	85.00	5.64	1.71	0.58	0.23	0.43	0.74	0.78	0.79	0.78	3.33	—
9	1000	80.6	liquid	11.50	7.16	5.27	4.31	1.76	3.29	4.69	5.07	4.37	4.41	19.80	28.39
9	1000	80.6	liquid	2.13	6.91	4.32	3.47	1.43	2.68	3.82	4.09	3.43	3.11	15.10	49.52
9	1000	80.6	gas	1.57	7.68	3.82	2.28	0.76	1.29	1.73	1.75	1.43	1.39	6.23	70.11

Table B.1 Continued

Run	Pressure	Percent Recovery	Phase	C_1	C_2	C_3	C_4	C_5	C_6	C_7	C_8	C_9	C_{10}	Soltrol	CO_2
10	1300	50.0	liquid	15.91	6.22	6.66	6.14	2.55	5.08	7.56	8.99	6.92	6.69	27.08	—
10	1300	73.2	liquid	17.35	6.69	7.07	6.50	2.69	5.10	7.05	7.52	6.32	5.90	27.80	—
10	1300	88.7	liquid	15.30	5.81	6.14	5.66	2.41	4.63	6.45	6.79	5.52	5.17	23.94	12.18
10	1300	90.6	liquid	12.61	4.85	5.10	4.70	2.00	3.74	5.24	5.56	4.63	4.40	20.95	26.23
10	1300	92.9	liquid	9.35	3.64	3.74	3.36	1.41	2.67	3.71	3.97	3.28	3.19	15.22	46.45
10	1300	94.7	liquid	5.33	2.20	2.33	2.24	1.06	2.14	2.71	3.07	2.58	2.29	11.06	62.98
12	1500	47.8	liquid	17.11	6.48	6.72	6.28	2.62	5.04	7.00	7.67	6.33	5.89	28.86	—
12	1500	84.6	liquid	28.68	6.21	5.80	5.20	2.11	4.00	5.55	5.84	4.79	4.58	20.11	7.14
12	1500	84.6	gas	66.13	3.90	1.30	0.72	0.20	0.26	0.77	1.01	0.89	1.02	10.05	13.75
12	1500	88.5	liquid	20.56	4.87	4.70	4.34	1.79	3.43	4.76	4.96	4.06	3.89	17.02	25.62
12	1500	91.2	liquid	13.09	2.46	2.33	1.77	0.63	1.06	1.63	1.79	1.56	1.56	9.87	62.26
13	1400	13.2	liquid	21.41	8.29	8.70	7.31	2.63	4.73	6.36	6.62	5.39	5.19	23.38	—
13	1400	77.9	liquid	30.58	6.63	6.58	5.86	2.25	4.25	5.80	6.10	5.01	4.84	22.12	—
13	1400	77.9	gas	86.62	4.52	1.42	0.63	0.24	0.48	0.77	0.83	0.67	0.61	3.16	—
13	1400	83.2	liquid	27.58	6.73	6.27	5.36	2.01	3.75	5.16	5.42	4.45	4.30	19.51	9.46
13	1400	83.2	gas	45.94	3.86	1.38	0.61	0.20	0.37	0.56	0.60	0.48	0.42	2.03	43.53
13	1400	86.6	liquid	19.64	5.32	4.67	3.81	1.45	2.74	3.71	3.87	3.14	3.00	14.19	34.48
13	1400	88.1	liquid	11.69	2.05	2.22	1.26	0.35	0.59	0.75	0.76	0.61	0.56	2.64	76.53
14	950	23.5	liquid	17.68	6.76	7.51	6.98	2.66	4.97	6.77	7.19	5.91	5.71	27.87	—
14	950	47.8	gas	83.68	5.53	1.80	0.76	0.29	0.60	0.91	0.98	0.78	0.67	4.02	—
14	950	47.8	liquid	21.65	6.88	7.30	6.64	2.56	4.79	6.50	6.78	5.59	5.44	25.86	—
14	950	67.9	liquid	27.31	7.62	7.27	6.09	2.23	4.15	5.69	5.93	4.86	4.67	22.82	1.35
14	950	67.9	gas	82.24	5.28	1.40	0.47	0.18	0.32	0.92	0.98	0.90	0.65	4.73	1.95
14	950	70.7	gas	30.16	6.43	1.49	0.38	0.08	0.12	0.35	0.35	0.32	0.23	1.79	58.30
14	950	70.7	liquid	8.17	7.42	5.43	4.34	1.64	3.10	4.22	4.45	3.66	3.53	17.06	36.98
15	1600	57.4	liquid	19.64	7.60	8.02	7.00	2.61	4.80	6.49	6.76	5.56	5.37	26.16	—
15	1600	86.0	liquid	20.04	6.37	6.43	5.56	2.06	3.80	5.16	5.38	4.41	4.27	20.59	15.93
15	1600	87.2	liquid	16.64	4.63	4.94	4.50	1.74	3.27	4.49	4.67	3.81	3.68	17.56	30.11
15	1600	90.0	liquid	16.49	3.35	3.45	3.07	1.19	2.36	3.11	3.36	2.67	2.55	12.22	46.39
15	1600	92.1	liquid	17.08	1.78	1.68	1.42	0.51	0.98	1.28	1.31	1.05	0.97	4.62	67.36
15	1600	92.6	gas	15.21	0.77	0.76	0.65	0.23	0.41	0.54	0.54	0.41	0.36	1.71	78.42
15	1600	93.5	gas	12.02	0.00	0.03	0.10	0.06	0.11	0.19	0.16	0.00	0.10	0.75	86.51

Table B.1 Continued

Run	Pressure	Percent Recovery	Phase	C_1	C_2	C_3	C_4	C_5	C_6	C_7	C_8	C_9	C_{10}	Soltrol	CO_2
16	2000	23.5	liquid	20.10	7.67	7.96	6.76	2.46	3.98	6.53	6.80	5.60	5.44	26.71	—
16	2000	38.2	liquid	21.16	8.09	8.38	7.10	2.59	4.22	6.33	6.59	5.41	5.22	24.91	—
16	2000	82.4	liquid	21.51	8.17	8.47	7.17	2.60	4.21	6.29	6.51	5.35	5.10	24.53	0.09
16	2000	85.5	liquid	22.23	6.44	6.70	5.77	2.13	3.50	5.35	5.62	4.63	4.46	21.45	11.70
16	2000	89.4	liquid	27.93	4.34	4.17	3.38	1.21	1.95	2.95	3.09	2.56	2.43	11.82	34.17
16	2000	91.3	gas	40.25	2.44	1.56	0.76	0.16	0.05	0.21	0.18	0.12	0.08	0.47	53.73
16	2000	91.3	liquid	24.74	2.69	2.71	2.28	0.85	1.37	2.03	2.00	1.57	1.42	6.53	51.81
17	1700	23.5	liquid	16.05	6.24	6.86	6.31	2.45	4.15	6.52	7.08	5.99	5.94	32.42	—
17	1700	42.9	liquid	17.31	6.84	7.70	7.09	2.70	4.48	6.80	7.17	5.95	5.80	28.17	—
17	1700	77.2	liquid	39.61	6.67	6.21	5.15	1.89	3.09	4.70	4.96	4.12	4.00	19.61	—
17	1700	77.2	gas	88.81	4.54	1.58	0.59	0.17	0.07	0.49	0.51	0.46	0.42	2.37	—
17	1700	80.0	liquid	39.09	7.09	6.21	4.95	1.80	2.99	4.59	4.85	4.02	3.87	18.92	1.62
17	1700	83.5	liquid	33.65	6.29	5.46	4.37	1.58	2.60	3.95	4.18	3.47	3.34	15.96	15.18
17	1700	83.5	gas	69.37	4.22	1.52	0.66	0.22	0.10	0.61	0.63	0.49	0.41	1.90	19.87
17	1700	85.3	liquid	24.95	5.27	4.64	3.62	1.33	2.18	3.27	3.37	2.77	2.61	12.64	33.36
17	1700	85.3	gas	51.77	4.00	1.65	0.63	0.16	0.06	0.35	0.34	0.25	0.21	0.72	39.88
18	1800	23.2	liquid	20.58	7.70	7.81	6.56	2.40	3.92	5.98	6.35	5.31	5.17	28.21	—
18	1800	39.3	liquid	18.28	7.07	7.65	6.78	2.53	4.14	6.28	6.59	5.47	5.36	29.85	—
18	1800	80.3	liquid	42.85	6.81	5.89	4.64	1.66	3.01	4.06	4.23	3.50	3.32	19.13	0.90
18	1800	80.3	gas	88.57	4.51	1.63	0.55	0.19	0.31	0.48	0.48	0.37	0.30	1.40	1.10
18	1800	82.1	liquid	37.15	6.50	5.94	5.03	1.88	3.07	4.64	4.85	4.01	3.81	18.52	4.60
18	1800	84.4	liquid	31.07	5.98	5.28	4.16	1.49	2.38	3.59	3.72	3.08	2.91	14.16	22.19
18	1800	85.9	liquid	25.58	4.71	4.36	3.48	1.24	1.97	2.91	2.96	2.42	2.25	10.86	37.26
18	1800	85.9	gas	48.21	3.68	1.73	0.66	0.14	0.19	0.26	0.22	0.17	0.11	0.50	44.13
19	1900	25.5	liquid	21.78	8.10	8.11	6.75	2.46	4.00	6.05	6.44	5.43	5.24	25.66	—
19	1900	41.3	liquid	18.60	7.19	7.77	6.93	2.61	4.32	6.63	7.04	5.85	5.66	27.42	—
19	1900	82.6	liquid	27.84	6.91	6.91	5.93	2.21	3.66	5.59	5.89	4.89	4.68	22.69	2.80
19	1900	85.3	liquid	31.26	6.38	6.09	5.16	1.92	3.16	4.86	5.13	4.24	4.04	19.67	8.09
19	1900	87.8	liquid	29.63	4.99	4.45	3.48	1.24	2.03	3.16	3.35	2.79	2.63	12.74	29.47
19	1900	87.8	gas	56.98	3.82	1.72	0.70	0.16	0.30	0.34	0.30	0.14	0.06	0.42	35.34

Table B.2

Fluid Compositions with Injected Gas Removed

(Mole %)

Run	Pressure	Injected Gas Composition	Percent Recovery	C_1	C_2	C_3	C_4	C_5	C_6	C_7	C_8	C_9	C_{10}	Soltrol
3	1100	CO_2	3.4	18.75	6.95	7.02	6.22	2.46	4.81	6.77	6.79	5.75	5.28	29.20
3	1100	CO_2	80.9	25.09	7.03	6.77	5.94	2.29	4.48	8.18	6.35	5.39	4.87	23.60
3	1100	CO_2	86.4	5.99	13.17	19.89	10.08	2.91	4.82	6.63	6.27	5.00	4.36	20.98
4	1850	CO_2	47.0	19.96	7.35	7.30	6.56	2.66	5.15	7.17	7.10	6.03	5.48	25.27
4	1850	CO_2	76.6	21.13	7.52	7.31	6.45	2.58	4.94	7.01	6.97	5.97	5.55	24.58
4	1850	CO_2	91.4	12.07	5.31	5.47	5.16	2.22	4.59	6.97	7.53	6.30	6.30	38.18
5	1200	CO_2	37.8	17.51	6.64	6.96	6.51	2.67	5.27	7.46	7.44	6.15	5.79	27.60
5	1200	CO_2	90.8	19.37	7.16	7.18	6.36	2.59	4.98	7.05	7.04	6.00	5.49	26.80
5	1200	CO_2	96.0	10.29	10.13	13.41	9.47	3.02	5.12	6.88	7.39	5.93	6.10	22.26
7	1200	CO_2	42.4	16.13	6.27	6.86	6.58	2.80	5.36	7.52	7.74	6.41	5.90	28.42
7	1200	CO_2	87.5	16.65	6.33	6.85	6.38	2.67	5.08	7.15	7.41	6.20	6.50	28.79
7	1200	CO_2	91.9	26.90	8.60	7.19	5.85	2.30	4.23	5.86	6.01	5.01	5.09	22.96
7	1200	CO_2	93.7	48.05	21.90	10.60	4.27	1.12	1.74	2.27	2.23	0.02	0.05	7.75
7	1200	CO_2	94.9	7.18	15.82	13.07	10.85	3.88	11.44	7.78	6.31	4.92	0.71	18.05
8	1500	CO_2	10.3	17.55	6.76	7.13	6.46	2.70	5.10	7.19	7.50	6.24	6.17	27.21
8	1500	CO_2	86.5	16.87	6.50	6.90	6.37	2.65	4.99	7.14	7.63	6.28	5.91	28.66
8	1500	CO_2	88.5	17.92	6.69	6.74	6.11	2.58	4.83	6.91	7.43	6.22	5.63	28.94
8	1500	CO_2	89.6	17.71	6.61	6.65	6.02	2.54	4.79	6.87	7.35	6.10	5.58	29.71
8	1500	CO_2	91.8	17.96	6.66	6.61	5.86	2.44	4.59	6.62	7.09	5.94	5.86	30.37
8	1500	CO_2	93.2	15.93	6.27	6.46	5.71	2.43	4.74	6.73	7.31	6.13	5.64	32.76
9	1000	CO_2	6.6	18.18	6.96	7.05	6.13	2.48	4.73	6.47	7.01	5.94	5.49	29.56
9	1000	CO_2	60.3	17.30	6.69	6.99	6.38	2.64	4.95	6.93	7.44	6.20	6.11	28.39
9	1000	CO_2	68.5	24.47	6.88	6.69	5.88	2.40	4.48	6.38	6.82	5.70	5.28	25.02
9	1000	CO_2	68.5	25.38	6.14	5.88	5.35	2.30	4.39	6.35	6.83	5.70	5.58	26.10
9	1000	CO_2	69.1	85.00	5.64	1.71	0.58	0.23	0.43	0.74	0.78	0.79	0.78	3.33
9	1000	CO_2	80.6	16.05	10.00	7.36	6.01	2.46	4.59	6.55	7.09	6.10	6.16	27.64
9	1000	CO_2	80.6	4.22	13.69	8.56	6.86	2.83	5.30	7.57	8.10	6.79	6.17	29.91
9	1000	CO_2	80.6	5.25	25.68	12.77	7.61	2.55	4.30	5.77	5.84	4.74	4.65	20.84

Table B.2 Continued

Run	Pressure	Injected Gas Composition	Percent Recovery	C_1	C_2	C_3	C_4	C_5	C_6	C_7	C_8	C_9	C_{10}	Soltrol
10	1300	CO_2	50.0	15.91	6.22	6.66	6.14	2.55	5.08	7.56	8.99	6.92	6.69	27.08
10	1300	CO_2	73.2	17.35	6.69	7.07	6.50	2.69	5.10	7.05	7.52	6.32	5.90	27.80
10	1300	CO_2	88.7	17.42	6.62	6.99	6.45	2.75	5.26	7.35	7.73	6.29	5.89	27.26
10	1300	CO_2	90.6	17.10	6.58	6.92	6.37	2.70	5.07	7.10	7.54	6.27	5.96	28.40
10	1300	CO_2	92.9	17.45	6.80	6.99	6.28	2.63	4.99	6.94	7.41	6.13	5.96	28.42
10	1300	CO_2	94.7	14.39	5.94	6.31	6.05	2.87	5.79	7.33	8.30	6.97	6.18	29.98
12	1500	12.5% C_1 87.5% CO_2	47.8	17.11	6.48	6.72	6.28	2.62	5.04	7.00	7.67	6.33	5.89	28.86
12	1500	12.5% C_1 87.5% CO_2	84.6	30.12	6.76	6.32	5.66	2.30	4.36	6.04	6.36	5.22	4.99	21.90
12	1500	12.5% C_1 87.5% CO_2	84.6	76.13	4.63	1.54	0.85	0.24	0.31	0.91	1.20	1.06	1.21	11.92
12	1500	12.5% C_1 87.5% CO_2	88.5	23.90	6.89	6.65	6.18	2.53	4.85	6.73	7.01	5.74	5.50	24.07
12	1500	12.5% C_1 87.5% CO_2	91.5	14.55	8.53	8.08	6.14	2.18	3.67	5.65	6.21	5.41	5.41	34.22
13	1400	12.5% C_1 87.5% CO_2	13.2	21.41	8.29	8.70	7.31	2.63	4.73	6.36	6.62	5.39	5.19	23.38
13	1400	12.5% C_1 87.5% CO_2	77.9	30.58	6.63	6.58	5.86	2.25	4.25	5.80	6.10	5.01	4.84	22.12
13	1400	12.5% C_1 87.5% CO_2	77.9	86.62	4.52	1.42	0.63	0.24	0.48	0.77	0.83	0.67	0.61	3.16
13	1400	12.5% C_1 87.5% CO_2	83.2	29.41	7.55	7.03	6.01	2.25	4.20	5.79	6.08	4.99	4.82	21.88
13	1400	12.5% C_1 87.5% CO_2	83.2	79.05	7.68	2.75	1.21	0.40	0.74	1.11	1.19	0.96	0.84	4.04
13	1400	12.5% C_1 87.5% CO_2	86.6	24.28	8.78	7.71	6.29	2.39	4.52	6.13	6.39	5.18	4.95	23.42
13	1400	12.5% C_1 87.5% CO_2	88.1	6.04	16.35	17.71	10.05	2.79	4.71	5.98	6.06	4.87	4.47	21.06
14	950	12.5% C_1 87.5% CO_2	23.5	17.68	6.76	7.51	6.98	2.66	4.97	6.77	7.19	5.91	5.71	27.87
14	950	12.5% C_1 87.5% CO_2	47.8	83.68	5.53	1.80	0.76	0.29	0.60	0.91	0.98	0.78	0.67	4.02
14	950	12.5% C_1 87.5% CO_2	47.8	21.65	6.88	7.30	6.64	2.56	4.79	6.50	6.78	5.59	5.44	25.86
14	950	12.5% C_1 87.5% CO_2	67.9	27.54	7.74	7.38	6.19	2.26	4.22	5.78	6.02	4.94	4.74	23.18
14	950	12.5% C_1 87.5% CO_2	67.9	83.83	5.40	1.43	0.48	0.18	0.33	0.94	1.00	0.92	0.66	4.84
14	950	12.5% C_1 87.5% CO_2	70.7	65.42	19.27	4.46	1.14	0.24	0.36	1.05	1.05	0.96	0.69	5.36
14	950	12.5% C_1 87.5% CO_2	70.7	5.00	12.85	9.41	7.52	2.84	5.37	7.31	7.71	6.34	6.11	29.55
15	1600	12.5% C_1 87.5% CO_2	57.4	19.64	7.60	8.02	7.00	2.61	4.80	6.49	6.76	5.56	5.37	26.16
15	1600	12.5% C_1 87.5% CO_2	86.0	21.72	7.79	7.86	6.80	2.52	4.65	6.31	6.58	5.39	5.22	25.17
15	1600	12.5% C_1 87.5% CO_2	87.2	18.81	7.06	7.53	6.86	2.65	4.99	6.78	7.12	5.81	5.61	26.77
15	1600	12.5% C_1 87.5% CO_2	90.0	20.99	7.13	7.34	6.53	2.53	4.81	6.62	6.94	5.68	5.43	26.01
15	1600	12.5% C_1 87.5% CO_2	92.1	32.40	7.73	7.30	6.17	2.22	4.13	5.56	5.69	4.56	4.21	20.07
15	1600	12.5% C_1 87.5% CO_2	92.6	38.62	7.42	7.32	6.26	2.22	3.95	5.20	5.20	3.95	3.47	16.48

Table B.2 Continued

Run	Pressure	Injected Gas Composition	Percent Recovery	C_1	C_2	C_3	C_4	C_5	C_6	C_7	C_8	C_9	C_{10}	Soltrol
16	2000	25.0% C_1 75.0% CO_2	23.5	20.10	7.67	7.96	6.76	2.46	3.98	6.53	6.80	5.60	5.44	26.71
16	2000	25.0% C_1 75.0% CO_2	38.2	21.16	8.09	8.38	7.10	2.59	4.22	6.33	6.59	5.41	5.22	24.91
16	2000	25.0% C_1 75.0% CO_2	82.4	21.51	8.18	8.48	7.18	2.60	4.22	6.30	6.52	5.36	5.11	24.56
16	2000	25.0% C_1 75.0% CO_2	85.5	21.72	7.63	7.94	6.84	2.52	4.15	6.34	6.66	5.49	5.28	25.41
16	2000	25.0% C_1 75.0% CO_2	89.4	30.38	7.97	7.66	6.21	2.22	3.58	5.42	5.68	4.70	4.46	21.71
16	2000	25.0% C_1 75.0% CO_2	91.3	78.77	8.60	5.50	2.68	0.56	0.18	0.74	0.63	0.42	0.28	1.66
16	2000	25.0% C_1 75.0% CO_2	91.3	24.16	8.70	8.76	7.37	2.75	4.43	6.57	6.47	5.08	4.59	21.12
17	1700	25.0% C_1 75.0% CO_2	23.5	16.05	6.24	6.86	6.31	2.45	4.15	6.52	7.08	5.99	5.94	32.42
17	1700	25.0% C_1 75.0% CO_2	42.9	17.31	6.84	7.70	7.09	2.70	4.48	6.80	7.17	5.95	5.80	28.17
17	1700	25.0% C_1 75.0% CO_2	77.2	39.61	6.67	6.21	5.15	1.89	3.09	4.70	4.96	4.12	4.00	19.61
17	1700	25.0% C_1 75.0% CO_2	77.2	88.81	4.54	1.58	0.59	0.17	0.07	0.49	0.51	0.46	0.42	2.37
17	1700	25.0% C_1 75.0% CO_2	80.0	39.40	7.25	6.35	5.06	1.84	3.06	4.69	4.96	4.11	3.96	19.34
17	1700	25.0% C_1 75.0% CO_2	83.5	35.85	7.89	6.85	5.48	1.98	3.26	4.95	5.24	4.35	4.19	20.01
17	1700	25.0% C_1 75.0% CO_2	83.5	85.36	5.74	2.07	0.90	0.30	0.14	0.83	0.86	0.67	0.56	2.58
17	1700	25.0% C_1 75.0% CO_2	85.3	24.91	9.49	8.36	6.52	2.40	3.93	5.89	6.07	4.99	4.70	22.77
17	1700	25.0% C_1 75.0% CO_2	85.3	82.17	8.54	3.52	1.35	0.34	0.13	0.75	0.73	0.53	0.45	1.54
18	1800	25.0% C_1 75.0% CO_2	23.2	20.58	7.70	7.81	6.56	2.40	3.92	5.98	6.35	5.31	5.17	28.21
18	1800	25.0% C_1 75.0% CO_2	39.3	18.28	7.07	7.65	6.78	2.53	4.14	6.28	6.59	5.47	5.36	29.85
18	1800	25.0% C_1 75.0% CO_2	80.3	43.07	6.89	5.96	4.70	1.68	3.05	4.11	4.28	3.54	3.36	19.36
18	1800	25.0% C_1 75.0% CO_2	80.3	89.52	4.58	1.65	0.66	0.19	0.31	0.49	0.38	0.38	0.30	1.42
18	1800	25.0% C_1 75.0% CO_2	82.1	37.94	6.92	6.33	5.36	2.00	3.27	4.94	5.17	4.27	4.06	19.73
18	1800	25.0% C_1 75.0% CO_2	84.4	33.62	8.49	7.50	5.91	2.12	3.38	5.10	5.28	4.37	4.13	20.11
18	1800	25.0% C_1 75.0% CO_2	85.9	26.15	9.36	8.70	6.92	2.46	3.91	5.78	5.88	4.81	4.47	21.58
18	1800	25.0% C_1 75.0% CO_2	85.9	81.39	8.94	4.20	1.60	0.34	0.46	0.63	0.53	0.41	0.27	1.21
19	1900	25.0% C_1 75.0% CO_2	25.5	21.78	8.10	8.11	6.75	2.46	4.00	6.05	6.44	5.43	5.24	25.66
19	1900	25.0% C_1 75.0% CO_2	41.3	18.60	7.19	7.77	6.93	2.61	4.32	6.63	7.04	5.85	5.66	27.42
19	1900	25.0% C_1 75.0% CO_2	82.6	27.95	7.18	7.18	6.16	2.30	3.80	5.81	6.12	5.08	4.86	23.57
19	1900	25.0% C_1 75.0% CO_2	85.3	32.02	7.15	6.83	5.78	2.15	3.54	5.45	5.75	4.75	4.53	22.05
19	1900	25.0% C_1 75.0% CO_2	87.8	32.71	8.22	7.33	5.73	2.04	3.34	5.21	5.52	4.60	4.33	20.99
19	1900	25.0% C_1 75.0% CO_2	87.8	85.48	7.22	3.25	1.32	0.30	0.38	0.47	0.38	0.26	0.11	0.79

APPENDIX C

VOLUMETRIC DATA

Table C.1

Composition and Volumetric Data for Reservoir Oil and CO_2

Composition

Component	Mole Percent
CO_2	0.0
C_1	17.67
C_2	6.93
C_3	7.46
nC_4	6.80
nC_5	2.65
nC_6	4.47
nC_7	6.90
nC_8	7.26
nC_9	6.00
nC_{10}	5.79
Soltrol	28.07

Volumetric Data

Pressure psig	Total Volume ml	Swelling Factor
445	140	
495	130	
545	121.5	
575	116.5	
615	111.5	
675	107.5	
750 (BP)	-	1.00
1150	102.5	
1555	101.5	
2070	100.5	
2695	99.5	

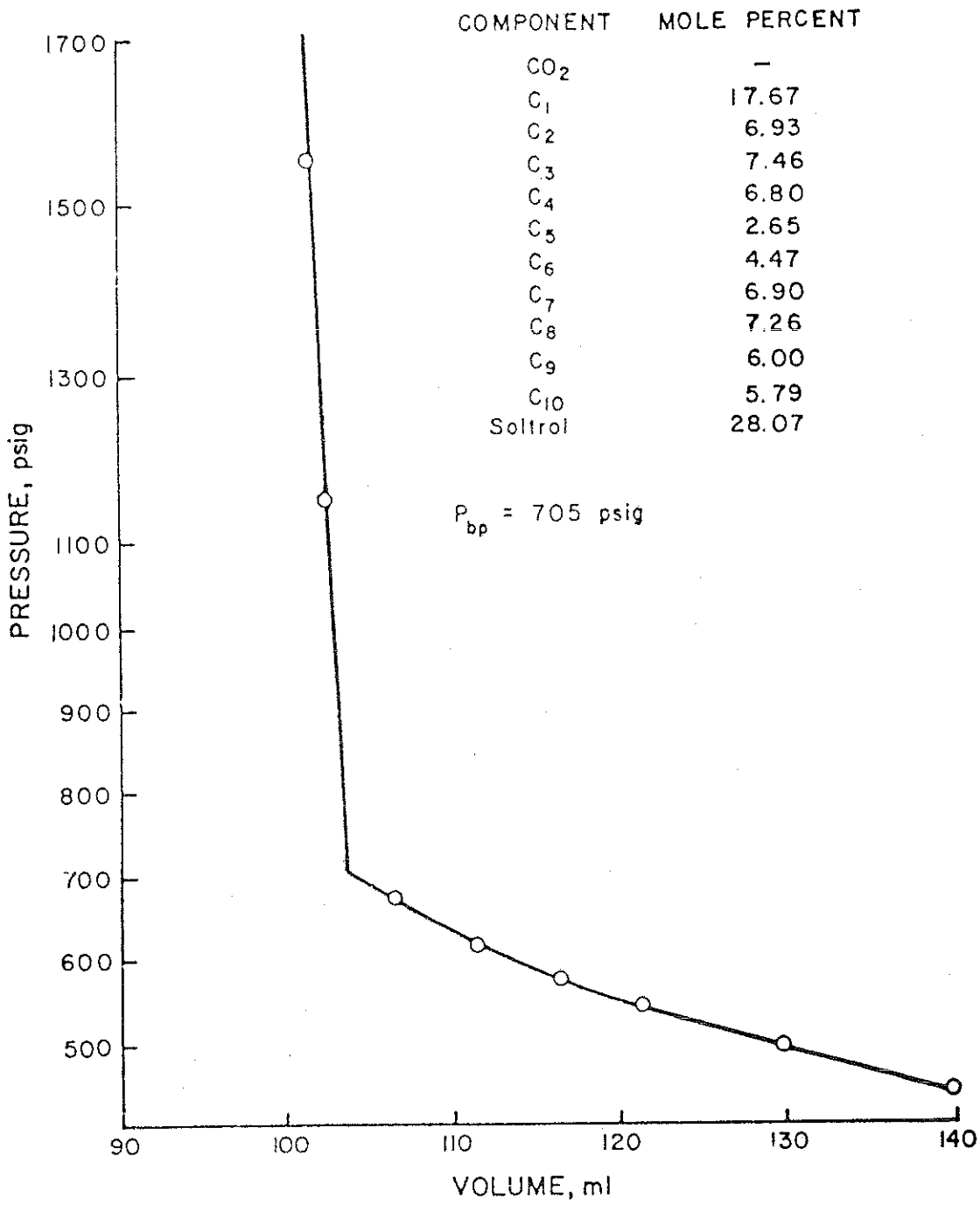

FIGURE C.1 PRESSURE-VOLUME BEHAVIOR

Table C.2

Composition and Volumetric Data for Reservoir Oil and CO_2

Composition

Component	Mole Percent
CO_2	21.62
C_1	13.78
C_2	5.40
C_3	5.82
nC_4	5.30
nC_5	2.07
nC_6	3.90
nC_7	5.38
nC_8	5.66
nC_9	4.68
nC_{10}	4.51
Solvent	21.88

Volumetric Data

Pressure psig	Total Volume ml	Swelling Factor
645	156	
700	146	
755	136	
825	126	
865	121	
910	117	
935	115	
955 (BP)	-	1.091
1185	113	
1565	112	
1980	111	
2465	110	

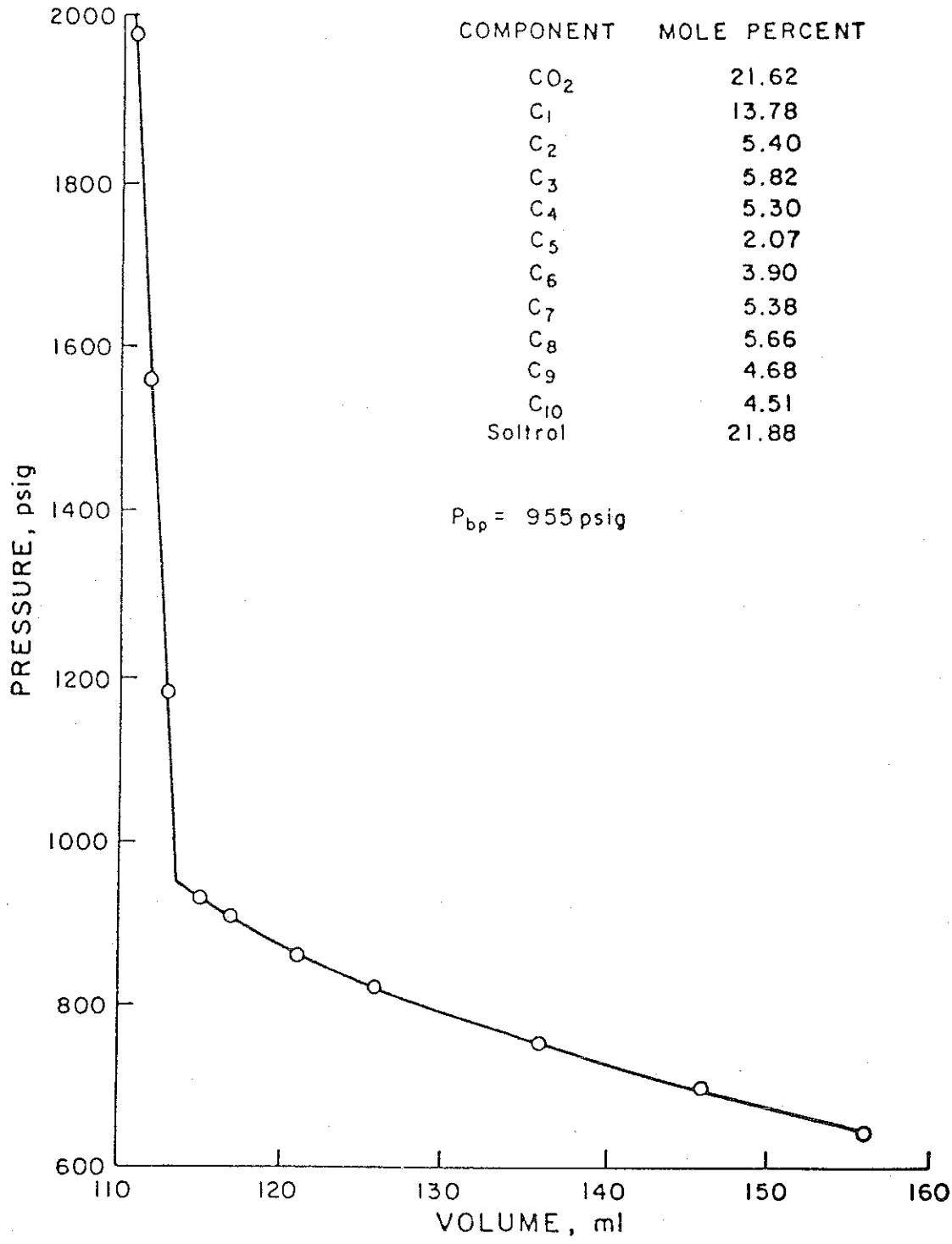

FIGURE C.2 PRESSURE - VOLUME BEHAVIOR

Table C.3

Composition and Volumetric Data for Reservoir Oil and CO_2

Composition

Component	Mole Percent
CO_2	46.01
C_1	10.24
C_2	3.98
C_3	4.10
nC_4	3.57
nC_5	1.62
nC_6	2.56
nC_7	3.53
nC_8	3.73
nC_9	3.08
nC_{10}	2.97
Soltrol	14.61

Volumetric Data

Pressure psig	Total Volume ml	Swelling Factor
935	170	
985	160	
1035	150	
1105	140	
1125	137	
1150 (BP)	-	1.288
1170	134	
1575	132	
1915	131	
2230	130	
2620	129	

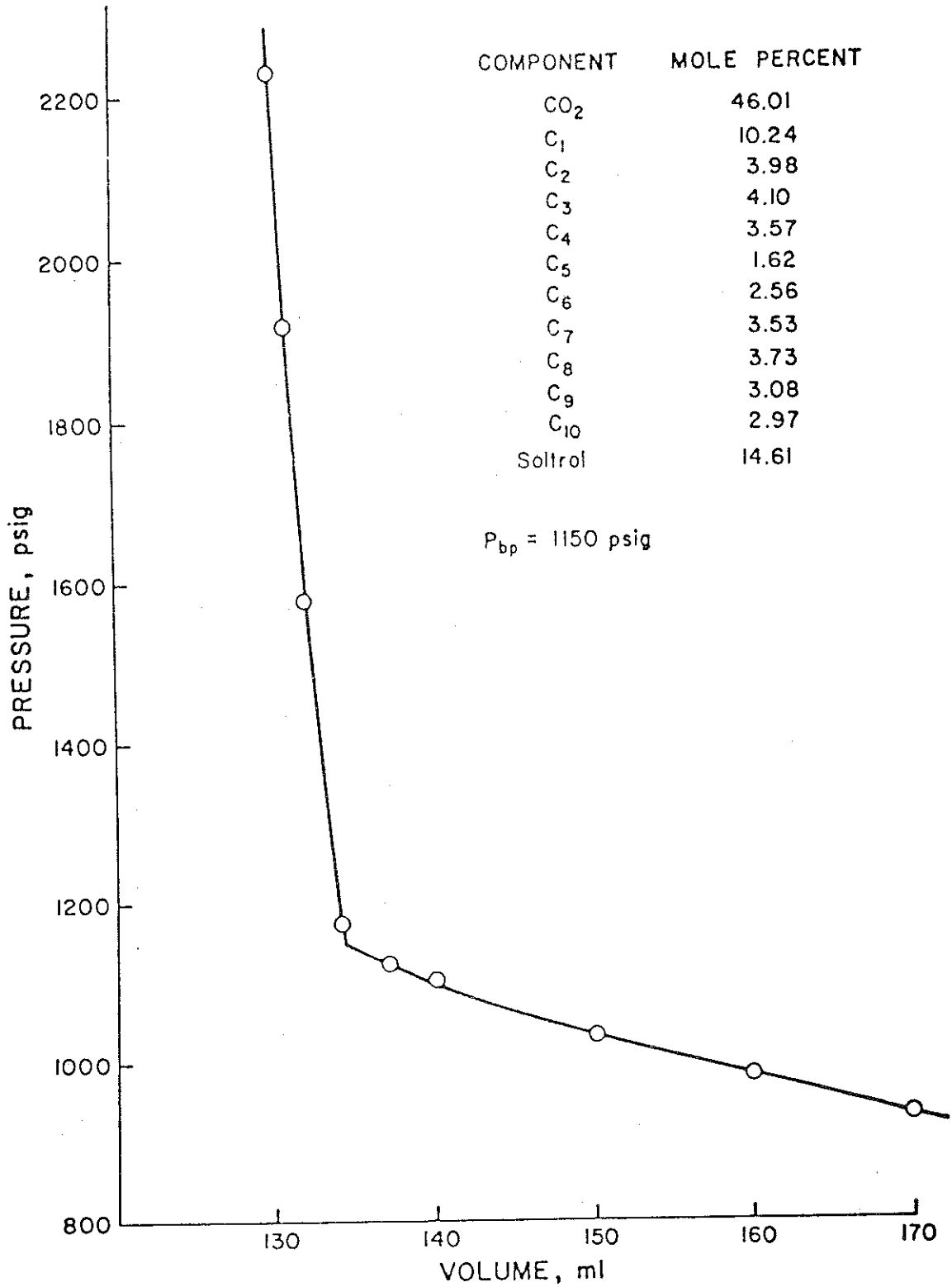

FIGURE C.3 PRESSURE-VOLUME BEHAVIOR

Table C.4

Composition and Volumetric Data for Reservoir Oil and CO_2

Composition

Component	Mole Percent
CO_2	60.48
C_1	7.51
C_2	2.91
C_3	3.00
nC_4	2.62
nC_5	1.11
nC_6	2.87
nC_7	2.58
nC_8	2.75
nC_9	2.27
nC_{10}	2.18
Solvol	10.73

Volumetric Data

Pressure psig	Total Volume ml	Swelling Factor
1075	190	
1115	180	
1145	170	
1190	161	
1215	158	
1220 (BP)	-	1.505
1720	155	
1995	154	
2235	153	
2510	152	

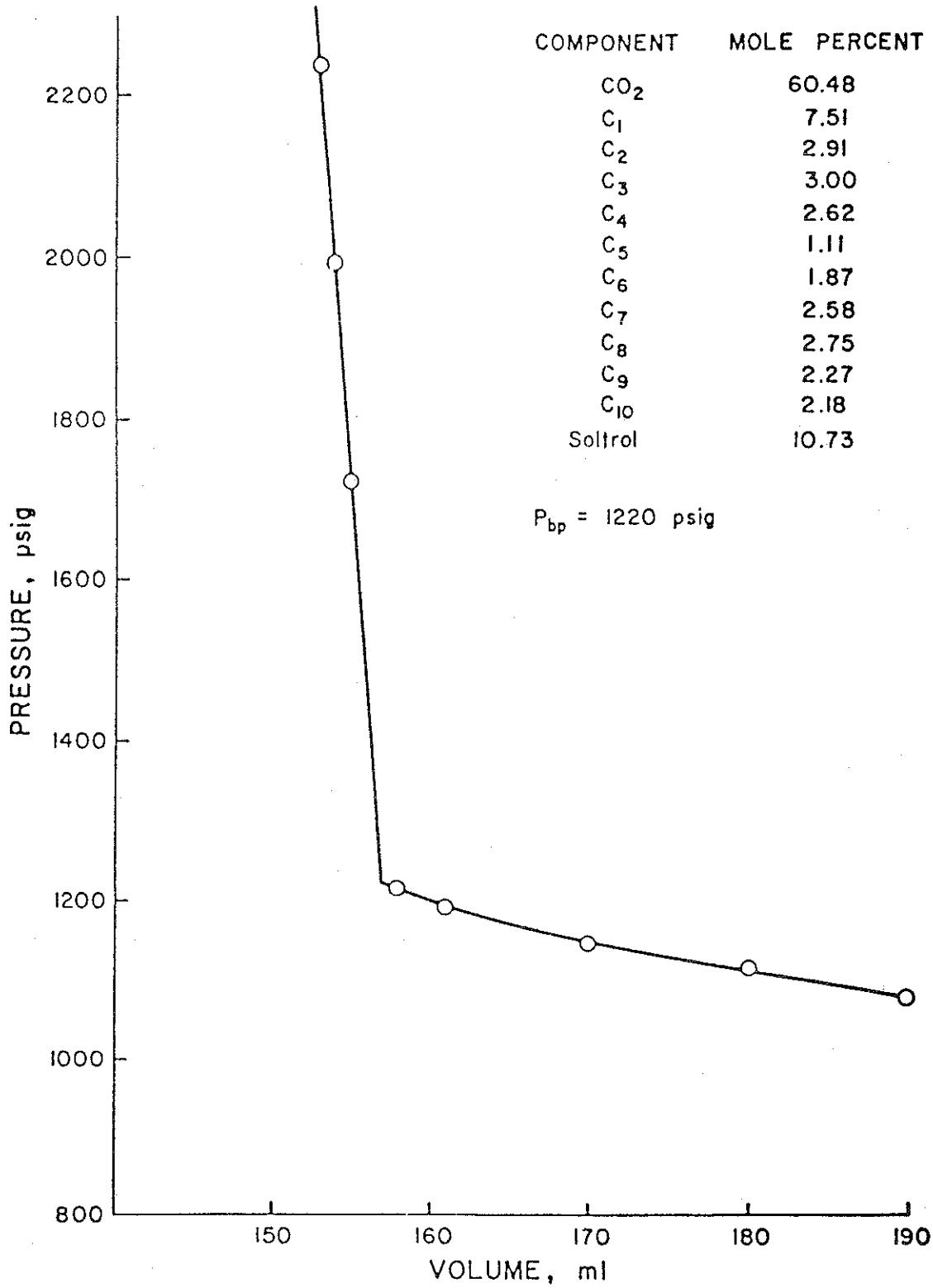

FIGURE C.4 PRESSURE - VOLUME BEHAVIOR

Table C.5

Composition and Volumetric Data for Reservoir Oil and CO_2

Composition

Component	Mole Percent
CO_2	75.00
C_1	5.42
C_2	2.06
C_3	2.03
nC_4	1.60
nC_5	0.56
nC_6	1.10
nC_7	1.55
nC_8	1.65
nC_9	1.36
nC_{10}	1.29
Soltrol	6.39

Volumetric Data

Pressure psig	Total Volume ml	Swelling Factor
1145	230	
1175	220	
1195	210	
1220 (BP)	-	1.942
1445	200	
1565	198	
1880	196	
2170	194	

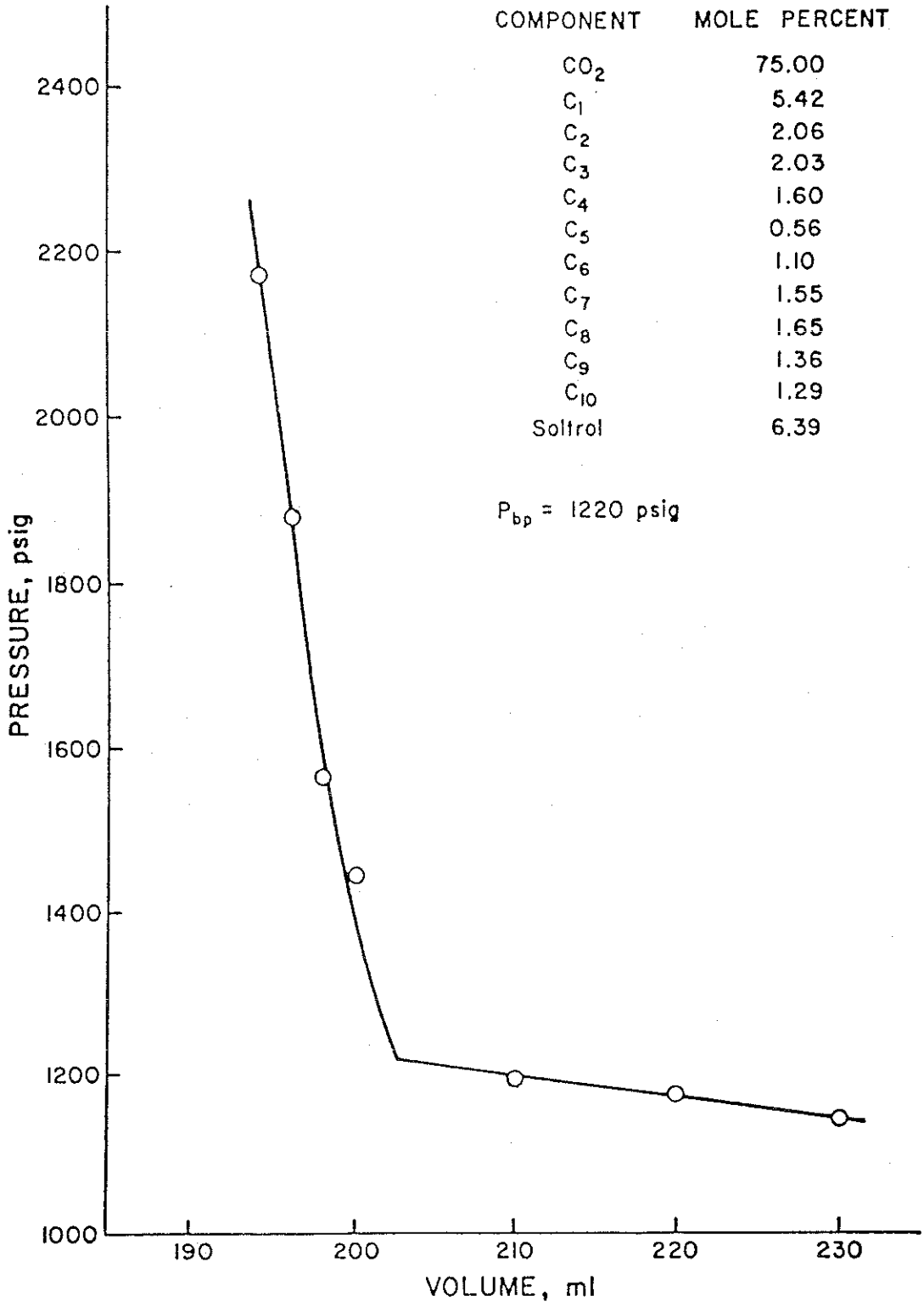

FIGURE C.5 PRESSURE-VOLUME BEHAVIOR

Table C.6

Composition and Volumetric Data for Reservoir Oil and CC_2

Composition

Component	Mole Percent
CO_2	79.95
C_1	4.18
C_2	1.58
C_3	1.60
nC_4	1.35
nC_5	0.48
nC_6	0.91
nC_7	1.25
nC_8	1.32
nC_9	1.09
nC_{10}	1.04
Soltrol	5.26

Volumetric Data

Pressure psig	Total Volume ml	Swelling Factor
1165	280	
1185	265	
1205	250	
1210(BP)	-	2.361
1230	245	
1350	243	
1535	241	
1705	239	
1910	237	
2075	235	

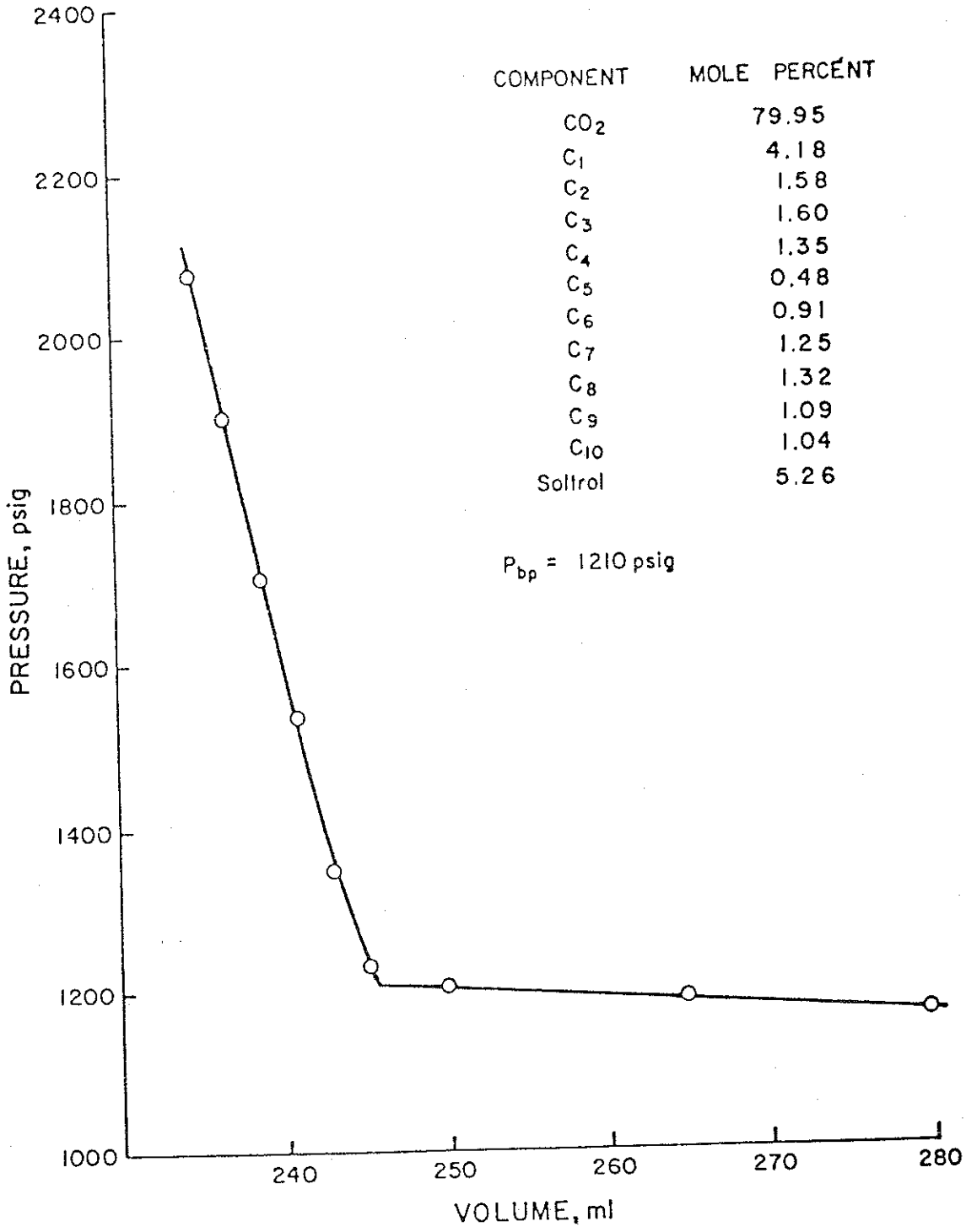

FIGURE C.6 PRESSURE-VOLUME BEHAVIOR

Table C,7

Composition and Volumetric Data for Reservoir Oil and

12.873% C_1H_4, 87.127% CO_2 Mixture

Composition

Component	Mole Percent
CO_2	14.17
C_1	18.67
C_2	6.57
C_3	6.77
nC_4	5.71
nC_5	2.42
nC_6	5.11
nC_7	5.17
nC_8	5.46
nC_9	4.50
nC_{10}	4.35
Soltrol	21.11

Volumetric Data

Pressure psig	Total Volume ml	Swelling Factor
620	140	
680	130	
755	120	
780	117	
810	114	
845	111	
890	109	
905 (BP)	-	1.043
965	108	
1390	107	
1860	106	
2375	105	

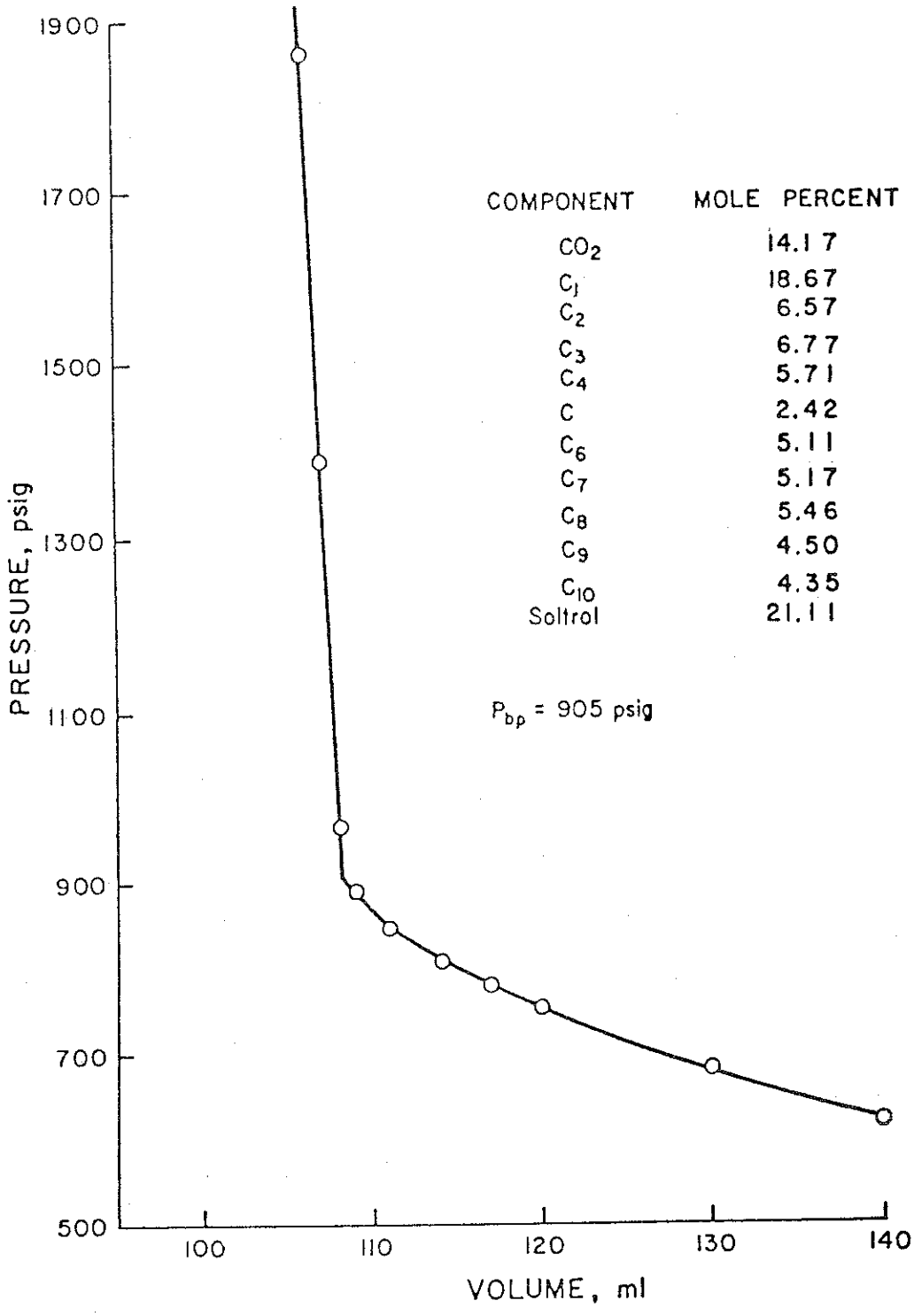

FIGURE C.7 PRESSURE-VOLUME BEHAVIOR

Table C.8

Composition and Volumetric Data for Reservoir Oil and

12.873% C_1H_4, 87.127% CO_2 Mixture

Composition

Component	Mole Percent
CO_2	29.43
C_1	16.18
C_2	4.82
C_3	5.08
nC_4	4.50
nC_5	2.02
nC_6	3.16
nC_7	4.34
nC_8	4.58
nC_9	3.82
nC_{10}	3.71
Soltrol	18.36

Volumetric Data

Pressure psig	Total Volume ml	Swelling Factor
865	150	
935	140	
1020	130	
1060	125	
1090	122	
1125	120	
1140(BP)	-	1.159
1460	118	
1735	117	
2035	116	
2330	115	

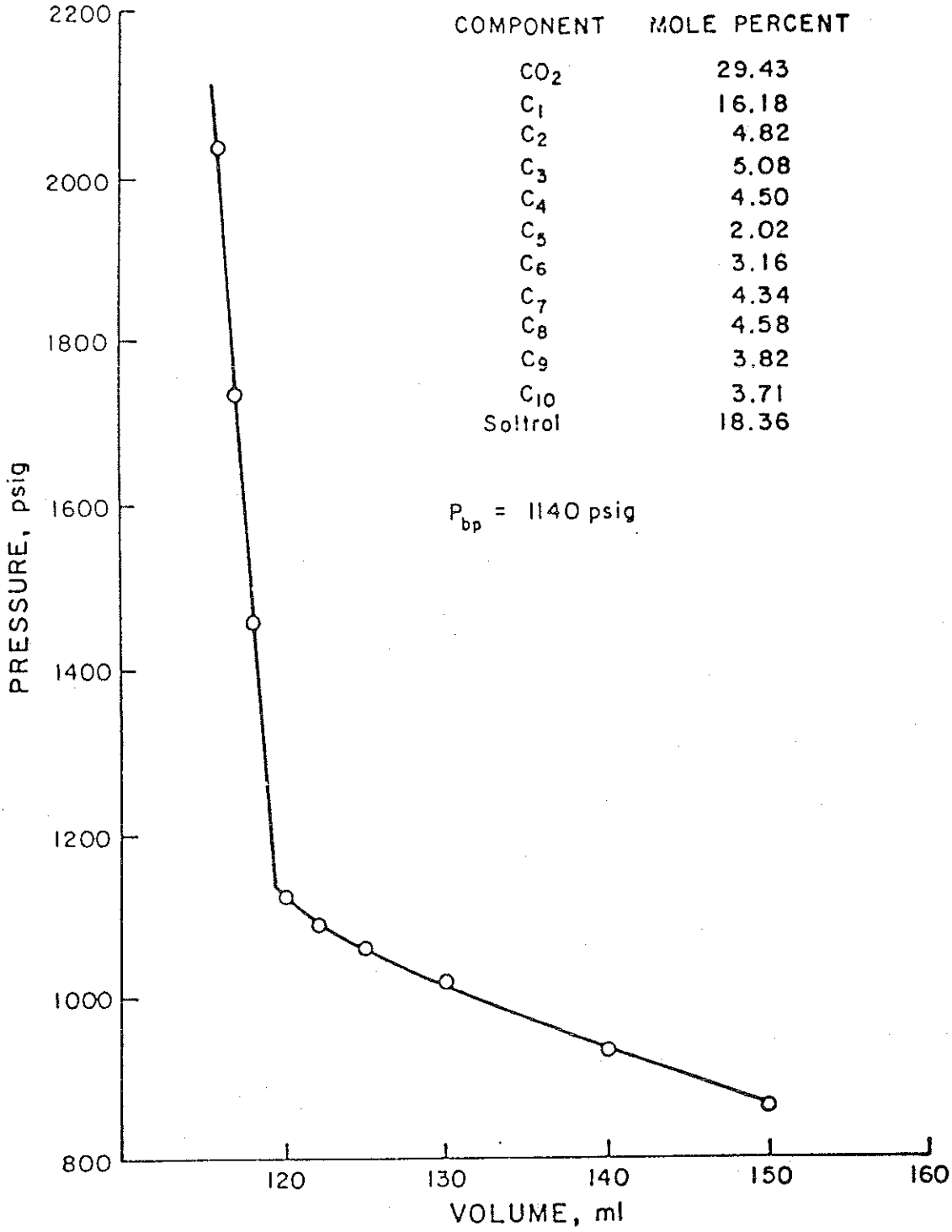

FIGURE C.8 PRESSURE-VOLUME BEHAVIOR

Table C.9

Composition and Volumetric Data for Reservoir Oil and

12.873% C_1H_4, 87.127% CO_2 Mixture

Composition

Component	Mole Percent
CO_2	55.05
C_1	14.99
C_2	2.87
C_3	2.95
nC_4	2.52
nC_5	0.91
nC_6	1.74
nC_7	2.37
nC_8	2.52
nC_9	2.09
nC_{10}	2.00
Soltrol	9.99

Volumetric Data

Pressure psig	Total Volume ml	Swelling Factor
1320	185	
1385	175	
1450	165	
1510	160	
1530	158	
1535 (BP)	-	1.522
1865	156	
2095	155	
2350	154	
2590	153	

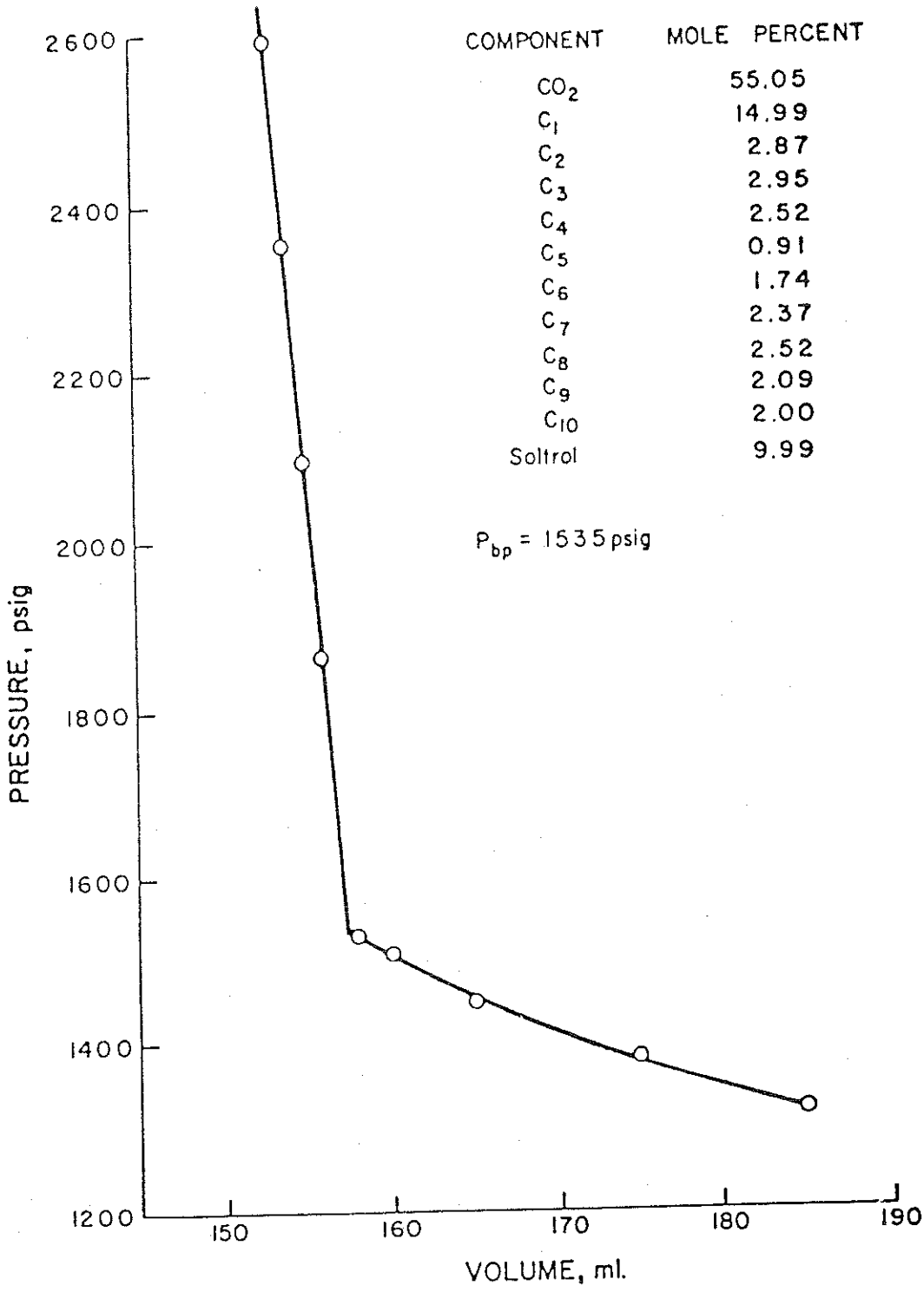

FIGURE C.9 PRESSURE - VOLUME BEHAVIOR

Table C.10

Composition and Volumetric Data for Reservoir Oil and

12.873% C_1H_4, 87.127% CO_2 Mixture

Composition

Component	Mole Percent
CO_2	65.40
C_1	14.29
C_2	1.96
C_3	1.97
nC_4	1.67
nC_5	0.61
nC_6	1.16
nC_7	1.60
nC_8	1.70
nC_9	1.41
nC_{10}	1.35
Soltrol	6.88

Volumetric Data

Pressure psig	Total Volume ml	Swelling Factor
1560	220	
1610	210	
1640	205	
1645 (BP)	-	1.971
1780	203	
1990	201	
2105	200	
2235	199	

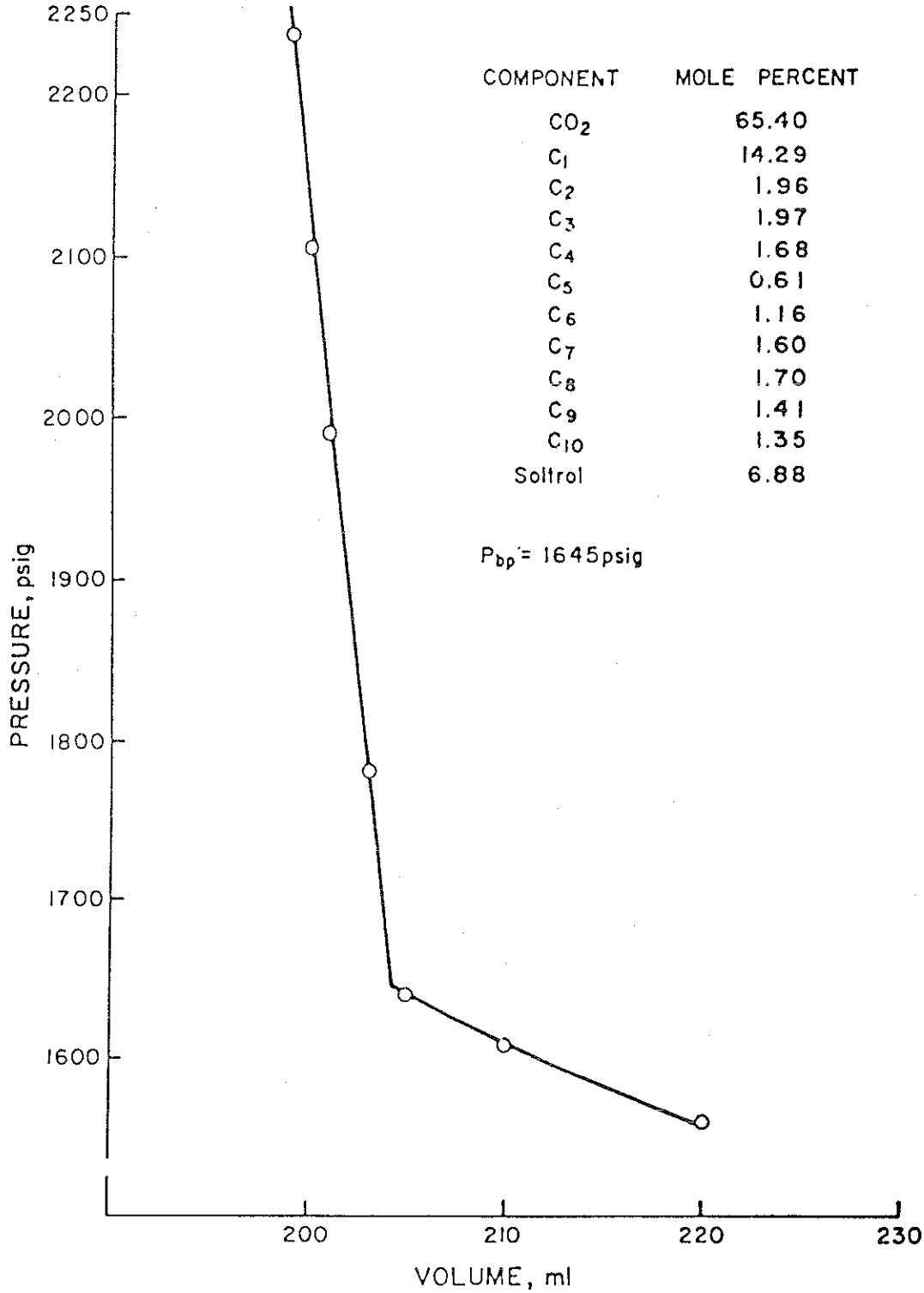

FIGURE C.10 PRESSURE VOLUME BEHAVIOR

Table C.11

Composition and Volumetric Data for Reservoir Oil and

12.873% C_1H_4, 87.127% CO_2 Mixture

Composition

Component	Mole Percent
CO_2	70.16
C_1	13.68
C_2	1.46
C_3	1.53
nC_4	1.33
nC_5	0.50
nC_6	0.93
nC_7	1.29
nC_8	1.36
nC_9	1.13
nC_{10}	1.08
Soltrol	5.55

Volumetric Data

Pressure psig	Total Volume ml	Swelling Factor
1575	280	
1615	270	
1665	260	
1675 (BP)	-	2.493
1880	255	
2005	253	
2165	251	
2305		

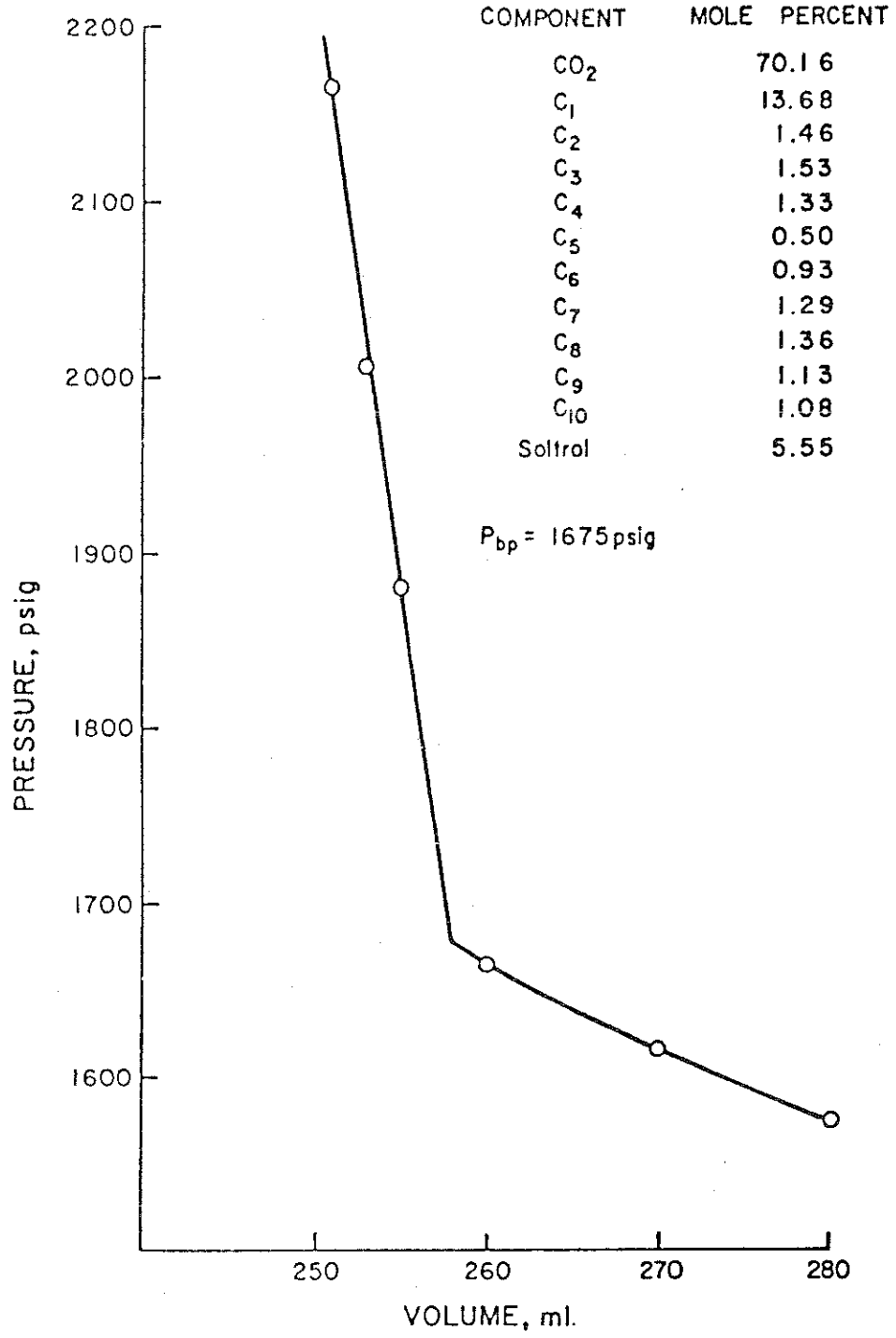

FIGURE C.11 PRESSURE-VOLUME BEHAVIOR

Table C.12

Composition and Volumetric Data for Reservoir Oil and

12.873% C_1H_4, 87.127% CO_2 Mixture

Composition

Component	Mole Percent
CO_2	74.15
C_1	13.49
C_2	1.14
C_3	1.17
nC_4	0.97
nC_5	0.55
nC_6	0.68
nC_7	0.96
nC_8	1.02
nC_9	0.85
nC_{10}	0.82
Soltrol	4.19

Volumetric Data

Pressure psig	Total Volume ml	Swelling Factor
1645	330	
1670	320	
1680	318	
1685	317	
1695(BP)	-	3.053
1760	314	
1850	312	
1925	310	
2000	308	

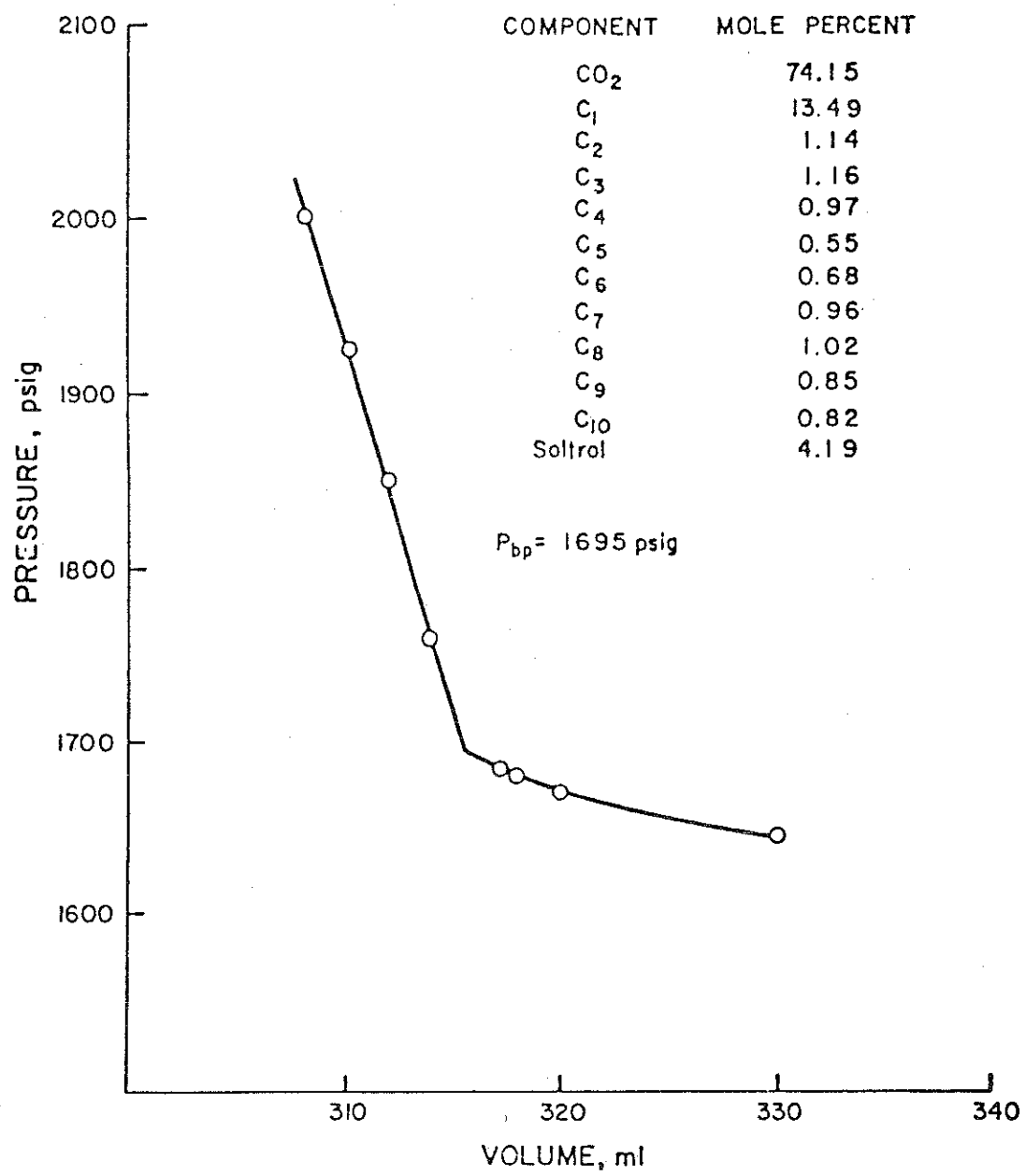

FIGURE C.12 PRESSURE - VOLUME BEHAVIOR

☆ U.S GOVERNMENT PRINTING OFFICE 1980—671-115/31

-END-

DATE FILMED

09/22/80